In vivo and *in vitro* studies on

the expression and function of TFF peptides in

the gastrointestinal tract and the central nervous system

Dissertation

zur Erlangung des akademischen Grades

doctor rerum naturalium
(Dr. rer. nat.)

genehmigt durch die Fakultät für Naturwissenschaften

der Otto-von-Guericke-Universität Magdeburg

von   M. Eng. Ting Fu

geb. am   25.03.1980 in Si Chuan, China

Gutacher: Prof. Dr. Werner Hoffmann

           Prof. Dr. Friedrich P. Paulsen

eingereicht am: 28.01.2014

verteidigt am: 27.05.2014

Acknowledgment

Foremost, I would like to express my sincere gratitude to my advisor, the Institute Director Professor Dr. Werner Hoffmann, for his encouragement and continuous support of my studies, for his patience, motivation, and immense knowledge.

My sincere thanks also go to Professor Dr. Daniela Dieterich and Dr. Anne Stellmacher from Institut für Pharmakologie und Toxikologie; Mr. Professor Dr. Dirk Schlüter and Dr. Ulricke Händel from IMMB (Institut für Medizinische Mikrobiologie), and also Dr. Ildiko Dunay (IMMB), for offering me the opportunities of cooperation with their groups and working on diverse exciting projects. My thanks are also extended to Priv.-Doz. Dr. Thomas Kalinski (Institut für Pathologie) for his valuable histological analysis, and also to Dr. Hubert Kalbacher (Interfakultäres Institut für Biochemie, Universität Tübingen) for providing the Tff peptides and anti-serum used in this study.

My special thanks go to Dr. Eva Znalesniak, for her genuine help with my work and valuable discussions and advices for this thesis.

To my fellow labmates of Institut für Molekularbiologie und Medizinische Chemie, Timo Albert, Jens Weste, Jana Reising, René Stürmer, Hubert Ragge, Andreas Kohnke, Franziska Richter, Jörn Heuer, Franz Salm and Elke Voß, thank you all for creating a pleasant working atmosphere and supporting me with my work.

Last but not least, I would like to thank my family for their support and encouragement during my study.

Parts of this work were published in the following paper:

<u>**Fu, T.**</u>, Kalbacher, H., & Hoffmann, W. (2013) TFF1 is differentially expressed in stationary and migratory rat gastric epithelial cells (RGM-1) after *in vitro* wounding: influence of TFF1 RNA interference on cell migration. *Cell. Physiol. Biochem.*, 32, 997–1010

Abbreviation

APS	Ammonium persulfate
BCA	Bicinchoninic acid
BP	Band pass (filter)
bp	Base pair
BSA	Bovine serum Albumin
CD	Cluster of differentiation
CNS	Central nervous system
Cy3	Cyanine dye 3
DAB	Diaminobenzidine
DAPI	4',6-Diamidino-2-phenylindole dihydrochloride
DCs	Dendritic cells
DMEM	Dulbecco's modified Eagle's Medium
DNase I	Deoxyribonuclease I
dNTP	deoxy-ribonucleoside triphosphate
DNA	Deoxyribonucleic acid
cDNA	Complementary DNA
ECL	Enhanced chemiluminescence
EDTA	Ethylenediamine tetraacetic acid · Na_2-salt
ES cell	Embryonic stem cell
FBS	Fetal bovine serum
FITC	Fluorescein isothiocyanate
FT	Farbteiler (filter)
GFAP	Glial fibrillary acidic protein
GI	Gastrointestinal
HBSS	Hank's balanced salt solution
H&E stain	Hematoxylin and eosin stain
HEPES	4-(2-Hydroxyethyl)piperazine-1-ethanesulfonic acid
HRP	Horseradish peroxidase
IFN	Interferon
IgG	Immunglobulin G
IL	Interleukin
i.p.	Intraperitoneal injection
LP	Long pass (filter)
LPS	Lipopolysaccharides
MAP2	Microtubule associated proteins 2
NF-κB	nuclear factor kappa-light-chain-enhancer of activated B cells
nt	Nucleotide
PBS	Phosphate buffered saline
PCR	Polymerase chain reaction
PFA	Paraformaldehyde
RISC	RNA-induced silencing complex
RNase	Ribonuclease
RNA	Ribonucleic acid
RNAi	RNA interference
dsRNA	Double-stranded RNA
mRNA	Messenger RNA
miRNA	Micro RNA
siRNA	Short/small-interfering RNA
shRNA	Short hairpin RNA
RT-PCR	Reverse transcription-PCR
PCR	Polymerase chain reaction
SDS	Sodium dodecyl sulfate
SDS-PAGE	SDS-polyacrylamide gel electrophoresis
SMCs	Surface mucous cells
T. gondii	*Toxoplasma gondii*
TE	*Toxoplasma*-Enzephalitis
TEMED	Tetramethylethylenediamine
Th1/2	Type 1/2 helper T cells
TFF	Trefoil factor family
TGF	Transforming growth factor
TLR	Toll-like receptor

TNF	Tumour necrosis factor
UV	Ultraviolet

Full name of genes mentioned in this study

ACTA2/α-SMA	Alpha-actin-2/Smooth muscle alpha-actin
ß-ACTIN	Beta actin
BIRC5	Survivin/Baculoviral IAP repeat-containing 5
CCNA2	Cyclin A2
CD4	T-cell surface glycoprotein CD4 antigen
CD8	T-cell surface glycoprotein CD8 antigen
CDH1/E-CDH	Cadherin 1, type 1/E-cadherin (epithelial)
CDH2/N-CDH	Cadherin 2, type 1/N-cadherin (neuronal)
CDK1(2)	Cyclin-dependent kinase 1 (2)
CXCL2/SDF-1	Chemokine (C-X-C motif) ligand 12
CXCR4	Chemokine (C-X-C motif) receptor 4
FCGBP	IgG Fc binding protein
GFAP	Glial fibrillary acidic protein
GKN2	Gastrokine 2
IBA1	Ionized calcium binding adapter molecule 1
IL-10	Interleukin 10
IL-12αp35-2	Interleukin 12 subunit alpha isoform 2
IL-1β	Interleukin 1 beta
IFNγ	Interferon gamma
LIPF	Lipase F/gastric lipase
LGR5	Leucine rich repeat containing G protein
LYZ	Lysozyme
MAP2	Microtubule-associated protein 2
MUC16	Mucin 16
PGC	Pepsinogen C
RhoA	Ras homolog family member A
TFF1	Trefoil factor family 1
TFF2	Trefoil factor family 2
TFF3	Trefoil factor family 3
T.g./Rhrep	*Toxoplasma gondii* strain RH repeat region
TGFα/β	Transforming growth factor α/β
TNFα	Tumour necrosis factor α
VIM	Vimentin

Full name of institutes mentioned in this study

IMMB	Institut für Medizinische Mikrobiologie
IMMC	Institut für Molekularbiologie und Medizinische Chemie
IPA	Institut für Pathologie
IPT	Institut für Pharmakologie und Toxikologie

Catalogue

Table list

Figure lists

Appendix list

1 Introduction

1.1 *Trefoil factor family (TFF)*

1.1.1 TFF peptides

The trefoil factor family (TFF) peptides belong to a family of mucin-associated small proteins containing seven conserved cysteine residues (Wright *et al.*, 1997; Emami *et al.*, 2004; Hoffmann, 2006). There are three members in the TFF family: TFF1, TFF2 and TFF3. All three TFF genes are clustered on chromosome 21q22.3 in a head-to-tail arrangement within a 54.5 kb region in the order of "telomere-TFF1-TFF2-TFF3-centromere" and the transcription directed toward the centromere (Beck *et al.*, 1996; Chinery *et al.*, 1996; Gött *et al.*, 1996; Seib *et al.*, 1997; Hoffmann, 2013a; Figure 1).
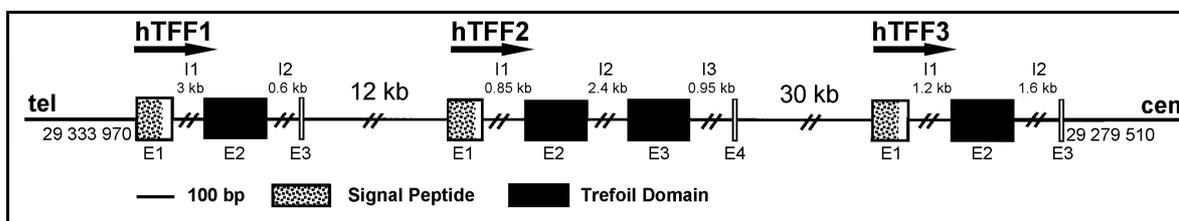
Figure 1: The region encoding human trefoil peptides on chromosome 21q22.3
Genomic organization of the human TFF gene locus harboring the genes hTFF1, hTFF2 and hTFF3. The orientation of the telomere (tel) and the centromere (cen) as well as the nucleotide positions are indicated. The introns are shown as I1, I2 or I3 with corresponding size. The exons (E) encoding the signal peptide (typical precursors of secretory proteins) are marked by dots, the TFF domains are shown in black. The size bar refers to these coding regions. The figure is modified from Seib *et al.* (1997) and Hoffmann (2013a).

All TFF peptides are synthesized via precursors containing a cleavable N-terminal signal sequence typical of secretory proteins. As a hallmark, they contain the unique TFF module comprised of about 42 amino acid residues and defining the TFF domain (formerly P-domain or trefoil domain; Thim, 1989; Hoffmann & Hauser, 1993; Wright *et al.*, 1997; Thim & May, 2005; Hoffmann, 2013a). Intramolecular disulfide bridges are formed from six of the conserved cysteine residues in the order of C^1–C^5, C^2–C^4, C^3–C^6 resulting in the characteristic three loop structure of the TFF domain (Thim & May, 2005). A planar projection of this structure resembles a trefoil (Hoffmann, 2013a; Figure 2). The complex pattern of disulfide bridges is probably one reason for the remarkable resistance of TFFs against proteolytic degradation, particularly in the stomach (Thim & May, 2005; Kjellev, 2009).

Not only the monomeric forms (Polshakov et al. 1997; Newton et al. 2000; Lemercinier et al. 2001; May et al. 2009) but also homodimeric and heterodimeric forms of TFF peptides have been detected *in vivo* (Gajhede *et al.*, 1993; Chadwick *et al.*, 1997; Newton *et al.*, 2000; Thim & May, 2005; Kouznetsova *et al.*, 2007b; May *et al.*, 2009; Albert *et al.*, 2010). The seventh free cysteine residue is essential for the formation of the dimeric forms of TFF1 and TFF3 (Chinery *et al.*, 1995; Thim *et al.*, 1995; Polshakov

et al., 1997; Williams *et al.*, 2001; Muskett *et al.*, 2003). In the human gastrointestinal (GI) tract, all TFFs are capable of forming heteromers with different partner proteins (Figure 2).

Figure 2: Structure of a typical Trefoil domain and different forms of TFF peptides in the mammalian GI tract
Schematically represented are: **(A)** typical disulphide-bond formation of the TFF domain (based on human TFF1). The conserved TFF domain (42 amino acids) is indicated in black with the proposed intradomain disulphide bonds; the amino acids outside of the trefoil domain are shown in grey; the seventh cysteine residue, at position 58, is shown in white (grey background) and in its reduced form; **(B)** the TFF1–GKN2 heteromer, the monomeric form of TFF2 (including the additional disulfide bridge), the high molecular weight complex of TFF2 (partner X is not known thus far) and the TFF3–FCGBP heteromer. The TFF1 and TFF3 heteromers are disulfide-linked. The figures are modified from Chadwick *et al.* (1995) and Hoffmann (2013)

The first discovered TFF member is TFF1 (formerly named pS2/BCEI/pNR-2/pNR-105/Md2). It has been initially found in the MCF-7 human breast cancer cell line, described as an estrogen-responsive gene (Masiakowski *et al.*, 1982; Jakowlew *et al.*, 1984; Nunez *et al.*, 1987). The human TFF1 gene codes for a small preprotein of 84 amino acids containing an amino terminal signal peptide characteristic of secreted proteins (Jakowlew *et al.*, 1984; Rio *et al.*, 1988b; Ribieras *et al.*, 1998) . The secreted mature form of TFF1 contains 60 amino acids (MW: ~6.67 kDa), forming one trefoil domain (Jakowlew *et al.*, 1984; Rio *et al.*, 1988a; Thim, 1989). TFF2 (formerly named [P]SP/[pancreatic] spasmolytic polypeptide) has originally been detected in porcine pancreas during purification of insulin (Jørgensen et al. 1982; Tomasetto et al. 1990; De et al. 1994; Beck et al. 1996). It contains 106 amino acids (MW: ~12 kDa) and consists of two TFF domains (Thim, 1997; Thim & May, 2005). TFF3 (formerly named ITF/P1.B), the last known mammalian member of the trefoil family, was recognized originally in rat intestine (Suemori *et al.*, 1991) and the human sequence was reported later (Hauser *et al.*, 1993; Podolsky *et al.*, 1993). It contains 59 amino acids (MW: ~6.6 kDa) forming one trefoil domain.

1.1.2   Expression of TFF peptides

TFF peptides are mainly expressed by normal mucous epithelial cells, predominantly found in the GI tract as exocrine products (Wong *et al.*, 1999; Hoffmann & Jagla, 2002;

Kjellev, 2009). They are also expressed in other parts of the human body, like the respiratory tract (Hoffmann, 2007), the salivary glands (Kouznetsova *et al.*, 2010) and the pancreas (Guppy *et al.*, 2012). Furthermore, TFF peptides are detectable in the human serum (Miyashita *et al.*, 1994; Higashiyama *et al.*, 1996; Grønbaek *et al.*, 2006), urine (Rinnert *et al.*, 2010) and are also found in minute amounts in the brain as neuropeptides (Hirota *et al.*, 1994a, 1994b, 1995; Hinz *et al.*, 2004).

1.1.2.1 TFF peptides in the gastrointestinal (GI) tract

TFF peptides are expressed in a tissue-specific manner within the GI tract (Table 1), which is the predominant expression site of all three TFF peptides (Madsen *et al.*, 2007; Hoffmann, 2013a) and are probably involved in various mucosal protection and repair processes.

Table 1: TFF peptides and co-expressed secretory mucins in the human GI tract

Organ	Cell	TFF Peptid	Secretory mucin
Stomach	Cardiac and antral SMCs	TFF1, TFF3	MUC5AC
	Corpus SMCs (surface mucous cell)	TFF1	MUC5AC
	Mucous neck cells	TFF2	MUC6
	Antral gland cells	TFF2	MUC6
Intestine	Brunner's glands	TFF2, TFF3	MUC6
	Goblet cells	TFF3	MUC2

The table is adapted from Hoffmann (2013a)

The major expression site of TFF1 is the stomach. Tff1 is expressed predominantly by the surface mucous cells (SMCs) in the surface/foveolar epithelium (Rio *et al.*, 1988a; Luqmani *et al.*, 1989; Tomasetto *et al.*, 1990; Hauser *et al.*, 1993; Machado *et al.*, 1996, 2000; Karam *et al.*, 2004; Ruchaud-Sparagano *et al.*, 2004; Hoffmann, 2012). A relative high level of TFF1 expression has also been described in the upper ducts and surface cells of Brunner's glands in the duodenum (Hanby *et al.*, 1993). The expression of TFF1 has also been observed in the intestinal part of the GI tract, e.g. the small and large intestine and rectum (Singh *et al.*, 1998; Madsen *et al.*, 2007). TFF2 is mainly expressed in the stomach (Madsen *et al.*, 2007) and secreted by gastric mucous neck cells and antral gland cells (Tomasetto et al. 1990; Hanby et al. 1993; Nogueira et al. 1999; Machado et al. 2000; Ota et al. 2006). In the duodenum, TFF2 expression is detected in acini and distal ducts of Brunner's glands (Piggott *et al.*, 1991; Regalo *et al.*, 2005). TFF2 expression was also shown in the mouse and rat antrum as well as in the intestine in only small amounts (Lefebvre *et al.*, 1993; Cook *et al.*, 1999). Additionally, Tff2 mRNA was reported to be expressed in the porcine ileum (Scholven *et al.*, 2009). TFF3 secretion was demonstrated in deep laying SMCs of the antrum, the pyloric region and the proximal duodenum (Hoffmann & Jagla, 2002; Kouznetsova *et al.*, 2004). The major expression sites of TFF3 are the goblet cells throughout the human and rodent intestine and also the gland acini and distal ducts of Brunner's glands (Suemori *et al.*, 1991; Hauser *et al.*, 1993; Podolsky *et al.*, 1993).

In general, the multiple molecular functions of TFF peptides include (a) constituents of mucus barriers, (b) enhancement of rapid mucosal repair by cell migration

("restitution"), (c) modulation of mucosal differentiation processes and (d) modulation of the mucosal immune response (Hoffmann, 2006, 2013b). Previous studies clearly demonstrated the protective and healing effects of all three TFF peptides after various mucosal damages (Hoffmann & Jagla, 2002; Zhang *et al.*, 2003; Beck *et al.*, 2004; FitzGerald *et al.*, 2004; Poulsen *et al.*, 2005; Hoffmann, 2006). TFFs support a variety of different mucosal defence and repair mechanisms, synergistically enhancing the surface integrity of the gastrointestinal mucosa and interact with mucins, influencing the rheological properties of viscoelastic mucous gels (Wong *et al.*, 1999; Thim *et al.*, 2002; Hoffmann, 2004, 2013a). The protective effect of TFF1 is reported in the jejunum of a transgenic mouse over-expressing Tff1, where the extent of jejunal damage caused by indomethacin was markedly reduced when compared with control animals (Playford *et al.*, 1996). Both Tff2 and Tff3 peptides were shown to enhance cell migration in the restitution phase of primary rabbit corneal epithelial cells *in vitro* (Göke *et al.*, 2001). TFF3 is reported to protect the intestinal epithelial barrier function by interaction with mucins in human (Kindon *et al.*, 1995) and to enhance the re-epithelialization of corneal wounds in the mouse (Paulsen *et al.*, 2008). Moreover, all three lines of Tff-deficient mice showed mucosal abnormalities: Tff1-deficient mice developed obligatory antropyloric adenomas, 30% of which progressed to carcinomas (Lefebvre *et al.*, 1996), Tff2-deficient mice had an increased number of parietal cells and showed increased susceptibility to gastric injury (Farrell *et al.*, 2002), Tff3-deficient mice showed a decreased resistance to colonic damage by dextran sulfate sodium (DSS; Mashimo *et al.*, 1996).

Many studies demonstrated a motogenic effect of all three TFF peptides (Dignass *et al.*, 1994; Playford *et al.*, 1995; Poulsom, 1996; Hoffmann & Jagla, 2002; Dürer *et al.*, 2007; Hoffmann, 2009). Their enhancing effect on cell migratory processes has been shown in various epithelial cell lines (Hoffmann *et al.*, 2001; Hoffmann & Jagla, 2002) pointing to a chemotactic but not a chemokinetic effect on cell migration (Chwieralski *et al.*, 2004; Hoffmann, 2009). There is increasing evidence indicating that TFF peptides modulate various mucosal differentiation processes that are crucial for the continuous regeneration of mucous epithelia from stem cells (Hoffmann, 2007, 2008), e.g., TFF1 is required for the commitment programme of mouse oxyntic epithelial progenitors (Karam *et al.*, 2004). TFF1 expression is up-regulated after mucosal injury (Rio *et al.*, 1991; Wright *et al.*, 1992; Taupin & Podolsky, 2003) and after total wounding (multi scratch assay) in the transformed human bronchial epithelial cell line (BEAS-2B) and human lung adenocarcinoma epithelial cell line (A549; Znalesniak, 2013).

TFFs were also demonstrated to participate in immune responses and inflammatory processes (Poulsen *et al.*, 2005; Hoffmann, 2009; McBerry *et al.*, 2012). TFF2 expression is found to be present in macrophages and lymphocytes (Göke *et al.*, 2001; Kurt-Jones *et al.*, 2007). The inflammatory and proliferative responses of these immune cells were shown to be dysregulated in TFF2-deficient mice (Kurt-Jones *et al.*, 2007). Not only TFF2 but also TFF3 expression has been observed in lymphoid tissues (e.g. spleen, lymph nodes and bone marrow; Cook *et al.*, 1999). They both are shown to play a role in gastrointestinal inflammation and systemic immune responses (Baus-Loncar *et al.*, 2005a; Poulsen *et al.*, 2005; Kurt-Jones *et al.*, 2007). A recent

study demonstrated that Tff2 suppresses *Toxoplasma gondii* driven type 1 inflammation in mice (McBerry *et al.*, 2012).

1.1.2.2 TFF peptides in the central nervous system (CNS)

The expression level of TFF peptides in the CNS is much lower when compared with the GI tract. Previous studies showed the expression of TFFs in the brain of human and mouse (Hirota *et al.*, 1994a, 1994b, 1995; Probst *et al.*, 1995, 1996; Schwarzberg *et al.*, 1999; Reymond *et al.*, 2002; Hinz *et al.*, 2004). In human, both TFF3 mRNA and protein was found in the hypothalamus and pituitary (Probst *et al.*, 1995, 1996; Jagla *et al.*, 2000). TFF3 peptide was also detected in the posterior lobe of pituitary and postmortem cerebrospinal fluid (Jagla *et al.*, 2000).

In the mouse, Tff1 mRNA is weakly expressed throughout the brain (Hinz *et al.*, 2004) and has been identified in cultured mouse astrocytes (Hirota *et al.*, 1994a, 1994b). Biosynthesis of TFF2 in the CNS has rarely been described. Faint level of Tff2 transcription has been reported in the mouse brain, with a higher concentration in the anterior but not the posterior lobe of the pituitary (Hinz *et al.*, 2004). Recently, Tff2 expression was found in the murine retina starting as early as embryonic day E15 and gradually increasing after postnatal day P5, with a high expression levels at P15 (Paunel-Görgülü *et al.*, 2011). In contrast, Tff3 expression is limited to the hippocampus, the temporal cortex and the cerebellum and the latter is the major site of expression (Hinz *et al.*, 2004). Moreover, a maximum expression of Tff3 was shown in the mouse brain at P15 (Hinz *et al.*, 2004). The high-resolution atlas of gene expression throughout the adult mouse brain (*in situ* hybridization (ISH) data) from the Allen Brain Atlas (http://mouse.brain-map.org/) shows that Tff1 positive cells are mainly found in the hippocampus and cerebellum, especially in the granular layer and Purkinje cells.

In the rat, Tff1 is widely distributed throughout the adult rat brain and the pronounced expression was found in the hippocampus, frontal cortex and the cerebellum (Hirota *et al.*, 1995). TFF1 expression was also detected in the substantia nigra pars compacta, the ventral tegmental area and in periaqueductal areas of adult rat midbrain, exclusively in neurons and not in astrocytes (Jensen *et al.*, 2013). There is still no data published concerning Tff2 in the rat brain. TFF3 expression is found predominantly in the rat cerebellum, and also in hippocampus, amygdala and cortex, especially in magnocellular neurons of the hypothalamus (Probst *et al.*, 1995).

The role of TFF peptides in the CNS is probably diverse and has not yet been clarified. TFFs have been described as the factors influencing the development of the CNS; e.g., rat hippocampal Tff1 mRNA is restricted mainly to astrocytes and its expression decreases significantly during postnatal development at P7 (Hirota *et al.*, 1995). Mouse Tff3 has been demonstrated as a typical neuropeptide of oxytocinergic neurons of the supraoptic and paraventricular nuclei (Hoffmann & Jagla, 2002) and improves learning and retention of novel object recognition memory in mice (Shi *et al.*, 2012). Generally, TFF peptides are expected to act as neurotransmitters/neuromodulators (Hoffmann & Jagla, 2002). For example, injected TFF3 in the basolateral nucleus of rat amygdala

exhibits fear-modulating activities (Schwarzberg *et al.*, 1999).

Some *in vitro* studies show an anti-apoptotic effect of TFF peptides in different cell culture systems (e.g., gastric, intestinal, colorectal or breast cancer cell lines; Lalani *et al.*, 1999; Chen *et al.*, 2000; Kinoshita *et al.*, 2000; Taupin *et al.*, 2000; Bossenmeyer-Pourié *et al.*, 2002; Siu *et al.*, 2004). Interestingly, in contrast to the survival promoting and anti-apoptotic effects, also pro-apoptotic activity was reported. The application of recombinant TFF3 to cultured primary human chondrocytes caused increased apoptosis *in vitro* (Rösler *et al.*, 2010). Moreover, the pro-proliferative and pro-apoptotic effects of Tff2 in the developing mouse retina cultured as organotypic whole mounts *in vivo* were demonstrated as well (Paunel-Görgülü *et al.*, 2011). Nevertheless, there were no obvious neural abnormalities reported in Tff1-, Tff2-, or Tff3-deficient mice (Lefebvre *et al.*, 1996; Mashimo *et al.*, 1996; Farrell *et al.*, 2002). However, from experiments with Tff3-deficient mice a participation of Tff3 in neurosensory signalling has been suggested (Lubka *et al.*, 2008).

1.1.2.3 Pathological expression of TFF peptides

Generally, TFF peptides are aberrantly expressed in inflammatory diseases and in a variety of neoplastic disorders (Wong *et al.*, 1999; Hoffmann *et al.*, 2001; Emami *et al.*, 2004; Tomasetto & Rio, 2005; Kjellev, 2009; Hoffmann, 2013a).

TFF expression is dysregulated during a wide range of inflammatory diseases, e.g. ileal Crohn's disease, ulcerative colitis, inflammatory bowel disease, gastric ulcer disease, acute cholecystitis, various types of metaplasia, different hyperplastic polyps, Barrett's oesophagus and pancreatitis (Hoffmann *et al.*, 2001; Hoffmann & Jagla, 2002). Furthermore, it was shown that the expression of TFFs is a typical response after gastric mucosal damage in various rat models of experimental ulceration (Alison *et al.*, 1995; Hoffmann *et al.*, 2001). Under these conditions, a unique glandular structure known as the ulcer-associated cell lineage (UACL) is a prominent site of TFF synthesis. The UACL delivers its secretion products, including EGF, to the lumen via excretory ducts and is thought to represent a natural repair kit activated after mucosal damage (Wong *et al.*, 1999; Kjellev, 2009; Hoffmann, 2013a). Moreover, TFF genes are differentially expressed within the UACL, e.g., TFF1 (together with MUC5AC) and TFF2 (together with MUC6 and EGF) were detected respectively in the upper and lower parts of the structure (acinar and proximal ductular structures) and TFF3 (together with MUC5B, TGF-α, and lysozyme) was infrequently detected in all parts of the UACL (Hoffmann & Jagla, 2002; Kjellev, 2009). TFF1 and TFF3 are considered to play an important role in the different responses of the stomach and the intestine to inflammation. An increased level of TFF1 expression was reported particularly during the healing of gastric ulcers (Saitoh *et al.*, 2000) and TFF1 is also expressed during the acute phase of acid-induced colitis in the rat rectum (Itoh *et al.*, 1996). Deregulation of TFFs is observed also after incisional wounds of GI tissue, in various induced gastric ulcerations as well as after irradiation and chemotherapy. Particularly, the late and sustained TFF1 and TFF3 responses are indicative for a role in late-stage repair processes (Hoffmann & Jagla, 2002). All the studies also provide the circumstantial

evidences that TFF peptides are differently involved in the mucosal epithelial regeneration (Hoffmann, 2013a).

Inflammation is a critical component of tumour progression. Pathological expression of TFFs is also observed in premalignant conditions, e.g. Barrett's metaplasia and metaplastic polyps, and dysregulated biosynthesis of TFFs is found in many epithelial tumours, e.g. in the esophagus, stomach, biliary tract, pancreas and intestine (Hoffmann & Jagla, 2002; Emami *et al.*, 2004; Tomasetto & Rio, 2005). Moreover, aberrant expression of the TFFs has been reported for a variety of important solid tumours in humans, including gastric, intestinal, breast, prostate and lung cancers (Perry *et al.*, 2008; Kjellev, 2009). Furthermore, unusual TFF plasma levels are indicative for the progression of certain cancers and can improve, for example, gastric cancer screening (Hoffmann, 2013a). All these data suggest a role of TFFs in the development and progression of human cancer. Particularly, expression of TFF1 is elevated in gastric mucosa with atypical hyperplasia and is not observed in poorly differentiated or intestinalized gastric cancer (Wong *et al.*, 1999). Furthermore, the co-expression of TFF1 and GKN2 that normally form a heterodimer, is deregulated in gastric cancer (May *et al.*, 2009). TFF3 is a marker for bad prognosis of both stomach and colon carcinomas and formation of the TFF3–FCGBP heteromer seems to be deregulated during colon carcinogenesis (Albert *et al.*, 2010; Hoffmann, 2013a).

In conclusion, TFF peptides are considered to play important roles not only in the physiological wound healing but also in the inflammatory processes, carcinogenesis, and metastasis.

1.2   Mucosal protection and repair

The large surface of the GI tract is exposed to numerous noxious agents and is vital for the complex communication with the environment. The protective mechanisms of the intestinal epithelium can be divided into three key components: (1) stratified mucus layer together with the glycocalyx of the epithelial cells, which provides a physical protection; (2) the single layer of epithelial cells forming a continuous cell sheet interconnected with tight junctions, which is characterized by self-renewal and restitution; (3) resident macrophages and dendritic cells (DCs) of the intestinal stroma completing the elements of the innate immune system. Furthermore, the adaptive immune system builds the fourth defence line both as master regulator and as an inducible system to remove microbiota that have sidestepped earlier defence lines (Sonnemann & Bement, 2011; Hansson, 2012).

1.2.1 Mucus

Mucus is an adhesive mixture of approximately 95% water, 5% mucin glycoprotein molecules, salts, immunoglobulins, cellular and serum macromolecules, as well as the mucin-associated TFF peptides, forming a continuous gel layer (Allen & Pearson, 1993; Wong *et al.*, 1999; Hoffmann & Jagla, 2002). This mucous gel layer covers the

mucosa throughout the GI tract and is, e.g., capable of withstanding the pH gradient in the stomach from acidic on its luminal side to near neutral at its apical cell membrane perimeter (Quigley & Turnberg, 1987). Generally, the mucus layer acts as a diffusion barrier against noxious agents, entraps microorganisms and interacts with the immune surveillance system (Allen & Pearson, 1993; Atuma, 2000). Moreover, it delivers also the tolerogenic signals to DCs influencing the function of intestinal antigen-presenting cells (e.g. DCs) and epithelial cells and thereby constrain the immunogenicity of gut antigens (Belkaid & Grainger, 2013; Shan *et al.*, 2013).

The gel-forming mucins such as MUC2, MUC5AC and MUC6 are secreted by gastrointestinal mucous cells (Matsuda *et al.*, 2008; Johansson *et al.*, 2011). The localization of the mucins varies throughout the GI tract (Table 1). In the stomach, MUC5AC together with TFF1 and MUC6 together with TFF2 are generally expressed in the surface epithelial cells and mucous neck cells, respectively. In the small intestine and colon, MUC2 is the one dominating mucin secreted from goblet cells together with TFF3 (Ho *et al.*, 1995; Wong *et al.*, 1999; Hoffmann & Jagla, 2002; Albert *et al.*, 2010; Hoffmann, 2013a). Recently, different mucus structures in the GI tract have been revealed. The stomach and colon were reported to have a two-layered mucus structure, from which the inner mucus layer is firmly attached to the epithelium and the outer mucus layer is easily removed and has a less defined outer border. In contrast, the small intestine has only one layer of mucus (Hansson, 2012) suggesting different protective mechanisms in the stomach and intestine.

1.2.2 Gastric self-renewal and restitution

When the mucus layer is unable to inactivate the injurious components, the epithelial barrier acts as a second defence line (Tobey & Orlando, 1991; Orlando *et al.*, 1992). This barrier is formed by epithelial cells linked together via cell-cell contacts (such as tight junctions, adherens junctions, and desmosomes; Balda & Matter, 2009).

The repair of the epithelial barrier following injury is accomplished by two processes covering different time scales (Hoffmann, 2012). One process is the self-renewal (continuous regeneration). This is an essential component of the multiple protection and defence mechanisms maintaining the surface integrity. It takes several days to months to refresh the mucous epithelia throughout the adult life and is required for the repair of extensive and deep mucosal wounds (Hoffmann, 2008, 2013b). The typical feature of the gastric epithelial barrier is the continual bi-directional self-renewal occurring via differentiation of stem cells and progenitor cells within the isthmus followed by apoptosis of the mature cells at the end of their life cycles, respectively (Kouznetsova *et al.*, 2011; Hoffmann, 2013b). Of note, the morphology and regeneration of the human stomach differ in some details from the rodent system (Hoffmann, 2008). The human stomach is divided histologically into three main regions: the fundus, corpus and pyloric antrum (Helander, 1981). The gastric epithelia, covered by surface mucous cells, differ much in their self-renewal rates and bidirectional renewal profiles. The antral units (combination of a pit [funnel-shaped faveolae] and a gland [divided into the isthmus, the neck, and the base region]) show a higher turnover

when compared with the corpus units (Figure 3; Hoffmann, 2008; Kouznetsova *et al.*, 2011). In addition to the isthmal somatic stem cells, at least a second stem cell population, defined by LGR5, is found at the bottom of the antral glands but not in fundic glands (Barker *et al.*, 2010; Hoffmann, 2012).
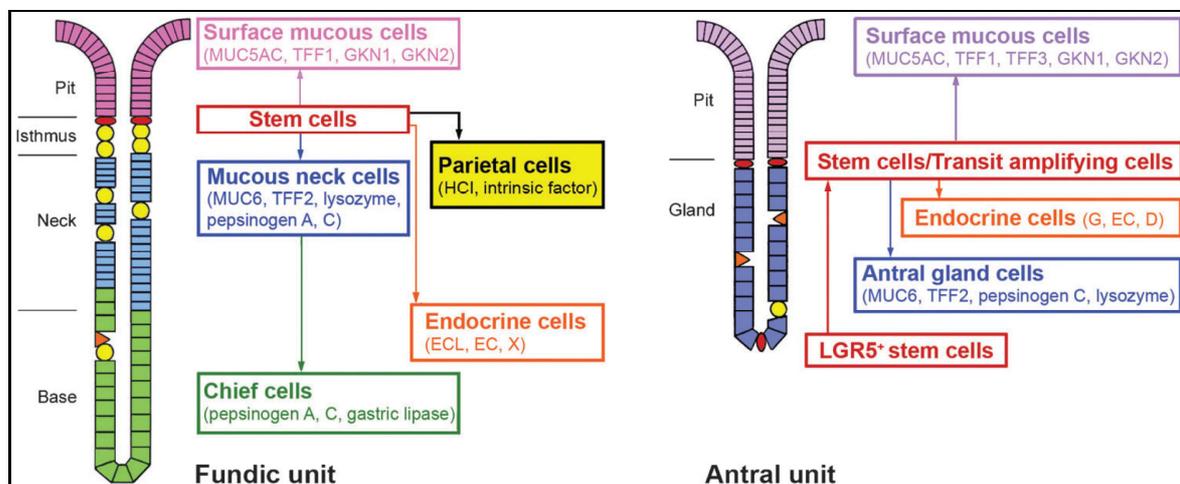
Figure 3: Schematic representation of the two gross types of human gastric units
Two gross types of human gastric units: fundic- and antral unit, and their continual renewal from stem and transit amplifying cells. The major cell types and some of their characteristic secretory products are shown. MUC: mucin, GKN: gastrokine, LGR5: Leucine rich repeat containing G protein. This figure is reproduced from Kouznetsova *et al.* (2011).

Nevertheless, minor disruptions of the surface layer of cells without damage of the basement membrane occur frequently, so speedy repair to restore epithelial continuity is essential. A sequence of events including epithelial cell dedifferentiation, forming of pseudopodia-like structures, reorganization of their cytoskeleton, migration into the site of defect to cover the exposed areas of the basement membrane and the redifferentiation after closure of the wound leading to a rapid epithelial repair has been referred as epithelial "restitution" (Silen & Ito, 1985; Taupin & Podolsky, 2003; Hoffmann, 2005; Sturm & Dignass, 2008). Restitution is a general phenomenon of mucous epithelia to superficial injury along the entire GI tract, as well as the respiratory tract, the urothelium, the oral epithelium, etc. (Hoffmann, 2005). It does not require cell proliferation and occurs within minutes to hours after the injury. Restitution is particularly well described to occur in the intestinal mucosa both *in vivo* (Feil *et al.*, 1989) and *in vitro* (Nusrat *et al.*, 1992; Znalesniak & Hoffmann, 2010). In the stomach, surface mucous cells are the major players during restitution (Hoffmann, 2005). *In vivo,* epithelial cells undergo restitution converting from polarized epithelial cells (with apical-basal polarity) to polarized migrating cells (with planar polarity; Etienne-Manneville, 2008).

Cell migration can be classified into single cell migration (amoeboid, mesenchymal) and collective migration modes (cell sheets, strands, tubes, clusters; Friedl, 2004; Friedl & Wolf, 2010). The collective cell migration as a cohesive group (maintaining cell–cell junctions) is typical of mucosal restitution (Znalesniak *et al.*, 2009). The rat gastric cell line RGM-1 (Kobayashi *et al.*, 1996) as an *in vitro* model for gastric

restitution (Nakamura *et al.*, 1998; Osada *et al.*, 1999; Ragasa *et al.*, 2007) shows predominantly collective migration (Figure 4) and is appropriate for the investigation of wound healing. It is comparable to the best studied *in vitro* models of migrating intestinal IEC-6 and IEC-18 cells (McCormack *et al.*, 1992; Znalesniak *et al.*, 2009). As so far, the only known non-transformed gastric epithelial cell line RGM-1 is a promising tool for the study of the TFFs function during migration *in vitro*.

Figure 4: Typical migratory RGM-1 cells after the wounding

Under certain circumstances, epithelial cells may undergo an epithelial-mesenchymal transition (EMT) to become migratory (Hay, 1995; Savagner *et al.*, 2005; Moreno-Bueno *et al.*, 2008; Yang & Weinberg, 2008). The EMT is characterized by trans-differentiation of epithelial cells into fibroblastoid, motile cells, accompanied by changes in the gene expression program (Jechlinger *et al.*, 2003; Huber *et al.*, 2004; De Wever *et al.*, 2008; Yang & Weinberg, 2008). The typical features for EMT are the down-regulation of epithelial-specific genes (e.g., tight- and adherens-junction proteins such as occludin and E-cadherin, respectively) and the induction of various mesenchymal genes (such as α-smooth muscle actin (α-SMA), vimentin and N-cadherin; Grünert *et al.*, 2003; Lee *et al.*, 2006; Znalesniak & Hoffmann, 2010). However, *in vivo* studies show that EMT is not complete in wound repair (Schäfer & Werner, 2008) and *in vitro* study shows that restitution is not fully accompanied by the unambiguous EMT (Znalesniak *et al.*, 2009).

The wound healing processe is modulated by numerous factors such as cytokines (Leaphart *et al.*, 2007), growth factors (Sturm & Dignass, 2008), adhesion molecules (Ivanov *et al.*, 2005), regulatory peptides (Moyer *et al.*, 2007) including TFF peptides (Taupin & Podolsky, 2003; Hoffmann, 2005, 2008). TFFs contribute to mucosal defence and repair enhancement after various types of induced mucosal damage by modulation of cell-cell contacts, motogenic activity and synergy with epidermal growth factor (Hoffmann, 2005).

1.2.3 Inflammatory process

Inflammation is an adaptive and immediate response that is triggered by noxious stimuli and conditions, such as chemicals, infection or tissue injury (Cotran *et al.*, 2004; Medzhitov, 2008; Weiss, 2008) and is mediated by tissue-resident leukocytes (e.g., macrophages), which can infiltrate the damaged region to remove the stimulus (Weiss,

2008; Sonnemann & Bement, 2011). The inflammatory response is regulated by various inflammatory mediators, like cytokines, chemokines, as well as small secreted proteins that are released by cells surrounding the damaged tissue and that act on immune system pathways leading to series of vascular and cellular reactions (Medzhitov, 2008). The vascular reactions resulting in the formation of inflammatory exudates include vasodilation with increased tissue perfusion and permeability. The cellular responses include the recruitment of leukocytes from the blood into the injured tissue by chemotaxis (margination and emigration) and the phagocytosis of invading microbes and apoptotic or necrotic cells (Böcker *et al.*, 2008).

Acute inflammation, as a component of wound healing, is a short-term response of the immune system to the damage. It usually limits the potential of infection and results in healing. A rapid repair of damaged mucosal epithelia is (therefore) essential for the prevention of chronic inflammation (Coussens & Werb, 2002). Furthermore, a prolonged, dysregulated and maladaptive response, which can be caused by the persistence of the initiating factors or a failure of mechanisms required for resolving the inflammatory reaction, as the hallmark of chronic inflammation (Coussens & Werb, 2002; Weiss, 2008), plays a decisive role at different stages of tumour development and in gastric cancer (Houghton *et al.*, 2004; Fox & Wang, 2007; Grivennikov *et al.*, 2010; Hoffmann, 2013b). Dysregulated self-renewal in the course of chronic inflammation is the basis for the development of neoplasias (Radtke & Clevers, 2005; Vries *et al.*, 2010). Approximately 90% of all human cancers originate from abnormal epithelial cell proliferation (Nollet *et al.*, 1999). There are studies reporting that TFFs, particularly TFF2 present in macrophages and lymphocytes (Kurt-Jones *et al.*, 2007), can participate in and regulate the intestinal inflammatory processes and systemic immune responses (Baus-Loncar *et al.*, 2005a, 2005b; Kurt-Jones *et al.*, 2007) and also stimulate the migration of monocytes (Cook *et al.*, 1999).

1.3 Investigated projects

TFF peptides are mainly expressed in the GI tract, where they not only play an important role in the wound healing of the gastrointestinal mucosa but also participate in the immune response. TFF peptides are also synthesized in the CNS. However, the function of TFF peptides in the CNS, especially in the immune response and during inflammatory processes is still unclear. In the context of the potential role of TFF peptides in wound healing and in the regulation of inflammatory processes of the GI tract and the CNS, four different model systems concerning various aspects of the synthesis and function of TFFs were investigated:

(a) *In vitro* model for the restitution of gastric epithelial cells (RGM-1) including RNA interference (RNAi) to study the function of TFFs during this process (described in 1.3.1).

(b) Two *in vivo* mouse models of inflammatory diseases using *Toxoplasma gondii* (*T. gondii*) induced ileitis (oral infection) and encephalitis (i.p. infection) to study the

expression of TFFs during the immune responses and to examine the phenotype of Tff-deficient mice (described in 1.3.2; cooperation with Dr. I. Dunay [IMMB] and Prof. Dr. D. Schlüter / Dr. U. Händel [IMMB], Magdeburg).

(c) *In vitro* study of the primary cell cultures of rat brain to study the cellular localization of TFFs in the rat brain (described in 1.3.3; cooperation with Prof. Dr. D. Dieterich / Dr. A. Stellmacher [IPT, Magdeburg]).

1.3.1 Function of TFFs in an *in vitro* model of gastric restitution

Here the non-transformed rat epithelial cell line RGM-1 (Kobayashi *et al.*, 1996) was used as an *in vitro* restitution model. These cells are expected to show characteristics of surface mucous cells. An established technique to separate migratory and stationary cells *in vitro* allowed expression profiling of these cells (Znalesniak *et al.*, 2009). Furthermore, RNAi was applied to investigate the function of TFFs for gastric restitution.

RNA interference

The mechanism of RNAi, discovered first in a worm (Fire *et al.*, 1998) and then in mammalian cells (Elbashir *et al.*, 2001), is a widely used method in biological and medical research. This RNA-dependent gene-specific silencing mechanism can be triggered both by endogenous and exogenous RNA and is used to drastically decrease the expression of a targeted gene (Hammond *et al.*, 2000; Bartel, 2004). Since it may not totally abolish expression of the gene, this technique is sometimes referred as "knockdown", to distinguish it from "knockout" procedures in which expression of a gene is entirely eliminated.

RNAi can be guided by small double-stranded RNA (dsRNA) including exogenous small interfering RNAs (siRNAs; Figure 5) or endogenous microRNAs (miRNAs). In the nucleus, endogenous dsRNAs with the imperfectly matched sequence to the target mRNA (Bernstein *et al.*, 2001), in form of primary miRNAs (pri-miRNAs), are processed by Drosha to the precursor miRNAs (pre-miRNAs). Pre-miRNAs are subsequently transported to the cytoplasm (He & Hannon, 2004; Kim & Rossi, 2007). In the cytoplasm, the pre-miRNAs are shortened and processed by the endonuclease Dicer (RNAse III enzyme) to produce the mature miRNAs. Then, the mature miRNAs proceed with the RNAi process in the cytoplasm similar as the process of exogenous short hairpin RNAs (shRNAs) or dsRNA, which have perfectly complementary sequence to the target mRNA.

In the cytoplasm, both the miRNA and shRNA are processed by Dicer to the siRNAs or miRNAs. They are 21-23 nucleotides (nt) -long with 2-base 3' overhangs. Afterward, the Ago2-RISC complex (Argonaute 2 - RNA-induced silencing complex) is activated by binding with the guide/antisense strand of siRNA or miRNA and meanwhile the passenger or sense strand is cleaved (siRNA) or released (miRNA; Matranga *et al.*, 2005). Subsequently, the activated Ago2-RISC complex binds to the mRNA bearing a

perfectly (siRNA) or not perfectly (miRNA) complementary sequence achieving the gene silencing.
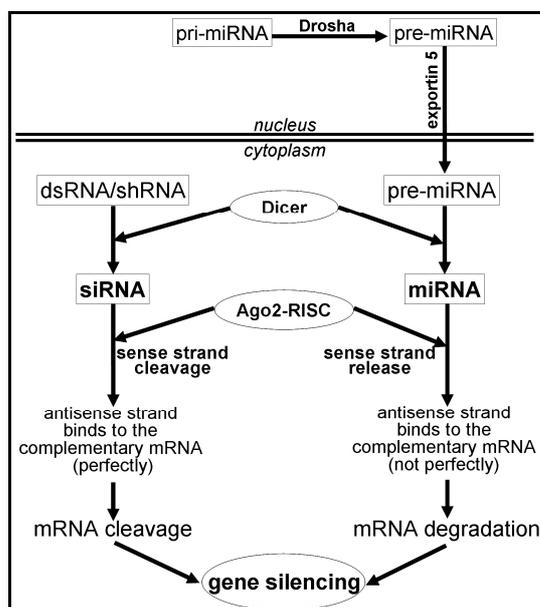
Figure 5: Mechanism of RNAi gene silencing in mammalian cells
RNA interference pathway is initiated with the exogenous dsRNA/shRNA or endogenous pri-miRNA, followed by various processes, e.g., the Dicer cutting, RISC processing, passenger/ sense strand cleavage or release, and the targeting mRNA cleavage or degradation to achieve the silencing of the target gene. This figure is modified based on de Fougerolles *et al.* (2007).

In the siRNA pathway, the silencing of gene expression is implemented by cleaving the mRNA strand between the nucleotides that are complementary to nucleotides 10 and 11 of the guide strand relative to the 5'-end (de Fougerolles *et al.*, 2007) The synthetically produced siRNAs are able to mediate gene silencing in mammalian system on any given target mRNA molecule (Caplen *et al.*, 2001; Elbashir *et al.*, 2001). The main advantage of using siRNAs is the ability to control the amount of transfected molecules and thereby their subsequent uptake into RISC. These characteristics might have a large impact on the putative off-target and anti-viral effects that partly depend on the siRNA concentration. In contrast, the relatively short duration of achieved gene silencing is the drawback of the siRNA usage. To target certain genes, siRNAs base-paired to mRNAs of the target genes must be designed following various rules (InvivoGen, 2003; LifeTechnologies, 2003). The designed siRNAs can be chemically synthesized and can be ordered from numerous commercial companies, sometimes with proprietary chemical modifications to ensure better RNAi results.

1.3.2 Mouse models of inflammatory diseases after *Toxoplasma gondii* infection

TFFs are known to be typically expressed during inflammatory conditions. Here, two mouse models for inflammatory diseases after *T. gondii* infection were investigated concerning the expression of TFFs and the influence of Tff-deficiency (Tff^{KO} mice): (i) mouse model of induced ileitis after oral *T. gondii* infection (Dunay *et al.*, 2008) and (ii) mouse model of induced encephalitis after i.p. *T. gondii* infection (Händel *et al.*, 2012).

Life cycle of *T. gondii*

T. gondii, first identified in *Ctenodactylus gundi* (Nicolle & Manceaux, 1908) and in rabbit (Splendore, 1908), is an obligate intracellular protozoan parasite that can invade and replicate in almost all nucleated cells in the host and causes toxoplasmosis (Dubey, 2008). Toxoplasmosis ranges from 15-85% in its worldwide prevalence and is estimated to be the third leading cause of food related deaths in the USA following salmonellosis and listeriosis (Mead *et al.*, 1999). During disease progression after *T. gondii* infection, tissue cysts are formed followed by multiplication of the parasites within the host cell cytoplasm (Hutchison *et al.*, 1970). There are three infectious stages including the tachyzoites (aggregate in any cell), the bradyzoites (in tissue cysts) and the sporozoites (in oocysts; Dubey *et al.*, 1998). Infection with *T. gondii* can be acquired through different ways: congenital infection with tachyzoites (Wolf *et al.*, 1939), ingestion of tissue cysts (Sabin & Olitsky, 1937) or food/water contaminated with oocysts (Frenkel *et al.*, 1970; Dubey *et al.*, 1998). After infection in the host, *T. gondii* is able to cross the intestinal epithelial barrier (Bates, 2006), the placenta (Havelaar *et al.*, 2007), as well as the blood–brain barrier (Feustel *et al.*, 2012) and disseminate rapidly throughout the body (e.g., muscle, blood), and especially into the brain.

The life cycle of *T. gondii* can be divided into feline (definitive host) and non-feline (intermediate host) infections, correlated with the sexual and asexual replication respectively (Figure 6). The sexual cycle of *T. gondii* begins when its definitive feline host ingests the *T. gondii* at any of the stages. After the ingestion, the parasites infect the epithelial cells in the ileum and then form zygotes fusing the extremely long-lived oocysts. Subsequently, oocysts are sporulated and shed from the feline intestines, whereby completing the sexual cycle (Dubey *et al.*, 1970, 1998). The ingestion of sporulated oocysts by intermediate hosts starts the asexual lifecycle of *T. gondii*, which consists of two distinct stages depending on whether the infection is in the acute or chronic phase (Black et al., 2000). In the acute phase, the sporulated oocysts transform into the rapidly proliferating tachyzoites and can enter all nucleated cells. The tachyzoites replicate rapidly, ultimately lead to cell death, disseminate to neighboring cells and spread through all tissues of the intermediate host, establishing infection (Radke & White, 1998). The immune response of the host can facilitate the differentiation of the tachyzoite to the bradyzoite, the slow replicating form of the parasite (Weiss & Kim, 2000). Bradyzoites can cluster and form tissue cysts localized predominantly in the CNS and muscle tissue of the host. This development of tissue cysts defines the chronic stage of the asexual cycle. Bradyzoites can reside in tissue cysts for the lifetime and can also be released by a dropping in the immune pressure and redifferentiated back into tachyzoites, thereby completing the asexual cycle. The conversion from bradyzoites back to tachyzoites frequently happens in immunocompromised individuals (Luft *et al.*, 1983; Wong, 1984) and can also happen when cysts are ingested through eating the infected or contaminated tissues and ruptured within the intestine of hosts.
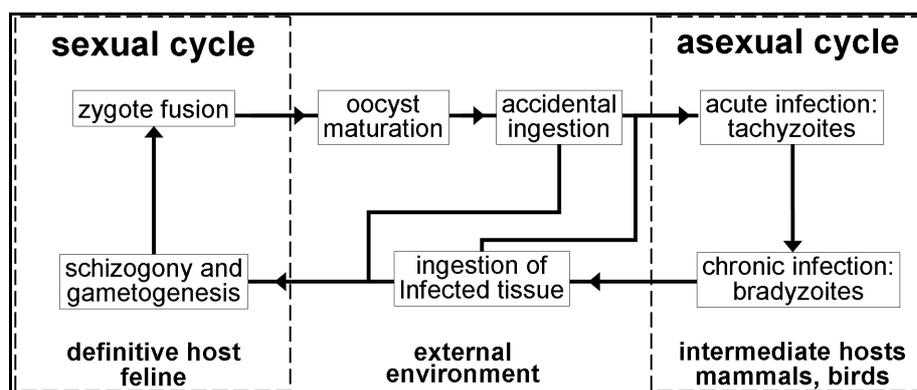
Figure 6: Life cycle of *T. gondii*
The sexual cycle is initiated when a member of the feline family ingests either oocysts or tissues that are infected with bradyzoite cysts. Following oocyst maturation (activated after being excreted from the cat), the oocysts become highly infectious and survive in the environment for months to years. Any warm-blooded animal that ingests these infectious oocysts becomes a host for the asexual cycle. Upon ingestion of these tissue cysts in raw or undercooked meat from a chronically infected host, the bradyzoites will infect the intestinal epithelium of the next susceptible host and differentiate back to the tachyzoite stage to complete the asexual cycle. If the ingesting animal is a cat, the bradyzoites can differentiate into the sexual stages, thereby completing the full lifecycle. The figure is modified based on Black & Boothroyd (2000).

Mouse models to study the immune response to *T. gondii* infection

As one of the most prevalent and successful parasite, *T. gondii* has been used as a model of intracellular pathogen to discover basic mechanisms of immune regulation and function in the host. Murine models of *T. gondii* infection, most often used for *T. gondii* studies, demonstrate the indispensability for the medical progress in the treatment of toxoplasmosis in human (Hunter *et al.*, 1994; Liesenfeld, 2002; Dunay *et al.*, 2010; Subauste, 2012).

There are three clonal lineages of *T. gondii*, designated type I, II and III strains that predominate in North America and Europe (Dubey *et al.*, 1970; Howe & Sibley, 1995; Sibley *et al.*, 2002) covering approximately 90% of the *T. gondii* isolates (Peyron *et al.*, 2006). Each type shows a different virulence and epidemiological pattern of infection (Vaudaux *et al.*, 2010). Type II strains (e.g., DX-strain, ME49-strain) are the predominant lineages causing toxoplasmosis in humans (Howe & Sibley, 1995) and are avirulent in murine infections. Type III strains are also avirulent, whereas the type I strains are highly virulent (uniformly lethal to mice; Howe & Sibley, 1995; Sibley *et al.*, 2002). Not only the strain of *T. gondii* but also the parasite stage, the genetic background of mice, the dose of inoculum and the inoculation route of infection are critical for the outcome of infection (Johnson, 1984; Blackwell *et al.*, 1993). To mirror the course of natural infection in immunocompetent humans, commonly the mouse-avirulent (type II) strains with cysts number between 1 and 20 are used for the infection (Dunay *et al.*, 2008; Munoz *et al.*, 2011). The natural infection of *T. gondii* is through the oral route by ingestion of the undercooked meat containing cysts or water/food contaminated with cysts or oocysts. Thus the oral infection of susceptible mice with *T. gondii* is the approach closest to the actual situation and will result in Th1-type immunopathology in the ileum. Although the natural route of infection with *T. gondii* is not intraperitoneal, the i.p. infection model has the advantage of allowing

15

direct access to the site of primary infection. Thus i.p. infection is also wildly used in the mouse model of *T. gondii* infection.

After *T. gondii* infection (either oral or i.p.), mice develop an acute infection (an acute phase, typically until 14 days after infection) followed by a chronic progressive infection (the chronic/latent stage), in which the parasites establish themselves in cysts, mainly in the CNS (Munoz *et al.*, 2011). Both the acute and chronic infections stimulate production of high levels of IL-12 and IFN-γ by cells of the innate immune system (Yap & Sher, 1999; Waree, 2008; Miller *et al.*, 2009; Dunay & Sibley, 2010; Figure 7). These two cytokines are essential for resistance to *T. gondii* infection and ultimately initiate the adaptive Th1 immune response (Denkers & Gazzinelli, 1998). Macrophages, neutrophils and DCs have been shown to produce IL-12 in response to parasites or antigens. DCs are the most significant source of IL-12 production after *T. gondii* infection (Liu *et al.*, 2006). They play a central role in T-cells antigen presentation and direct polarisation towards the Th1 adaptive response, as well as the production of IFN-γ (Miller *et al.*, 2009). Moreover, IL-1β is also required for IL-12 to stimulate natural killer (NK) cells to produce IFN-γ (Hunter *et al.*, 1995), which is also secreted by CD4+ and CD8+ T-cells (Bliss *et al.*, 2000; Dunay & Sibley, 2010). Thus, *T. gondii*-induced IFN-γ production is largely IL-12-dependent and plays an important role for the regulation of IL-2 and TNF-α as co-factors (Gazzinelli *et al.*, 1993a, 1993b, 1994; Hunter *et al.*, 1994; Tait & Hunter, 2009). IL-2 produced by CD4+ T-cells is an important T-cell mitogen and can enhance NK cell expansion (Kobayashi *et al.*, 1989; D'Andrea *et al.*, 1992; Denkers & Gazzinelli, 1998; Tait & Hunter, 2009). TNF-α is essential for the activation of macrophages and is released by monocytes, T-lymphocytes, as well as macrophages themselves (Stafford *et al.*, 2002). The pro-inflammatory effects of the *T. gondii* induced Th1 cytokines (e.g. IFN-γ, IL-2 and TNFα) are eventually inhibited by the anti-inflammatory cytokines (e.g., IL-10 and TGF-β) that suppress the inflammatory damage from the *T. gondii* infection (Wilson *et al.*, 2005; Miller *et al.*, 2009; Saraiva & O'Garra, 2010).

During the course of oral infection with *T. gondii* (Figure 7), bradyzoites are first released from the cysts in the intestine and then convert to tachyzoites, and move through the intestinal epithelium by infecting enterocytes. These enterocytes secrete chemokines and cytokines such as IL-12, chemokine (C-C motif) ligand (CCL) 3 and CCL4 that attract neutrophils, macrophages and help in DCs maturation, resulting in ileitis and ultimately initiating the Th1 immune response in the host (Miller *et al.*, 2009). After having passed through the intestinal epithelium, the parasites proceed into the CNS, localize in the brain and finally initiate the encephalitis.

In contrast to oral infection, i.p. infection-mediated encephalitis is caused without direct invasion of the intestinal epithelium but by spreading through blood vessels of the peritoneum. Thus, an ileitis is not arising in the early phase of i.p. infection.
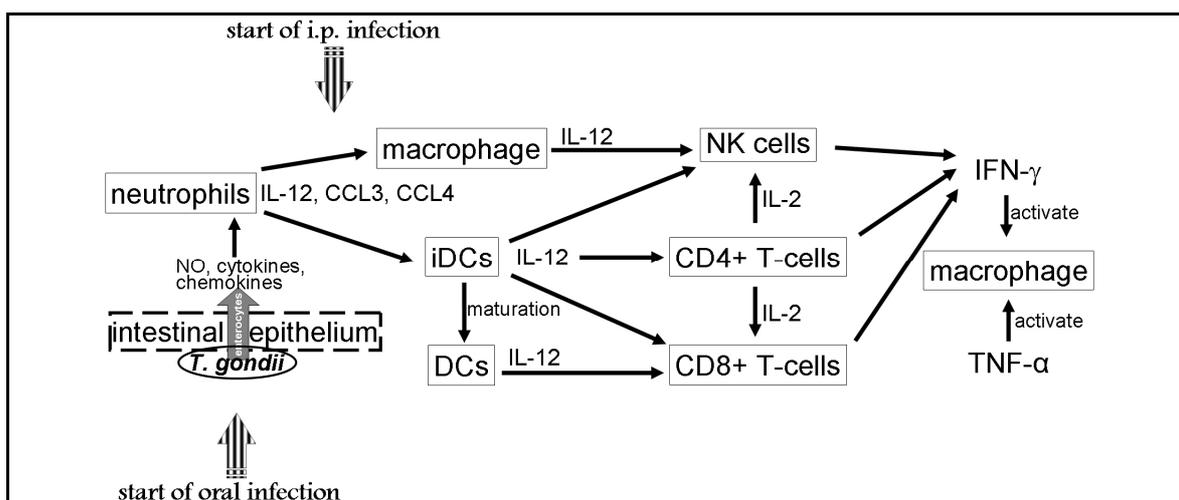
Figure 7: Innate immune responses after *T. gondii* infection
The immune responses of oral *T. gondii* infection start with the invasion of enterocytes in the intestinal epithelium and then followed by a series of Th1 immune responses. Of note, the intestinal epithelium is not involved after i.p. infection with *T. gondii*. After the i.p. infection, the parasites first activate the macrophage or DCs directly by spreading through blood vessels and induce the Th1 immunity. DCs: dendritic cells, NK cells: natural kill cells. This figure is modified from Waree (2008) and Miller *et al.* (2009).

1.3.3 Expression of Tffs in primary cell cultures from rat brain

Thus far, the cellular localization of TFFs in the brain is still unclear. In order to gain more insights which cells of the CNS express TFFs at least *in vitro*, different primary cell culture from rat brain were investigated by RT-PCR analysis and immunohistochemistry. First, neural cell cultures containing mix cell population of neuron and glial cells (Goslin *et al.*, 1998) were analyzed. Second, a glial cell-enriched population (Guizzetti & Costa, 1996) was studied.

1.4 Aims of this study

Generally, this study was designed to gain insight into the expression and function of TFFs in the GI tract and CNS considering four different aspects. The aims of the four projects outlined in chapter 1.3 were as follows:

(1) to gain new insights into the expression of TFFs after *in vitro* wounding of RGM-1 cells and to analyze the expression profile of stationary and migratory cells and investigate the role of TFF1 by the help of RNAi;

(2) to gain new insights into the expression of TFFs in the intestine during inflammatory conditions in a mouse model of induced ileitis after oral *T. gondii* infection and to investigate the phenotype of Tff3^{KO} mouse in this model;

(3) to gain new insights into the expression of TFFs in the brain during inflammatory conditions in a mouse model of induced encephalitis after i.p. *T. gondii* infection and to investigate the phenotype of different Tff^{KO} mice in this model;

(4) to gain new insights into which cell types cells (neurons, astrocytes, microglial cells) express TFFs in primary cell cultures from rat brain.

2 Materials

2.1 Cell culture

2.1.1 Materials

Application	Description	Cat.-No.	Producer
Cell cultivation	CELLLSTAR® 6/24 well cell culture multiwell plates	6xx160	Greiner Bio-One, Frickenhausen
	CELLLSTAR® 12/48/96 well cell culture multiwell plates	6xx180	
	CELLSTAR® standard cell culture Flasks 50/250 ML, 25/75 cm²	6xx170	
	CELLSTAR® cell culture dishes, 100 X 20 mm	664160	
	Corning® cell lifter	3008	Corning® Inc. Costar, MA, USA
	Sterile glass cover slips, 22x22 mm	BB02202 2A1	Gerhard Menzel, Braunschweig
	Microscope cover slip circles, 12 mm	CB00120 RA1	
	BD falcon™ conical tubes, 15, 50 mL	352096	BD Biosciences, Heidelberg
Pipettes and tips	SafeSeal tips premium 1000/100/10 µl, sterile	692xxx	Biozym Biotech Trading, Oldendorf
	Serological pipettes 1 mL, 2 mL, 5 mL, 10 mL, 25 ml	612-12xx	VWR International, Darmstadt
	Tips 10 µL, 50 µL, 100 µL	0300 xxx.xxx	Eppendorf AG, Hamburg
	Tips 2 µL, 200 µL, 1000 µL	D10,200, 1000	Gilson, Limburg

2.1.2 Media and reagents

Application	Description	Cat.-No.	Producer
Media	DMEM high glucose (4.5 g/L)	E15-009	GE Healthcare Life Sciences/PAA GmbH, Cölbe
	Leibovitz´s L-15	E15-020	
	Neurobasal® medium (1X), liquid	21103-049	Life Technologies GmbH, Darmstadt
Reagents	Dulbecco's PBS (1x)	H15-002	GE Healthcare Life Sciences/PAA GmbH, Cölbe
	Fetal bovine serum gold (FBS)	A15-151	
	MycoKill (50x)	P11-016	
	G418-BC (100x)	A 2912	Biochrom AG, Berlin
	NEA-Non essential amino acids(100x)	K 0293	
	Sodium pyruvate 1 mM	L 0473	
	HBSS Hanks´s balanced salt solution	14170	Life Technologies GmbH, Darmstadt
	L-glutamine (200 mM)	25030-081	
	BSA (Bovine Serum Albumin)	15561-020	
	Opti-MEM® I reduced serum medium	31985-047	

Application	Description	Cat.-No.	Producer
Reagents	B-27® Serum-free supplement (50X)	17504-044	Life Technologies GmbH, Darmstadt
	Lipofectamine® 2000 transfection teagent	11668-027	
	0.25% Trypsin-EDTA (1X),PhenolRed	25200-056	
	0.05% Trypsin-EDTA (1X),PhenolRed	25300-054	
	L-glutamine solution	59202C	Sigma-Aldrich Chemie GmbH, München
	Penicillin-streptomycin solution stabilized (100x)	P 4333	
	Trypsin inhibitor from glycine max	T6522	
	Poly-D-lysine hydrobromide	P7280	
	Deoxyribonuclease I	DN25	

2.2 Basic experiments

2.2.1 Extraction

Applications	Description	Cat.-No.	Producer
Tissue preparation	Sterile disposable scalpel standard	No. 10	FEATHER Safety Razor Co., Ltd. PFM, Köln
RNA, DNA and protein Extraction	TRIzol® reagent	10296 -028	Life Technologies GmbH, Darmstadt
	ISOLATE RNA mini Kit	BIO -52073	Bioline GmbH, Luckenwalde
	Complete protease inhibitor cocktail tablets	0469311 6001	Roche, Mannheim
	Guanidine hydrochloride	0037.1	Carl Roth GmbH, Karlsruhe
	Invisorb® spin tissue mini kit	1032100 300	STRATEC Molecular GmbH, Berlin

2.2.2 RT-PCR

Applications	Description	Cat.-No.	Producer
Concentration determination	Semi-micro plastic UV-cuvettes	Y199.1	Carl Roth GmbH, Karlsruhe
	Cuvettes for absorption measurements	6040-UV-10-531	Hellma GmbH & Co. KG, Müllheim
	Bio-Rad protein assay dye reagent concentrate	500-0006	Biorad, München
	BCA (bicinchoninic acid) protein assay reagent	23225	Thermo Fisher Scientific, Bonn
Reverse transcription	RiboLock RNase-inhibitor	EO0384	Thermo Fisher Scientific, Bonn
	DNase I, RNase-free	EN0521	
	RevertAid H minus reverse transcriptase	EP0452	
	dNTP set	R0181	
	Oligo(dT)18 primer	SO132	
	Safe-lock tubes 0,5/1.5/2 mL	0030-120	Eppendorf AG, Hamburg
	Safe-lock tubes, biopur, 0,5/1,5 mL	0030-121	

Applications	Description	Cat.-No.	Producer
PCR	PCR-oligos (primers)		Metabion, Martinsried
	DreamTaq green DNA Polymerase	EP0714	Thermo Fisher Scientific, Bonn
	Mineral oil	M5904	Sigma-Aldrich Chemie Gmbh, München
	PCR- reaction tubes, 200 µL	GS001- x	Kisker Biotech GmbH & Co. KG, Steinfurt

2.2.3 Western blotting

Applications	Description	Cat.-No.	Producer
Western blotting	Gel-blotting paper BF2	FT-2-519 -580600N	Sartorius AG, Göttingen
	Luminol p-Cumaric acid	123072 537-98-4	Sigma-Aldrich Chemie Gmbh, München
	Protein-marker I	27-1010	Peqlab Biotechnologie GmbH, Erlangen
	Whatman PROTRAN BA79 nitrocellulose transfer membrane	10402096	Whatman, Dassel
	Ponceau S	1142750 010	Merck, Darmstadt
Gel electrophoresis	Agarose gel for DNA electrophoresis research	11404.05	Serva, Heidelberg
	1% Ethidium bromide solution (10 mg/mL)	331564	Merck, Darmstadt
	GeneRuler™ 1kb Plus DNA ladder, ready-to-use 6x Loading dye	SM1333	Thermo Fisher Scientific, Bonn
	Rotiphorese$^{®}$ Gel 30 (30% acrylamide/ bisacrylamide = 37.5:1.)	3029.1	Carl Roth GmbH, Karlsruhe
	TEMED	2367.3	
	APS (Ammonium persulfate)	9592.3	

2.2.4 Immunostaining

Description	Cat.-No.	Producer
Goat serum	B15-035	PAA GmbH, Cölbe
Dako fluorescent mounting medium	S 3023	Dako GmbH, Hamburg
Triton™ X-100	100-155	Sigma-Aldrich Chemie Gmbh, München
Sodium azide (NaN_3)	S 2002	
Horse serum	H0146	
HEPES (4-(2-hydroxyethyl)piperazine-1-ethanesulfonic acid)	H3375	
Saponin	47036	
BSA (bovine serum albumin)	A7888	
DPX mountant	44581	
Tris ultrapure	A1086	AppliChem GmbH, Darmstadt
EDTA (ethylenediamine tetraacetic acid · Na_2-salt)	11280	SERVA Electrophoresis GmbH, Heidelberg
PFA (paraformaldehyde)	0335.2	Carl Roth GmbH, Karlsruhe

Description	Cat.-No.	Producer
D(+)-saccharose/sucrose	4621.1	Carl Roth GmbH, Karlsruhe
Sodium periodate	2603.2	
Boric acid	5935	
Gelatine	4274.1	
L-Lysine hydrochloride	1700.2	
Methanol	P717.2	
Ethanol	0342.2	
Mowiol 4-88	0713.2	
VECTASTAIN® Elite ABC Kit	PK-6100	BIOZOL Diagnostica Vertrieb GmbH, Eching
Tissue-Tek® O.C.T™ Compound	4583	Sakura Finetek GmbH, Staufen

2.3 Peptides and antibodies

2.3.1 Synthetic peptides and antiserum

Two antisera (anti-mTff1-1 and anti-rTff3-2) raised against synthetic peptides were used in this study. The peptides were both provided by Dr. H. Kalbacher and they present partial sequences of mouse Tff1 (Karam *et al.*, 2004) or rat Tff3 (GenBank® accession No.: NP_037174.2; see below). The peptides were purified using reversed phase-HPLC and their identities were confirmed by MALDI-MS (matrix-assisted laser desorption/ionization mass spectrometry), then coupled to KLH (keyhole limpet hemocyanin) via glutaraldehyde and used to immunize rabbits (Charles River Laboratories, Sulzfeld).

Affinity purification of anti-mTff1-1 was performed as described previously (Wiede *et al.*, 1999). Briefly, the mTff1 peptide was coupled to BSA via glutaraldehyde, diluted to 20 mg/mL with PBS and loaded onto nitrocellulose membranes for 5 h at room temperature. The membranes were washed with PBS and residual protein binding capacity was blocked by incubation with 5% normal goat serum in PBS for 30 min. Then, loaded membranes were incubated with antiserum anti-mTff1-1 diluted 1:50 in 5% normal goat serum in PBS supplemented with 0.1% sodium azide overnight at room temperature. After a washing with PBS, bound antibodies on the membranes were eluted with 0.2 M glycine–HCl buffer/pH 2.5 (containing 150 mM NaCl and 1 mg/mL BSA) for 30 min. Eluted antibodies were neutralized by adding 1/10 of volume 2 M Tris-base/pH 8.0 and dialyzed against PBS overnight at 4°C. Finally, purified antibodies were concentrated by ultrafiltration using Vivaspin tubes (GE Healthcare Europe GmbH, Freiburg). The affinity-purified antiserum anti-mTff1-1 was tested via ELISA for reactivity against the BSA conjugate or synthetic peptide.

Description	Sequences	Source
Tff1 peptide, representing the C-terminus of mouse Tff1	FHPMAIENTQEEECPF (1-16)	H. Kalbacher (Karam *et al.*, 2004)
Tff3 peptide, representing rat Tff3	Whole rat Tff3 peptide sequence (1-59)	H. Kalbacher (GenBank® accession No.: NP037174.2)

2.3.2   Primary antibodies

Antiserum	Description	Size kDa	Origin	Dilution	Species Reactivity	Source /Cat. Nr
anti-Actin (20-33)	N-terminal region universal for all actins	42	rabbit polyclonal	WB: 1:50 - 200 IF: ---	Human, Rat, Mouse	Sigma-Aldrich, München /A5060
anti-Human beta Actin (N-21)	N-terminal region	42	rabbit polyclonal	WB: 1:200 IF: ---	Human, Mouse	Santa Cruz, Heidelberg / sc-130656
anti-mTff1-1	against sequence: FHPMAIENTQEEE CPF	6.7	rabbit polyclonal	WB: 1:1000 IF: 1:500	Mouse Rat	Fu et al. (2013)
anti-rTff3-2	against sequence: rat Tff3 protein sequence 1-59	6.6	rabbit polyclonal	WB: 1:2000 IF: 1:500	Rat Mouse	IMMC
anti-MAP2	specific for all forms of MAP2 (a, b, c)	280	mouse monoclonal	IF: 1:500	Human Rat Mouse, etc.	Sigma-Aldrich, München /M4403
anti-GFAP	against full length native protein	~50	chicken polyclonal	IF: 1:1000	Human Rat Mouse, etc.	Abcam, Cambridge, UK ab4674 ab5076
anti-Iba-1	against sequence: CTGPPAKKAISELP (135-147)	17	goat polyclonal	WB: 1:1000 IF: 1:500	Human Rat Mouse, etc.	
anti-Iba-1	against Iba1 C-terminal sequence	17	rabbit polyclonal	WB: 1:1500 IF: 1:1000	Human Rat Mouse	Wako Chemicals GmbH,Neuss 019-19741
anti-*Toxoplasma gondii*	stains *Toxoplasma gondii* by immunohistoemical techniques	---	rabbit polyclonal	WB: --- IF: 1:1000	Human Rat Mouse, etc.	BioGenex, CA, USA PU125-UP

2.3.3   Secondary antibodies

Antiserum	Origin	Dilution	Cat. Nr	Producer
Biotinylated goat anti-rabbit IgG antibody		WB: 1:2000	BA-1000	Biozol Diagnostica Vertrieb GmbH, Eching
Peroxidase anti-rabbit IgG(H+L)	goat	WB: 1:4000	PI-1000	
Alexa Fluor® 488 anti-rabbit IgG (H+L)	goat	IF: 1:1000	A-11008	Invitrogen, Life Technologies GmbH, Darmstadt
anti-goat IgG (H+L)-Cy3	donkey	IF: 1:500	705-165-003	Dianova, Hamburg
DyLight™ 649 anti-chicken	donkey	IF: 1:1000	703-496-155	
anti-chicken IgG (H+L)-Cy3	donkey	F: 1:1000	703-165-155	
anti-mouse IgG (H+L)-Cy3	donkey	IF: 1:1000	715-165-150	
anti-rabbit IgG whole molecule F(ab´)₂ fragment-**Cy3**	goat	IF: 1:100-200	C2306	Sigma-Aldrich, München
DAPI (4',6-Diamidino-2-Phenylindole Dihydrochloride)		IF: 1:1000	D9542	

2.4 Animals

2.4.1 Transgenic mice

Three different transgenic mice were used in this study, i.e., Tff1-deficient mice (Tff1^{KO} mice), Tff2-deficient mice (Tff2^{KO} mice) and Tff3-deficient mice (Tff3^{KO} mice). The result for the weight control experiment is present in the Appendix I (on page i).

2.4.1.1 Tff1-deficient mice (Tff1^{KO} mice)

Tff1-deficient mice were generated by Lefebvre et al. (1996) and kindly provided by Dr. M.-C. Rio: To inactivate the mouse Tff1 gene, a targeting vector was constructed by inserting the *neomycin* resistance gene (*neo*) cassette into exon 2 of mTFF1 to achieve the disruption (Figure 8) and was electroporated into D3 embryonic stem (ES) cells (129S2/SvPas). C57BL/6J blastocysts microinjected with one positive clone were reimplanted in pseudo gestante females to generate the chimeric male. Then the mutant allele was transmitted to offspring by mating the generated chimeric male with 129/Svj females, yielding Tff1$^{+/-}$ heterozygotes. These mice were subsequently mated to yield Tff1$^{-/-}$ homozygous (Tff1^{KO}), as well as Tff1$^{+/+}$ homozygous (wild type). They were used as Tff1-deficient mice and wild type mice, respectively, in this study.
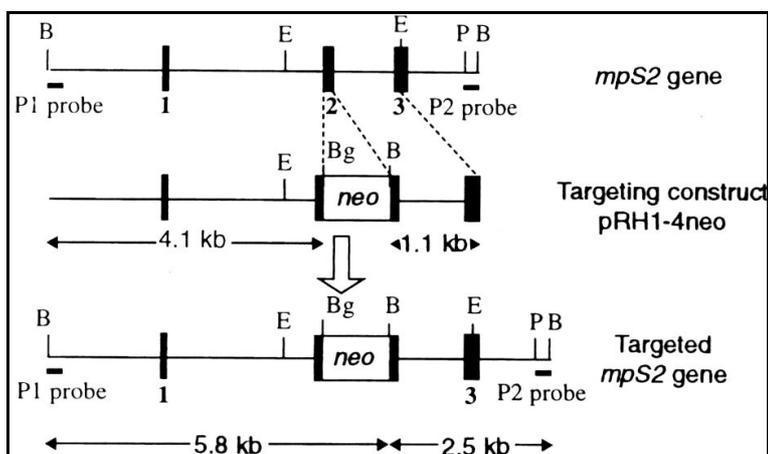
Figure 8: Targeting strategy of the mTFF1 gene (Lefebvre et al. 1996)

2.4.1.2 Tff2-deficient mice (Tff2^{KO} mice)

Tff2-deficient mice were generated by Baus-Loncar *et al.* (2005b) and kindly provided by Prof. N. Blin: To inactivate the mouse Tff2 gene, targeting vector was constructed by replacing exon 1 and exon 2 of mTFF2 (encoding one functional Tff2 domains) with *neo* gene cassette (Figure 9) and electroporated into AB2.2 (129SvEv) ES cells. After microinjection of the positive clone into blastocysts from C57BL/6, high percentage chimaeric mice were obtained. Subsequently, germline transmission of the disrupted Tff2 allele was generated and confirmed. Without adverse effects on ability of reproduction, the Tff2$^{-/-}$ homozygous (Tff2^{KO}) were subsequently reproduced and also used for this study.
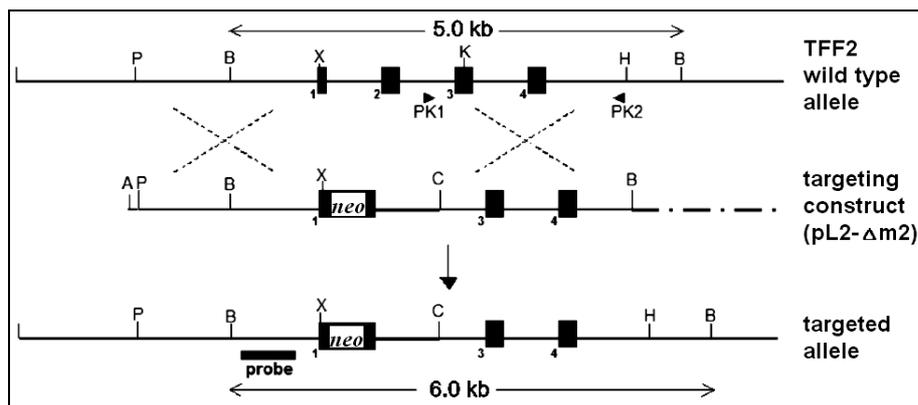
Figure 9: Targeting strategy of the mTFF2 gene (Baus-Loncar *et al.*, 2005b)

2.4.1.3 Tff3-deficient mice (Tff3^{KO} mice)

Tff3-deficient mice were generated by Mashimo et al. (1996): The targeting vector, in which the entire exon 2 of mTff3 gene (encoding most of the TFF domain) was replaced with the *neo* gene cassette (Figure 10), was homologous recombinated in J1 ES cells (129/Sv-Aguti). The original strain of the Tff3$^{-/-}$ mice (Tff3^{KO}) was kindly provided by Prof. D.K. Podolsky (Harvard Medical School), which have a mixed background of 129/Sv and C57BL/6 (Lubka *et al.*, 2008; Blaschke, 2010). After backcrossing these Tff3$^{+/-}$ heterozygotes (homozygous sister lines) for more than 10 generations, Tff3$^{+/+}$ mice (wild type strain) as well as Tff3$^{-/-}$ mice (TFF3^{KO}) were obtained with the same genetic background and were used for this study. The pedigree for the backcrossing culture is presented in the Appendix II (on page ii).
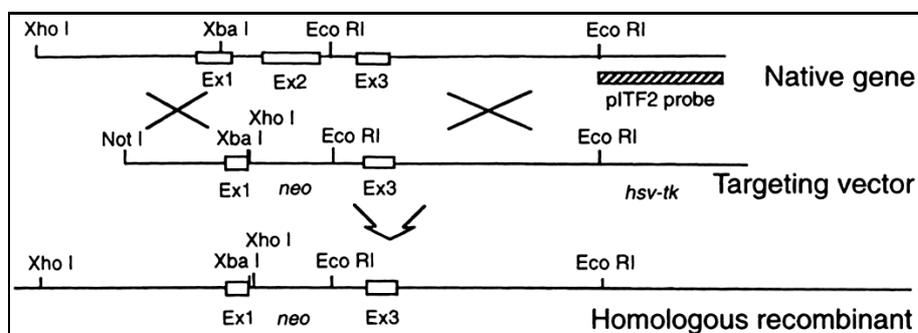
Figure 10: Targeting strategy of the mTFF3 gene (Mashimo *et al.*, 1996)

2.4.2 Materials

Description	Cat.-No.	Producer
Normal saline, 0.9% NaCl	89167-772	VWR International, Darmstadt
Tweezers and scissors	-----	
BD butterfly needles	367344	BD Biosciences, Heidelberg
BD Falcon® cell strainers	3523x0	
Sterile disposable scalpel standard	No. 10	FEATHER Safety Razor Co., Ltd. PFM, Köln

2.5 Transformation and transfection

Description	Cat.-No.	Producer
Competent cells E. coli TOP10	5-1600-020	IBA GmbH, Göttingen, Germany
pGEM®-T easy vector system I	A1360	Promega GmbH, Mannheim, Germany
HotStar HiFidelity polymerase kit	202602	Qiagen, Hilden, Germany
QIAquick gel extraction kit	28706	
pIRES vector	631605	Takara Bio Europe/Clontech Saint-Germain-en-Laye, France
JetStar® plasmid mini prep kit	200200	Genomed GmbH, Löhne
BD Falcon™ round bottom tubes, 5 mL PS with cap	352003	BD Biosciences, Heidelberg
LB broth (lennox)	L7275	Sigma-Aldrich Chemie Gmbh, München
LB broth with agar (lennox)	L7025	
IPTG (isopropyl β-D-1-thiogalactopyranoside)	16758	
Ampicillin sodium salt	A9518	
SOC medium	BIO-86033	Bioline GmbH, Luckenwalde
Glycerol from plant (glycerin)	23176	SERVA Electrophoresis GmbH, Heidelberg
Calcium chloride/$CaCl_2$	CN93.2	Carl Roth GmbH, Karlsruhe
X-gal (5-Bromo-4-chloro-3-indolyl-beta -D-galactopyranoside, light prevented)	203782	Merck Chemicals GmbH, Schwalbach
T4 DNA ligase	M0202S	New England Biolabs GmbH, Frankfurt am Main
Restriction enzymes	RxxxxS	
Sterile plastic loop	510-1001-STR	Elkay Products, Inc., Massachusetts, USA

2.6 Stealth RNAi duplexes

Stealth RNAi™ compounds, provided from Invitrogen, are 25-mer dsRNA molecules containing proprietary chemical modifications that enhance nuclease stability and reduce off-target effects by limiting sense strand activity (Carstea *et al.*, 2005). The three rat Tff1 stealth RNAi™ and the negative control duplexes used in this study had the following sequences:

Name	Cat. No.		Sequence	Nucleotide positions	GC%
rTff1-siRNA1	Tff RSS 350528	sense anti-sense	CAUGGUGCUUCCGACCUCUGGUCAU AUGACCAGAGGUCGGAAGCACCAUG	218-242	56.01% Hi GC
rTff1-siRNA2	Tff RSS 350530	sense anti-sense	CCAGAACCAGGAAGAAACAUGUGCC GGCACAUGUUUCUUCCUGGUUCUGG	93-117	52.00% Hi GC
rTff1-siRNA3	Tff RSS 350529	sense anti-sense	GCAAGAAGAAGAAUGUCCCUUCUAA UUAGAAGGGACAUUCUUCUUCUUGC	252-276	40.00% Low GC
Negative Control	12935-114	sense anti-sense	GGUAGGUGAGUGUACAGACGCAAUA UAUUGCGUCUGUACACUCACCUACC		50.00% Hi GC

2.7 Equipment and software

Devices/Function	Description	Producer/Distributor
Homogenization	Precellys 24	Peqlab Biotechnologie GmbH, Erlangen
	Ultraturrax T25 basic	IKA Werke GmbH, Staufen
Heating/shaking/ stirring	Thermomixer	Eppendorf AG, Hamburg
	IKA magnetic stirrer COMBIMAG REO Magnetic stirrer RCT bank	IKA Werke GmbH, Staufen
	Innova® 4200 incubator shaker	New Brunswick Scientific, Edison, NJ, USA
Concentration measurement	NanoDrop ND-1000 Spectrophotometer	Thermo Fisher Scientific, Bonn
	Libra S12 spectrophotometer	Biochrom Ltd.,Omnilab, Bremen
Gel electrophoresis	Agagel maxi Casting system compact L/XL	Biometra, Göttingen
	Electrophoresis supplier EPS 3500	Amersham Pharmacia Biotech, Freiburg
	Heinzinger economy line LNG350 06	Herolab, Wiesloch
	Mini-protean PowerPac™ basic power supply	Biorad, München
Microtome	Leica Jung CM3000 cryostat microtome	Leica Mikrosysteme Vertrieb GmbH, Wetzlar
Microwave	Micromat Txp EEH8733	AEG-Elektrolux, Nürnberg
Microscope	Axiovert 40, 135	Carl Zeiss Microscopy GmbH, Göttingen
	Axiophot/axiocam HRC	
	Axio observer.Z1/AxioCamMRm	
	BZ-8000	Keyence, Frankfurt
Objectives and filter	Filterset 01, BP 365 nm +/- 12 nm, FT 395 nm, LP 420 nm	Carl Zeiss Microscopy GmbH, Göttingen
	Filterset 10, BP 450-490 nm, FT 395 nm, LP 397 nm	
	Filterset 15, BP 546 nm +/- 12 nm, FT 580 nm, LP 590 nm	
	Ph1 Plan-NEOFLUAR 10x/0,30	
	Ph2 Plan-NEOFLUAR 20x/0,50	
	Ph3 Plan-APOCHROMAT 63x/1,40	
	Plan-NEOFLUAR 40x/0,75	
PCR/RT	Robocycler gradient 96	Stratagene,Heidelberg
Protein Transfer	Heidolph polymax 1040	Carl Roth GmbH, Karlsruhe
	Heinzinger economy line LNG 350 06	Amersham Pharmacia Biotech, Freiburg
	Semi dry blotter 20 x 20	Biostep, Jahnsdorf
Incubators	Hera cell 150	Haereus, Hanau
	US autoflow	Nuaire, Integra Biosciences GmbH, Fernwald
Safety bench/ laminar flow	Biological safety cabinets class II	Nuaire, Integra Biosciences GmbH, Fernwald
	Hera safe	Haereus, Hannau
Balance	Sartorius analytic A2000S	Sartorius, Göttingen

Devices/Function	Description	Producer/Distributor
Documentation & semi-quantitative analysis	GeneGnome	Syngene Bioimaging Synoptics Ltd., Cambridge, England
	Herolab E.A.S.Y RH3	Amersham *Pharmacia Biotech*, Freiburg
Vortex	Vortex-Genie 2	Carl Roth GmbH, Karlsruhe
Centrifugation	Biofuge primo R	Haereus, Hanau
	Micro centrifuge	Carl Roth GmbH, Karlsruhe
	Mikro 200R Universal 30RF Universal 329R	Hettich Lab Technology, Tuttlingen
Software	AxioVision 3.1 AxioVision release 4.8	Carl Carl Zeiss Microscopy GmbH, Göttingen
	Adobe® photoshop 7.0	Adobe System GmbH, München
	Adobe® Reader® XI	
	GeneTools	Syngene Bioimaging, Synoptics Ltd., Cambridge, UK
	BZ observation application	Keyence, Frankfurt
	Herolab E.A.S.Y Win32	Amersham *Pharmacia Biotech*, Freiburg
	Microsoft® Office 2003	Microsoft Corporation, Redmond, WA, USA

2.8 Oligodeoxynucleotides List

Table 2: RT-PCR analyses of RGM-1 cells (*Rattus norvegicus*)

Genes	Accession No.	Primer No.	Primer Pairs	nucleotide positions	Tm (°C)	Size (bp)
Tff1 **Trefoil factor family 1**	NM_057129.1	MB1547 MB1548	CCCAGAACCAGGAAGAAACA ACCAGTTCTCTCGGATGGAC	92-111 297-278	60	206
Acta2 **Actin, alpha 2 (aortic smooth muscle)**	NM_031004	MB671 MB672	CGATAGAACACGGCATCATCAC TCCAGAGCGACATAGCACAG	257-278 713-694	60	457
Ccna2 **Cyclin A2**	NM_053702.3	MB661 MB662	TGTCTGTGTTAAGAGGAAAGC GTGAAGGTCCATGAGACAAG	796-816 1244-1225	57	449
Birc5 **Survivin/Baculoviral IAP repeat-containing 5**	M_022274.1	MB2270 MB2271	ACCACCGGATCTACACCTTC GTGAAGGTCCATGAGACAAG	51-70 563-544	60	513
Vim **Vimentin**	NM_031140.1	MB673 MB674	TTTCCAAGCCTGACCTCAC GAGAAATCCTGCTCTCCTCC	859-877 1317-1298	60	459
ß-Actin **Actin, beta**	NM_031144.3	MB2158 MB2159	AAGTACCCCATTGAACACGG CAGCTCAGTAACAGTCCGC	280-299 1225-1207	60	946
Pgc **Pepsinogen C**	NM_133284.2	MB1169 MB1170	TGGGTGTCTTCTGTCTACTGC GCATGACGAGCAGAGAGGT	361-381 925-907	60	565
Gkn2 **Gastrokine 2**	NM_001039686.1	MB2164 MB2165	ATGCTCTTCCACCACCATTT GCAGATAGAGATCCCCAGGA	202-221 568-549	60	367
Muc16 **Mucin 16**	XM_235886.7	MB2242 MB2243	CCCCTAGTGGCTATGTACCG AGGGTAGGTTGGTGATGGTG	314-333 766-747	60	453

Genes	Accession No.	Primer No.	Primer Pairs	nucleotide positions	Tm (°C)	Size (bp)
Cxcl2/Sdf-1 **chemokine (C-X-C motif) ligand 12**	NM_022177.3	MB2298 MB2299	CAGAGCCAACGTCAAACATC ACTGGAAAAAGGAGCCTCTG	201-220 912-893	60	712
Lgr5 **Leucine rich repeat containing G protein**	NM_001106784.1	MB1151 MB1152	ACTGGAGCAAAGATCTCGTC TTATTCCGGGCTAAGTTCAG	1006-1025 1226-1207	57	221
Tff3 **Trefoil factor 3**	NM_013042.1	MB1551 MB1552	GACTCCAGCATCCCAAATGT GCAGATCAGGGGTGAGTGTT	198-217 349-330	60	152

Table 3: RT-PCR analyses of mouse tissue (*Mus musculus*)

Genes	Accession No.	Primer No.	Primer Pairs	nucleotide positions	Tm (°C)	Size (bp)
ß-Actin **Actin, beta**	NM_007393.3	MB1912 MB1913	CCCTCACGCCATCCTGCGTC ACGCAGCTCAGTAACAGTCCGC	592-611 1208-1229	60	638
Tff1 **Trefoil factor family 1**	NM_009362.2	MD7 MD8	ATCTGTGTCCTCGCTGTGGT GGGGAAGCCACAATTTATCC	128-145 450-429	57	323
Tff2 **Trefoil factor family 2**	NM_009363.3	MD5 MD6	TTCCACCCACTTCCAAAC AATGCTGTGTCTAGCCACTG	242-259 532-551	57	310
Tff3 **Trefoil factor family 3**	NM_011575.2	MB1847 MB1848	TCTGGCTAATGCTGTTGGTG TCAGATCAGCCTTGTGTTGG	443-424	60	392
Ifnγ **Interferon gamma**	NM_008337.3	MB2054 MB2055	TCCTCCTGCGGCCTAGCTCTG TGGCGCTGGACCTGTGGGTT	83-103 494-475	60	412
Il-12αp35-2 **Interleukin 12 subunit alpha isoform 2**	NM_008351.2	MB2133 MB2134	CACAGTCCTGGGAAAGTCCTG TAGCCAGGCAACTCTCGTTC	9-029 410-391	60	402
Il-1β **Interleukin 1 beta**	NM_008361.3	MB2038 MB2039	GTGGCTGTGGAGAAGCTGTGGC CAGGGTGGGTGTGCCGTCTT	270-291 659-640	60	390
Il-10 **Interleukin 10**	NM_010548.2	MB2154 MB2155	CTGCTCTTACTGACTGGCAT GGAGTCGGTTAGCAGTATGT	95-114 274-255	60	180
Tnfα **Tumour necrosis factor α**	NM_013693.2	MB2052 MB2053	GCAGCCAACCAGGCAGGTTCT ACGTAGTCGGGGCAGCCTTGT	83-103 611-591	60	592
T529 *Toxoplasma gondii* **strain RH repeat region**	AF487550.1 **(T.g./RHrep)**	MB2066 MB2067	ACTACAGACGCGATGCCGCTC CTCTCCGCCATCACCACGAGGAA	107-127 328-306	60	222
Iba1 **Ionized calcium binding adapter molecule 1**	NM_019467	MB1727 MB1728	GGATTTGCAGGGAGGAAAAG GCCACTGGACACCTCTCTAA	329-349 523-243	60	215
Cd4 **T-cell surface glycoprotein CD4 antigen**	NM_013488.2	MB2117 MB2118	ACCCCTTGACAGAGTGCAAA TCCTGATGCAGTGTCCCTTT	630-649 1101-1082	60	472
Cd8 **T-cell surface glycoprotein CD8 antigen**	NM_001081110.2	MB2119 MB2120	CCCGAACTCCGAATCTTTCC CAAACACGCTTTCGGCTC	200-239 806-789	60	587

Table 4: RT-PCR analyses of rat primary cell cultures (*Rattus norvegicus*)

Genes	Accession No.	Primer No.	Primer Pairs	nucleotide positions	Tm (°C)	Size (bp)
Tff1 **Trefoil factor family 1**	NM_057129.1	MB1547 MB1548	CCCAGAACCAGGAAGAAACA ACCAGTTCTCTCGGATGGAC	92-111 297-278	60	206
Tff2 **Trefoil factor family 2**	NM_053844.1	MB45 MB46	GCAGAACACCCAGGTCCAG CTTGGAAAGACACTGTGTC	001-19 556-538	60	556

Genes	Accession No.	Primer No.	Primer Pairs	nucleotide positions	Tm (°C)	Size (bp)
Tff3 **Trefoil factor family 3**	NM_013042.1	MB1551 MB1552	GACTCCAGCATCCCAAATGT GCAGATCAGGGGTGAGTGTT	198-217 349-330	60	152
Map2 **Microtubule-associated protein 2**	NM_013066.1	MB2143 MB2144	CATCATTCGCACTCCTCCAA GAGGAGACATTGCTGAGTCG	MB2143 MB2144	60	462
Gfap **Glial fibrillary acidic protein**	NM_017009.2	MB2145 MB2146	AGGGACAATCTCACACAGGA GGCGATAGTCATTAGCCTCG	416-435 854-835	60	439
Iba1 **Ionized calcium binding adapter molecule 1**	NM_017196.3	MB2141 MB2142	TTGGATGGGATCAACAAGCA ATCTCTTGCCCAGCATCATT	168-187 441-422	60	274

3 Methods

3.1 Cell culture

3.1.1 RGM-1 cells

The non-transformed rat gastric epithelial cell line RGM-1 (Kobayashi *et al.*, 1996), kindly provided by Dr. S. J. Hagen (Boston, USA), was maintained in 75 cm^2 cell culture flasks with filter caps at 37°C in a humidified atmosphere with 5% (v/v) CO_2. DMEM (Dulbecco's modified Eagles medium) with 4.5 g/L glucose was routinely used as cell culture medium and was supplemented with 1% (v/v) 100x non-essential amino acids, 1 mM sodium pyruvate, 2 mM glutamine (see below), and 10% (v/v) FBS (fetal bovine serum). For the migration experiments, cells between the 10th and 20th sub-cultivation were used. Before scratch-wounding, cultures were incubated in serum free, full supplemented growth medium (see below) for 12-15 h.

Full supplemented medium

Non-essential amino acids 100x	1% (v/v)
Sodium pyruvate	1 mM
Glutamine	2 mM

10% (v/v) FBS was added if needed

3.1.2 Primary cell cultures

3.1.2.1 Neural cell cultures

Primary hippocampal and cortical cultures were prepared by Dr. A. Stellmacher (IPT, Magdeburg) according to Goslin et al. (1998) from hippocampi and cortices, respectively, of E18 rat embryos (Sprague Dawley; Harlan, Rossdorf, Germany). Briefly, hippocampi or cortices were carefully dissected from rats on embryonic day 18 respectively and treated with 0.05% trypsin for 20 min at 37°C. After an incubation with trypsin inhibitor (0.5 mg/mL trypsin inhibitor with 0.24 mg/mL DNase I (Dn25)), hippocampi and cortices were triturated respectively in HBSS plus 3 mg/mL BSA with needles of decreasing diameters and cell strainers until cells were fully suspended. Then 20,000 to 40,000 cells were plated on prepared poly-D-lysine coated cover slips (diameter 12 mm) and cultivated in Neurobasal® medium supplemented with 0.8 mM glutamine and 1x B-27® serum-free supplement at 37°C with 5% CO_2 (v/v). Cells were feed with 1/10 of fresh culture medium every week, i.e. 50 µL fresh medium was added to each well of 24-well plate every week.

3.1.2.2 Glial cell-enriched cultures

Glial cell-enriched cultures were prepared by Dr. A. Stellmacher (IPT, Magdeburg) according to Guizzetti & Costa (1996). In brief, cortices of P2 rats (Sprague-Dawley; Harlan, Rossdorf, Germany) were dissected and trypsinized (0.25% v/v trypsin, 20 min at 37°C). Trituration was performed with needles and cell strainers as described in

chapter 3.1.2.1. Cells were cultivated in flasks in DMEM supplemented with 2 mM glutamine and 1x penicillin/streptomycin (100 U/mL). Medium was changed every 3-4 days. After the cells reached confluency, they were detached with trypsin/EDTA and collected from the culture flask and plated onto cover slips (diameter 12 mm, placed in 24-well plate) at a dilution of 1:12 with the same supplemented DMEM medium.

3.2 *In vitro scratch wound assays and RNA interference*

3.2.1 *In vitro* wounding of RGM-1 cells

For the further use for immunocytochemistry, sterile glass cover slips (22 x 22 mm) were first placed in 6-well plate. RGM-1 cells were suspended in fully supplemented growth medium (see chapter 3.1.1) with 10% v/v FBS, seeded at a density of 4.5×10^5 in each well and cultured with 2.5 mL same medium. When cells were confluent, this medium was replaced by 2.5 mL serum free medium. After 12 h incubation, the cell monolayer was scratched under sterile conditions with a cell lifter (19 mm blade). Routinely, 2 wound sides (~18-19 mm) were created on each cover slip. The wounded cell cultures were carefully rinsed with serum free medium to remove residual cell debris. Cells were further incubated in 2.5 mL fresh serum free medium for 24 h and were then used for immunocytochemistry (see chapter 3.7.1.1).

The cells used for RT-PCR analysis were prepared with a similar procedure as for immunocytochemistry. Instead of cover slips, cells were seeded in 100 mm cell culture dishes at a density of 2×10^6 in fully supplemented growth medium with 10% v/v FBS. After reaching the cell confluence and following a 12 h serum free medium incubation, the cell monolayer was scratched under sterile conditions with a cell lifter (19 mm blade). Routinely, 5 rectangular wound zones (~5 x 40-80 mm) were created on each 100 mm culture dish according to the pattern marked on the outer bottom surface of the cell culture dishes. The wounded cells were then carefully rinsed with 37°C serum free medium, further incubated in fresh serum free medium for 24 h at 37°C and then sorted as stationary and migratory cells (Figure 12, on page 33) for further experiments.

3.2.2 siRNA and transfection

Three non-overlapping stealth RNAi™ duplexes were designed to rat Tff1 (NM_057129.1): site 1 (Tff1-siRNA1), site 2 (Tff1-siRNA2), and site 3 (Tff1-siRNA3). Sequence information for the three stealth RNAi™ duplexes as well as the stealth RNAi™ negative control used is provided in chapter 2.6.

One day before transfection, RGM-1 cells were seeded in 100 mm cell culture dishes at 2×10^6 cell density in fully supplemented growth medium with 10% v/v FBS. This medium was replaced by 15 mL Opti-MEM® I reduced serum medium 4 h before transfection. Then cells were transfected with 125 nM stealth RNAi™ for Tff1 or stealth RNAi™ negative control, respectively, using the cationic lipid-based transfection

reagent Lipofectamine 2000 at 1 µg/mL according to the manufacturer's instructions. Shortly, for each cell culture dish, 120 µL stealth RNAi™ duplexes (20 µM) was diluted and gently mixed with 1.5 mL Opti-MEM® I reduced serum medium. Meanwhile 30 µL Lipofectamine® 2000 was gently mixed with 1.5 mL Opti-MEM® I reduced serum medium, then incubated for 5 min at room temperature. All these steps were finished within 25 min. Then the diluted RNA oligomer and the diluted Lipofectamine® 2000 were gently mixed and incubated for another 15 min at room temperature. At the end, RNA oligomer-Lipofectamine® 2000 complexes was added to the culture dish containing cells and 15 mL Opti-MEM® I reduced serum. The medium was then mixed gently by rocking forth and back.

After 8 hours, 10% FBS was added to the transfection mix. At 24 hours after transfection, the medium was replaced with normal growth medium, fully supplemented including 10% (v/v) FBS. Cells were cultured for another 48-72 h. When cells were confluent, this medium was replaced by 15 mL of serum free medium. After 12 h incubation, the cell monolayers were scratched under sterile conditions with a cell lifter (19 mm blade).

3.2.3   Scratch wounding of cells after transfection

In the process of scratch wounding, 5 rectangular wound zones (~5 x 40-80 mm) were created as described in chapter 3.2.1 (also see Figure 12a).

The wound areas were photographed immediately (0 h) and 24 h after the scratch at exactly the same positions according to the pattern on the outer bottom (Figure 11a). The growth area between the two time points (0 h and 24 h) was then analyzed by Adobe Photoshop 7.0 by counting the pixel numbers (Figure 11b, c).
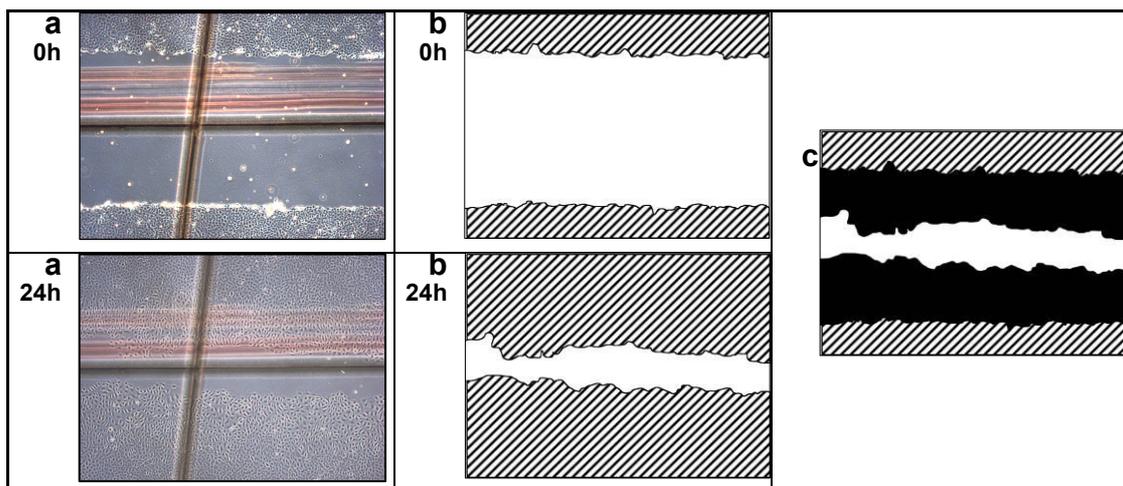
Figure 11: Photograph and analysis process of the growth area after wound healing
a: cell photos, made at exactly the same positions 0 h and 24 h after the scratch. **b**: cell edges (black line) as determined from the corresponding photos (the area with cells were marked with slashes) **c**: growth area of cells (marked in black) after 24 h wound healing

3.2.4   Isolation of stationary and migratory cells

After the scratch wound assays (either from normal or siRNA transfected RGM-1 cells) "stationary cells" and then the "migratory cells" were isolated (Znalesniak *et al.*, 2009) for further analysis. Cell isolation begins with collection of the "stationary cells". In this step, only cells that did not have direct contact with the border zone (i.e., cells from one half of the culture dish which has not been scratch wounded; see Figure 12a) were harvested with a plastic cell scraper.

Then, all remaining stationary cells as well as the migratory cells close to the stationary cells were removed with 4-5 mm fragments of double edge stainless-steel razor blades as described previously (Dürer *et al.*, 2007; Znalesniak *et al.*, 2009). The remaining migratory cells were rinsed gently with 37°C serum free medium (~5 times), so that only a population of "pioneer" cells were left over (i.e., about 10 rows of cells directly behind the migratory front) and collected (Figure 12b, c, d). All procedures of cell wounding and cell sorting were controlled with a microscope.

After a short rinse with PBS/pH 7.4 at 20°C, total RNA was isolated from the separated "migratory cells" and "stationary cells" respectively. RNA isolation was preceded with 450 µL lysis buffer of ISOLATE RNA mini kit (Bioline GmbH) or 1 mL TRIzol® reagent according to the manufacturer's protocol (see chapter 3.4.2).
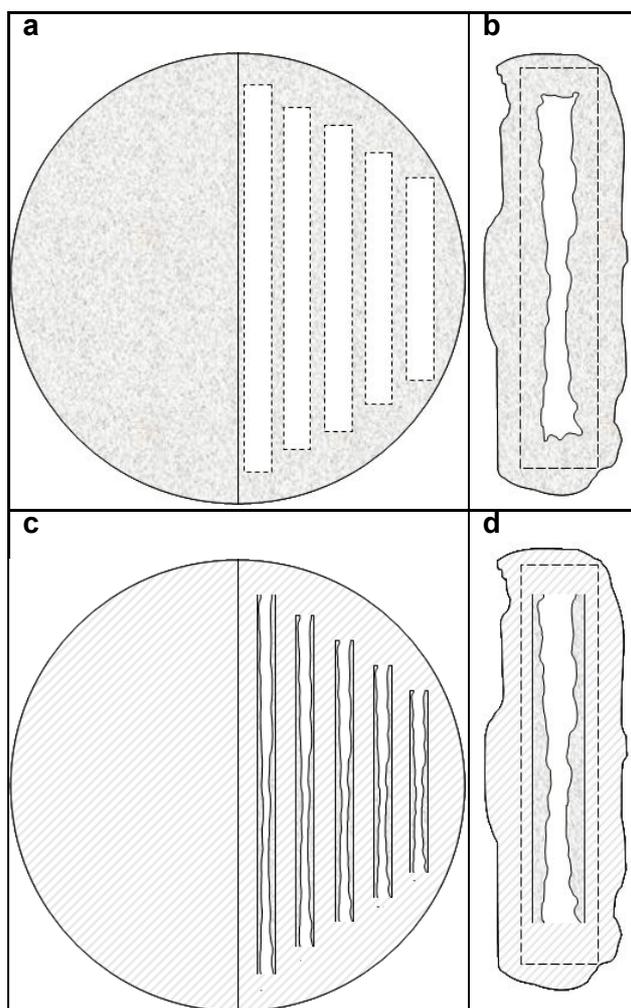
Figure 12: Scratch wound assay and isolation of stationary and migratory cells **(a)** Five rectangular wound zones were created on the right side of 100 mm culture dish according to the pattern marked on the outer bottom surface, i.e. all cells in the white area were carfully removed. Cells on the unwounded left side were used as stationary cells. **(b)** Cell growth pattern in one of the five wound zones, 24h after the scratch wounding. **(c)** Stationary cells were collected from left side of the dish. After having removed the other cells, only a population of pioneer cells were left over and collected as migratory cells (10 narrow rows of cells on right side of the dish). **(d)** "Pioneer" cells, left over in the wound zone and collected as the migratory cells.

3.3 Animal experiments

3.3.1 Animal maintenance and genotyping

Animal care and experimental procedures were performed according to legal regulations, and experiments with *T. gondii* infection were approved by state authorities (Landesverwaltungsamt, Saxony-Anhalt, Halle, Germany; AZ: IMMC/G/01-1004/10, 2-1174 Uni MD). Tff-deficient mice Tff1^{KO}, Tff2^{KO}, Tff3^{KO} and the corresponding wild type mice were used for the study (see chapter 2.4.1). Animals were kept at the animal facility of the Medical Faculty, housed in standard cages at a steady room temperature (22°C), maintained under controlled conditions with a regulated twelve hour light cycle (lights was available at 7 a.m.) and provided with food and water ad libitum.

Genomic DNA used for genotyping was isolated from tail clippings taken at weaning and purified with Invisorb® spin tissue mini kit (STRATEC GmbH) following the manufacturer's instruction (see also in chapter 3.4.4). All primer sequences and corresponding gene maps are listed in Table 5. For Tff1^{KO} mice, the reverse primer MB990 annealed within the intron after exon2 of mTFF1 recognized both the knock out and wild type alleles. Paired with MB990, forward primer MB989 annealed to the intron before exon2 giving rise to a 215 bp amplicon, whereas forward primer MB988 annealed within the targeted deletion neomycin cassette producing a 505 bp amplicon. For Tff2^{KO} mice, the reverse primer MB820 annealed within intron after exon4 recognized both the null and wild type alleles. Paired with MB820, forward primer MB821 annealed within exon2 giving rise to a ~2.65kb amplicon, whereas forward primer MB819 annealed within the targeting vector producing a ~2.4kb amplicon. For Tff3^{KO} mice, to recognize the wild type alleles, forward primer MB1871 annealed within exon2 and reverse primer MB98 annealed intron after exon2 giving rise to a 291 bp amplicon, whereas to recognize the knock out alleles, primer pair MB1920 and MB1921 annealed within the targeted deletion neomycin cassette producing a 637 bp amplicon.

Table 5: Primer list for genotyping

Genes	Primer No.	Sequence	Nucleotide positions	Size (bp)
Tff1 forward	MB989	CCATGACTCACCCTGCTTTT	intron before exon 2	215
Tff1 reverse	**MB990**	CCCCTACTGTGCTGAGAGATG	intron after exon 2	

Tff1 MB989 MB990 exon1 — exon2 — exon3

| Neo forward | MB988 | AGGATCTCCTGTCATCTCACCT | targeting vector | 505 |
| Tff1 reverse | **MB990** | CCCCTACTGTGCTGAGAGATG | intron after exon 2 | |

Neo/Tff1 MB989 MB990 exon1 — neo — exon3
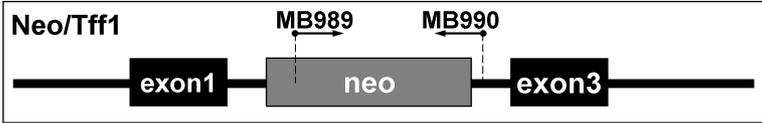
Genes	Primer No.	Sequence	Nucleotide positions	Size (bp)
Tff2 forward	MB821	GTCCCTTGGTGTTTCCACCC	exon2	~2.65k
Tff2 reverse	**MB820**	ACTGTGATCAGCAGTCATGCG	intron after exon4	

Tff2

MB821   MB820

exon1   exon2   exon3   exon4

Genes	Primer No.	Sequence	Nucleotide positions	Size (bp)
Neo/Tff2 forward	MB819	GGTACCCCGGGTTCGAAATC	targeting vector	~2.4k
Tff2 reverse	**MB820**	ACTGTGATCAGCAGTCATGCG	intron after exon4	

Neo/Tff2   MB819   MB820

neo   exon3   exon4

Genes	Primer No.	Sequence	Nucleotide positions	Size (bp)
Tff3 forward	MB1871	CTGTCACATCGGAGCAGTGT	exon 2	291
Tff3 reverse	MB98	TGACCCTGTGTCATCACCCT	intron after exon 2	

Tff3   MB1871   MB98

exon1   exon2   exon3

Genes	Primer No.	Sequence	Nucleotide positions	Size (bp)
Neo forward	MB1920	TGCTCTGATGCCGCCGTGTT	targeting vector	637
Neo reverse	MB1921	GCACGAGGAAGCGGTCAGCC	targeting vector	

Neo (Tff3)   MB1920   MB1921

exon1   neo   exon3

3.3.2 *Toxoplasma gondii* infection

Mice used for *T. gondii* infection were kept under specific-pathogen free (spf) conditions. To obtain *T. gondii* cysts for *in vivo* experiments, NMRI mice (Harlan-Winkelmann, Borchen, Germany) were orally infected with 5 cysts of a type II strain of *T. gondii* (DX or ME49) at the age of 2 to 3 months, as described (Deckert et al. 2006; Dunay et al. 2008; Händel et al. 2012; performed and provided by IMMB, Magdeburg). Cysts formed in the brain of these mice and were then used for the experimental infection. These chronically *T. gondii* infected mice were sacrificed 3 to 5 months after infection to obtain the cysts produced (approximately 50 cysts per total mouse brain). The mice were deeply anesthesized with isoflurane and decapitated. Brain tissues were removed and dispersed in 2 mL 0.1 M PBS/pH 7.4 using button needles and injection needles. Then 20 µL of this suspension was spread on a microscope slide, covered with a cover slip. The number of cysts was counted under the microscope with magnification of 10 and was then adjusted to a concentration of 25 cysts / mL in 0.1 M PBS. The adjusted suspension was administered (i.p. or p.o.) to the experimental mice (Tff1^{KO}, Tff2^{KO} and Tff3^{KO} mice). DX-strain suspension (200 µL) was intraperitoneally injected (i.e., 5 *T. gondii* cysts per mouse) by Dr. U. Händel (IMMB, Magdeburg) and ME49-strain suspension (120 µL) was orally administered (i.e., 3 cysts pro mouse) by Dr. I. Dunay (IMMB, Magdeburg).

3.3.3   Perfusion, organ collection and tissue processing

Four weeks after the i.p. infection (performed by Dr. U. Händel, IMMB, Magdeburg) or 7 days after the oral infection (performed by Dr. I. Dunay, IMMB, Magdeburg), organs of the experimental mice were harvested. Animals were deeply anaesthetized with isoflurane and perfused transcardially with 50 mL saline to remove contaminating intravascular leukocytes from the brains and other organs and then decapitated. The skull bone was carefully removed to obtain an injury-free brain. The brain was then sagittally cutted through the midline of the brain into two parts. The left half of the brain was used for immunohistochemistry (see chapter 3.7.2), and the right half of the brain was used for RNA and protein extraction and proceeded for further processing of experiments (see chapter 3.4.2). Ileum (only from orally infected mice), colon and stomach were also collected.

3.4   Extraction from Tissue and Cells

3.4.1   Preparation of tissue and cells

Fresh tissue or tissue kept at -80°C was cooled on ice, cut with a scalpel into small pieces (0.2-0.5 g) and filled in a 2 mL tube added with corresponding buffer for RNA/protein extraction. After cooling in liquid nitrogen for 10 s, the suspension was homogenized with the Precellys 24 (2 x 20 s, 6800 rpm, 30 s pause). After centrifugation at 16,000 g for 5-10 min at 4°C, the supernatants were transferred to new tubes and used for RNA/protein extraction.

Collected cells were washed 3 times with 1x PBS and added with corresponding buffer for extraction, then homogenized by pipetting up and down. Suspensions were centrifuged at 16,000 g for 5-10 min at 4°C when needed. The supernatants were transferred to new tubes for RNA/protein extraction.

3.4.2   Total RNA extraction

Total RNA of tissues and cells was isolated and purified using TRIzol® reagent or ISOLATE RNA mini kit, according to the manufacturer's protocol.

When using the ISOLATE RNA mini kit, the chaotropic lysis buffer was used to lyse the cells and inactivate RNases. After homogenizing, the sample lysate was applied to a spin column to selectively remove genomic DNA. RNA was then bound to a silica membrane. Remaining cell debris was removed by subsequent wash steps. Pure RNA was eluted in the final step with RNase-free water.

Sample lysate was centrifuged at maximum speed for 1 min and was carefully transferred to spin column R1 placed in a 2 mL collection tube. After 2 min centrifugation at 10,000 g, spin column R1 was discarded, and 1 volume (usually 400µL) of 70% ethanol was added to the filtrate and well mixed by pipetting. The mixture was then transferred to spin column R2 placed in a new collection tube and centrifuged at 10,000 g for 2 min. The filtrate was discarded. Spin column R2 was

placed in a new collection tube, filled with 500 µL wash buffer "AR" and centrifuged at 10,000 g for 1 min. Then the filtrate was discarded. Spin column R2 was placed in a new collection tube, filled with 700 µL wash buffer BR and centrifuged at 10,000 g for 1 min. The filtrate was discarded and spin column R2 was placed in a new collection tube centrifuged at 10,000 g for another 2 min to remove all traces of ethanol. Then the spin column R2 was placed in an elution tube and 30 µL RNase-free water was directly added to spin column membrane. After 1 min incubation at room temperature, the elution tube was centrifuged at 6000 g for 1 min to elute the RNA.

The extraction with TRIzol$^{®}$ Reagent uses the acid guanidinium thiocyanate-phenol-chloroform method (Chomczynski & Sacchi, 1987). Under acidic conditions (pH 4-6), proteins and DNA partitioned into the organic phase, while RNA remained in the aqueous phase. RNA is then recovered from the aqueous phase by precipitation with isopropanol or ethanol.

The supernatant (1 mL) of TRIzol$^{®}$ Reagent was first incubated for 5 min at room temperature to permit complete dissociation of the nucleoprotein complex, and then 200 µL chloroform were added and shaked vigorously by hand for 15 seconds. After 2-3 min incubation at room temperature, the mixture was centrifuged at 12,000 g, 4°C for 15 min. Three phases were formed: a lower red phenol chloroform phase, an interphase, and a colourless upper aqueous phase. The aqueous phase was carefully aspirated into a new tube to precede the procedure for RNA extraction. The interphase and organic phenol-chloroform phase were saved for the protein extraction. For 1 mL of TRIzol$^{®}$ Reagent 0.5 mL of 100% isopropanol was added to the aqueous phase. After 10 min incubation at room temperature, the mixture was centrifuged at 12,000 g, 4°C for 10 min. After 2 times wash with 1 mL of 75% ethanol, the RNA pellet was air dried for 5-10min. The RNA pellet was then resuspended in RNase-free water and incubated at 60°C for 10 min. The isolated RNA was used for further studies or frozen at -80°C for long-term storage.

3.4.3   Total protein extraction

Total protein of cells and tissues was isolated using either protein extraction buffer (self-configured, see below) or the TRIzol$^{®}$ reagent according to the manufacturer's protocol.

When using the protein extraction buffer (see below), 4-fold volume of buffer (0.8 - 2 mL) with 50 mg/mL protease inhibitor was added to tissue (0.2 – 0.5 g); alternatively 150 µL extraction buffer was added to the cells. The supernatant was added to the same volume of chloroform (0.8 - 2 mL) and incubated for 30 min at 4°C to remove non-polar interfering substances. The mixture was then centrifuged at 16,000 g for 10 min at 4°C. Supernatant was used for further experiments or frozen at -20°C for long-term storage.

When using the TRIzol$^{®}$ Reagent, the interphase and the organic phenol-chloroform phase left from TRIzol$^{®}$ Reagent RNA extraction were used for protein extraction. The proteins were denatured by this chaotropic agent (guanidinium thiocyanate) in the

organic phase. For 1 mL TRIzol® Reagent used in the initial homogenization, 1.5 mL of isopropanol was added to the phenol-ethanol supernatant. After 10 min incubation at room temperature, the mixture was centrifuged at 12,000 g, 4°C for 10 min. The protein pellet was then washed three times with 2 mL 0.3 M guanidine hydrochloride in 95% ethanol and once with 2 mL of 100% ethanol for 20 min each at room temperature and centrifuged at 7500 g for 5 min at 4°C after every wash step. Supernatant was discarded and the protein pellet was air dried for 5-10min and dissolved in 1% SDS (sodium dodecyl sulfate) solution. For long-term storage, protein was frozen at -20°C.

Protein extraction buffer (500mL)

1 M Tris/HCl, pH 8.0	10 mL
4 M NaCl	3.75 mL
deionized water	add to 500 mL

3.4.4   Genomic DNA extraction

Genomic DNA for genotyping was isolated from tail clippings taken at weaning and further purified with Invisorb® Spin Tissue Mini Kit following the manufacturer's instruction. Briefly, tail clippings were digested in 400 µL lysis buffer G with protein kinase K, shaked at 52°C for 2 h. After 1 min centrifugation, the suspension was transferred to a new tube and filled with 200 µL binding buffer T. The mixture was mixed thoroughly and transferred to the column set in a 2 mL tube. The tube was centrifuged 1 min and filtration was discarded. The column was then washed two times with wash buffer and centrifuged 1 min, and then the column was centrifuged for another 2 min to remove the remaining buffer. The elution buffer E was applied to the centre of the membrane in column and centrifuged for 2 min. The eluted DNA can be directly used for PCR for genotyping.

3.5   RT-PCR analysis

3.5.1   RNA quantification

RNA (DNA) concentration was calculated from the absorption measured at a wavelength of 260 nm as well as 280nm by NanoDrop ND-1000 spectrophotometer following the instruction. RNA solution (1-2 µL) was applied to the sensor of the spectrophotometer and the concentration was determined directly from the measurement.

3.5.2   Removal of genomic DNA and reverse transcription

Before reverse transcription, total RNA (normally 2 µg RNA for tissues and 0.5 µg RNA for cells) from each sample was first digested with DNase I to eliminate the rest of genomic DNA. According to the manufacturer's instructions, RNA was incubated with the enzyme at 37°C for 45 min (see below), and DNase I was then inactivated by 10 min incubation with EDTA at 65°C.

Digestion of RNA

RNA 0.5-2 μg	x μL
10x Reaction buffer with MgCl$_2$	1 μL
DNase I, RNase-free (1 u)	1 μL
RiboLock^{TM} RNase inhibitor (40 u)	1 μL
DEPC-treated water	to 10 μL

After the DNA digestion, RNA was used for the first strand cDNA (complementary DNA) synthesis. The reaction was primed with oligo(dT)$_{18}$ using RevertAid H Minus reverse transcriptase according to the manufacturer's protocol. RNA was incubated with oligo(dT)$_{18}$ primer at 65°C for 5 min to allow denaturation and then was chilled immediately on ice for 3 min to prevent renaturation. After a gentle mix and a brief centrifugation, RNA was incubated with reverse transcriptase, mixed with 5x reaction buffer, RNase inhibitor and dNTP, at 42°C for 60 min. The reaction was terminated by heating at 70°C for 10 min (see below). The mix was subsequently diluted to 100 μL with sterile deionized water. After a brief centrifugation, the cDNA was used for further studies or frozen at -20°C for long-term storage.

Reverse transcript reaction (20 μL reaction)

Total RNA after DNA digestion (with EDTA)	11 μL
Oligo(dT)$_{18}$ primer	1 μL
	5 min, 65°C
5x Reaction buffer	4 μL
RiboLock RNase inhibitor (40 u)	0.5 μL
dNTP Mix, 10 mM each	2 μL
RevertAid H Minus reverse transcriptase (200 u)	1 μL
	60 min, 42°C, then 10min, 70°C

3.5.3   PCR

The relative expression level of selected genes was monitored by RT-PCR analysis. DreamTaq Green DNA Polymerase was used for amplification. The reaction mix was prepared (see below) and overlaid with light mineral oil. PCR amplification was then performed in the programmed (see below) thermo Robocycler. Beta-actin transcripts were amplified in parallel reactions as an internal control for the integrity of the cDNA preparations. The cDNA was also checked for contaminating chromosomal DNA by amplification of a promoter sequence (from the beta-actin gene). All the specific primer pairs used in this study are listed at chapter 2.8.

RT-PCR reaction (10 μL reaction)

cDNA (equivalent of 2 mg/L RNA)	1-4 μL
10x DreamTaqGreen buffer*	1 μL
dNTP Mix, 2 mM each	1 μL
7.5 μM primer-mix (forward + reverse)	1 μL
DreamTaq DNA polymerase	0.1 μL
autoclaved deionized water	to 10 μL

*10x DreamTaq Green Buffer contains 20 mM MgCl$_2$ and loading dye

Thermal cycling programs for RT-PCR reaction

Step	Temperature	Time	Number of cycles
initial denaturation	95°C	3 min	1
denaturation	95°C	45 s	
annealing	57/60°C	45 s	24-40
extension	72°C	45 s	
final extension	72°C	5 min	1

3.5.4 Electrophoresis

After PCR, the size of the products was confirmed by electrophoresis on a 1.5% agarose gel. For preparation of the gel, 8 g agarose were dispersed in 500 mL 1x TBE buffer (see below) and heated in a microwave oven until completely dissolved. Before casting the gel, 10 mg/L ethidium bromide was added to the dissolved agarose. Then the horizontal agarose gel was casted in the leveled casting chamber with comb teeth. Comb teeth were slowly removed once the gel solidified. Each amplification reaction (8.5 µL from the 10 µL reaction) was loaded into the gel slots. The electrophoresis was run using power supply system (Heinzinger Economy Line LNG 350 06) at 150 V in 1x TBE buffer. The PCR products resolved in the gel were visualized (exposure at 254 nm UV light) and documented by the Herolab E.A.S.Y system.

1x TBE buffer (1L)

Tris	10.8 g
H_3BO_3 (solid)	5.5 g
0.5 M EDTA, pH 8	4.0 mL
deionized water	to 1 L

3.5.5 Semi-quantitative analysis

All relative expression levels of selected genes were determined by semi-quantitative analysis of the DNA bands with the GeneTools software. As a control gene β-actin was amplified in parallel reactions. All data were then analyzed with Excel 2003.

3.6 Western blotting

3.6.1 Protein quantification

Total protein concentration of cell or tissue extracts were determined using two protein quantitation methods: BCA (bicinchoninic acid) method and Bio-Rad Protein Assay method.

The BCA method is a quick and highly accurate protein quantitation method. The BCA reagent reacts with protein and changes color from light blue to purple. The intensity of purple color is based on the amount of total protein concentration in the sample. Total protein concentration of the sample was determined by comparing absorbance (562 nm) readings to serially diluted BSA standards. The BCA protein assay reagent was used following the manufacturer's instructions. All samples were prepared in duplicate and incubated for 30 min at 37°C. Absorbance was measured with the NanoDrop ND-1000 spectrophotometer following the instructions. The protein concentrations of the sample were calculated out automatically from the standard curve.

The Bio-Rad protein assay is based on the reaction of proteins with an alkaline copper tartrate solution and Folin reagent. It was also used for protein quantitation following the manufacturer's instructions. The BSA standards were the same as for the BCA method. All standards and samples were prepared in duplicate. The Bio-Rad assay dye was diluted 1:5 with deionized water and well mixed. For each measurement 1 mL

diluted dye with 1 µL standard or sample was mixed thoroughly and then transferred to a disposable plastic cuvette. The absorbance was read at 595 nm by Libra S12 spectrophotometer. The concentration was then determined using the standard curve equation in Excel 2003.

3.6.2 SDS-PAGE (sodium dodecyl sulfate- polyacrylamide gel electrophoresis)

Proteins were separated by SDS-PAGE based on molecular weight. The SDS-PAGE gel consists of two sections: the upper stacking gel (see below) focused the proteins and the running gel (see below). The two sections were prepared from different buffers, and combined with different pH values. Protein samples were mixed (3:1) with corresponding 4x loading buffer (reducing or non-reducing, see below) and boiled for 5 min. Then samples were immediately cooled in ice for 5 min to prevent renaturation, and were briefly centrifuged.

Samples with equal amounts of proteins (10 or 20 µg) were loaded in each lane. Protein-Marker I (7 µL) was loaded into one lane in order to provide a reference. The gel was run in electrophoresis buffer Laemmli (see below) at 75 mA until the protein samples entered the running gel, then the current was raised to 100 mA until desired protein separation was achieved.

6% Stacking gels for Western blot (for 2 gels)

4x stacking gel buffer	3.125 mL
30% acrylamide/bisacrylamide (37.5:1)	3.125 mL
20% SDS (w/v)	0.125 mL
TEMED	12.5 µL
20% APS (w/v)	125 µL
deionized water	9mL

4x Stacking gel buffer (500 mL): 60.57 g Tris (1 M), adjusted to pH 6.8 with HCl

15% Running gels for Western blot (for 2 gels)

4 x running gel buffer	3.8 mL
30% acrylamide/bisacrylamide (37.5:1)	10.0 mL
TEMED	8 µL
20% APS (w/v)	80 µL
deionized water	6.2 mL

4x Running gel buffer (500 mL): 90.86 g Tris (1.5 M) + 10 mL SDS (10% (w/v)), adjusted to pH 6.8 with HCl; add APS and TEMED shortly before overlaying

4x Reducing loading buffer (10 mL)

0.5 M Tris/HCl, pH 6.8	2.5 mL
glycerol	2.0 mL
10% SDS (w/v)	4.0 mL
0.1% bromophenol blue (w/v)	0.5 mL
2-mercaptoethanol	0.5 mL
deionized water	0.5 mL

For non-reducing buffer, use 0.5 mL deionized water   instead of 2-mercaptoethanol

Electrophoresis buffer Laemmli (500 mL)

Tris	1.52 g
glycine	7.13 g
20% SDS (w/v)	2.5 mL
deionized water	add to 500 mL

pH approx. 8.8

3.6.3   Western blot

After the protein separation, the SDS-PAGE gel was carefully removed from the chamber. Protein transfer (from the polyacrylamide gel to the nitrocellulose membrane) was carried out with a 20x20 cm semi dry blotter. The gel was carefully placed on the top of the membrane to avoid any air bubble. The membrane was placed on three layers of filter papers (gel-blotting-paper BF2) on the anode side of the semi dry blotter, and the gel was covered with another three layers of filter papers to form a sandwich-structure. All materials in this step were pre-wetted in transfer buffer (see below). After covering the cathode on this sandwich-structure, the transfer was for 70 min at 0.8 mA /cm^2 (approx. 90 mA for each membrane). To control the transmission efficiency, the membrane was shortly treated with Ponceau S solution (see below), a negatively charged stain that can bind to positively charged amino groups of the blotted polypeptides.

Transfer buffer for electro-blot (1000 mL)

Tris	5.81 g
glycine	2.93 g
20% SDS	1.85 mL
methanol	200 mL
deionized water	add to 1000 mL

pH approx. 8.8

Ponceau S solution (500 mL)

Ponceau S	1.0 g
Trichloroacetic acid	15 g
deionized water	add to 500 mL

3.6.4   Immunological detection of proteins

In order to detect the protein of interest, mono- or polyclonal antibodies can be used. The membrane needs first to be blocked with a blocking solution to prevent non-specific antibody binding, and then be incubated with primary antibodies which bind the protein of interest. After extensive washing, the membrane is incubated with the appropriate secondary antibody that binds the primary antibody. Usually the secondary antibody is conjugated to an enzyme, for instance horseradish peroxidase, which aids in visualization (Alberts *et al.,* 2002). After the enhanced chemiluminescence (ECL) treatment, the oxidized form of luminol from horseradish peroxidase (HRP) produces chemiluminescence, which can be detected at 428 nm.

For this purpose, the transferred protein on nitrocellulose membrane was fixed by treating with 0.2% glutaraldehyde in 1x PBS (see below) for 30 min. After washing two times with 1x PBS-T (see below) and once with 1x TBS-T (see below) for 5 min each, the unspecific binding sites on the membrane were blocked with blocking buffer (consisting of 1% BSA and 1% dry milk in 1x TBS-T) for 60 min. Then the membrane was incubated with primary antibody diluted in 1x TBS-T (see chapter 2.3.2) at 4°C overnight or at room temperature for 60-120 min. After three times 5 min washing with 1x TBS-T, the membrane was incubated with the corresponding secondary antibody conjugated with HRP (see chapter 2.3.3) at room temperature for 45-60 min. Dilution was with 1x TBS-T diluted. Then the membrane was washed two times, 10 min each

with 1x TBS-T. The ECL solution (see below) was prepared during this washing step. For one membrane, 2.5 mL of each fresh ECL solution were mixed and the mixture was pipetted onto the membrane. After 2 min incubation, the membrane was visualized with Gene Gnome. The exposure times of each membrane differed from 5 x 2 min to 5 x 3 min depending on the signal strength.

1x PBS (2000 mL)

Na_2HPO_4	2.3 g
KH_2PO_4	0.5 g
NaCl	18.0 g
deionized water	add to 2000 mL

KH_2PO_4 dissolves at last, adjust to pH 7.4 with NaOH before making up to 2000 mL

1x PBS-T (1000 mL)

1x PBS	999 mL
Tween 20	1 mL

1x TBS-T (2000 mL)

Tris	4.84 g
NaCl	17.52 g
Tween 20	2 mL
deionized water	add to 2000 mL

ECL solution (10 mL)

solution A	250 mM luminol (44.29 g/L)	100 µL
	90 mM p-coumaric acid (14.77 g/L)	44 µL
	1 M Tris/HCl, pH 8.5	1000 µL
	deionized water	8856 µL
solution B	30% H_2O_2 (w/v)	6.1 µL
	1 M Tris/HCl, pH 8.5	1000 µL
	deionized water	8993.9 µL
	mix solution A and B (1:1) shortly before use	

3.6.5   Competitive inhibition

The specificity of the staining with anti-mTff1-1 and anti-rTff3-2, respectively, was tested by competition with the corresponding synthetic peptides (see chapter 2.3.3). One mL antiserum (anti-mTff1-1 or anti-rTff3-2, diluted in 1x TBS-T buffer, 1:500) was pre-adsorbed with 10 µg corresponding synthetic peptide by shaking at 4°C overnight and then used for Western blot analysis.

3.7   *Immunohistochemistry*

3.7.1   Cell cultures

3.7.1.1   *RGM-1 cells (after in vitro wounding)*

Cells on glass cover slips (22 x 22 mm, see chapter 3.2.1) were fixed with cold methanol at -20°C for 5 min and then washed 3 times for 5 min each with PBS/pH 7.4 at room temperature. Non-specific antibody binding sites were blocked with blocking buffer (see below) at room temperature for 1 h. The primary antibody anti-mTff1-1 (see chapter 2.3.2) was 1:500 diluted with blocking buffer. The incubation with the primary antibody was at 4°C overnight. The cover slips were rinsed with PBS/pH 7.4 3 times 5

min each at room temperature, and then incubated with the secondary antibody, Cy3-labeled anti-rabbit-IgG F(ab')2 fragment from sheep antiserum (see chapter 2.3.3), 1:200 diluted in blocking buffer at room temperature for 1 h (from this step, the incubation and all following steps were carried out in the dark) and rinsed again with PBS/pH 7.4 2 times 5 min each at room temperature.

Blocking buffer (10 mL)

goat serum	1 mL (final conc. 10%)
10% NaN$_3$	100 µL (final conc. 0.1%)
10% Triton™ X-100	300 µL (final conc. 0.3%)
1x PBS/pH 7.4	add to 10 mL

The cell nuclei were stained with DAPI (4',6-diamidino-2-phenylindole dihydrochloride) at room temperature for 5 min using a 1:1000 diluted DAPI stock solution (0.1 mg/mL in PBS/pH 7.4). Subsequently, the cover slips were rinsed twice with PBS/pH 7.4 at room temperature for 5 min and once with deionized water for 5 min. The cover slips were embedded on the microscope slides using DAKO fluorescent mounting medium. The slides were photographed with an Axiophot microscope equipped with an AxioCam digital camera. The following filter sets were used: filterset 01 for DAPI and filterset 15 for Cy3 (see chapter 2.7). The images were processed with the AxioVision 3.1 software.

3.7.1.2 *Primary rat brain cells*

All procedures were performed at room temperature. After 20–22 DIV (days *in vitro*), primary culture cells (provided from Dr. Stellmacher, IPT, Magdeburg) grown on glass cover slips were fixed with periodate-lysine-paraformaldehyde (PLP) fix (see below) for 30 min. Cells were washed with PBS 3 times and blocked with blocking solution (see below) for 1 h. Subsequently, cells were incubated with primary antibody (see chapter 2.3.2) diluted in blocking solution for 1 h. After 3 times washing with PBS, cells were incubated with secondary antibodies (see chapter 2.3.3) diluted in block solution for 1 h. Cells were incubated with DAPI for 3 min to stain the cell nuclei. Subsequently, cells were washed 2 times with PBS, once with water, and mounted with Mowiol 4-88 onto the slide. The following antibodies were used (see also in chapter 2.3): primary antibodies: goat anti-Iba-1, rabbit anti-Iba-1, chicken anti-GFAP, mouse anti-MAP2, and rabbit anti-rTff3-2 antiserum; secondary antibodies: donkey anti-goat Cy3, Alexa Fluor™ 488 goat anti–rabbit, donkey anti-chicken Cy3, DyLight™ 649 donkey anti–chicken, donkey anti-mouse Cy3, goat anti-rabbit Cy3.

PLP fix

PFA (paraformaldehyde)	4%
sucrose	5.4%
NaIO$_4$	0.01 M
lysine HCl	0.1M

dissolved in 0.1M sodium phosphate buffer/pH 7.4

Blocking solution

horse serum	10%
sucrose	5%
BSA	0.01 M
saponin	0.2 mg/mL

dissolved in PBS buffer, pH 7.4

Cells were viewed and recorded digitally using the Zeiss microscope Axio Observer.Z1 equipped with a camera AxioCam MRm and the AxioVision Release 4.8 software. The excitation and emission spectra of the fluorescent markers for all the immunofluorescence staining are listed below. Images were processed using Adobe Photoshop 7.0.

Excitation and emission spectra of the fluorescent markers

Fluorescence Marker	Excitation (nm)	Emission (nm)	Colour/Spectrum
Alexa Fluor 488	499	519	green
Cy3	552	565	red
Alexa Fluor 647	652	668	infrared
DyLight 649	654	673	infrared
DAPI	345	455	blue

3.7.1.3 Quantitative analysis

Photos of the RGM-1 cells after *in vitro* wounding were captured in such way that both stationary and migratory cell regions were visible. All photos had the same frame size. For each photo, the total Tff1 immunofluorescence signal was analyzed within a normalized area of stationary and migratory cells, respectively, with GeneTools (Figure 13). This signal was divided by the number of cells in order to obtain the Tff1 staining per cell. All data were then analyzed with Excel 2003.
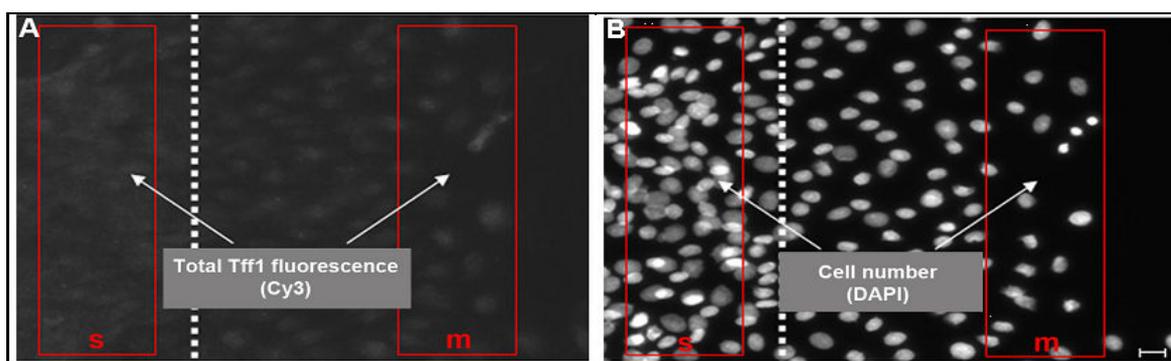
Figure 13: Schematic presentation of total Tff1 immunofluorescence signal analysis
The rectangular standardized zones (stationary (s) and migratory (m)) were marked by a red line. The scratch wound is indicated by the white dotted line. **(A)** Using GeneTools software, total Tff1 immunofluorescence was measured within a pair of rectangular standardized zones (s and m). **(B)** The cell number within the corresponding areas was counted after staining the nuclei with DAPI. Scale bar: 20µm.

3.7.2   Tissues

3.7.2.1   Tissue preparation

Mouse brains were carefully dissected (see chapter 3.3.3). The right half used for freeze sections was immediately fixed in 4% PFA (in 50 mM HEPES-Puffer/pH 7.4) overnight at 4°C, and then transferred to 1 M sucrose (dissolved in 1x PBS/pH 7.4) overnight at 4°C. Subsequently, the tissues were embedded in OCT compound (Tissue-Tek®), frozen in 2-methylbutane (pre-frozen at -60°C) for 2 min, and then stored at -80°C. To prepare sagittal sections for free floating immunohistochemical staining, the frozen half hemisphere was cut using Leica Jung CM3000 Cryostat Microtome at -20°C. The 25 µm sagittal sections were cut and carefully collected into

24-well plate containing 1x PBS and used for further experiments. For long-term storage, sections were frozen in 1 M sucrose at -20°C.

3.7.2.2 Free floating immunohistochemistry

Free-floating sections were washed 3 times for 10 min each with PBS/pH 7.4 at room temperature. Sections were then incubated in 50% (v/v) methanol solution in 1x PBS/pH 7.4 with 1% (v/v) H_2O_2 (fresh made) at room temperature for 10 min to block the endogenous peroxidase activity. Then sections were washed again 3 times for 10 min each with PBS/pH 7.4 at room temperature. The non-specific background staining of sections were blocked with freshly made blocking buffer I (see below) at room temperature for 60 min. Then, sections were incubated with the primary antibodies mTff1-1 and Iba-1 (see chapter 2.3.2), diluted in blocking buffer I, for 1-3 days at 4°C. Sections were then washed 3 times for 10 min each with PBS/pH 7.4 at room temperature and blocked again with blocking buffer II (see below) for 60 min at room temperature. Sections were incubated with the secondary antibody (biotinylated goat anti-rabbit IgG antibody, see chapter 2.3.3) diluted in blocking buffer II at room temperature overnight. After that, sections were washed 3 times for 10 min each with PBS/pH 7.4 at room temperature.

The avidin-biotin peroxidase complex (ABC) method (VECTASTAIN® Elite ABC Kit, BIOZOL GmbH) was used following the manufacturer's instructions. First, sections were blocked with 1x BSA (0.2%) solution at room temperature for 60 min. During this time, solution A and solution B from the VECTASTAIN® Elite ABC Kit were both 1:1000 diluted in 1x BSA solution (see below) and incubated at room temperature for 30 min. After the blocking, sections were further incubated with this mixture, overnight at 4°C or more than 4 h at room temperature. Then, sections were washed two times with 1x PBS/pH 7.4 and once with 1x Tris-buffer/pH 7.6 (0.05 M) for 10 min each at room temperature. During this washing step, 0.5 g/L DAB (diaminobenzidine) solution (in 1x Tris-buffer/pH 7.6) as chromogen was freshly made and 0.5 mL DAB solution was added to each well of the 24-well plate containing sections. To start the staining reaction, 20 µL 3% H_2O_2 was added to each well and incubated for 2-4 minutes under visual control to avoid strong background. The reaction was stopped with PBS washing for three times and then mounted onto gelatine-coated slides (pretreated with 0.5% gelatine; air dried and stored at 4°C). After being air-dried, the slides with mounted sections were progressively dehydrated: first with series of ethanol (concentration elevated from 70% to 100%), 2 min each; then with xylol (two times, for 2 min and 5 min). At the end, cover slips were mounted with DPX mounting medium on the slides. After air drying overnight, the slides were examined under the microscope BZ-8000 (Keyence) and then processed with the BZ observation application software (Keyence).

Blocking buffer I for immunohistochemical staining (10 mL)

goat serum	1 mL (final conc. 10%)
10% NaN$_3$	100 µL (final conc. 0.1%)
10% Triton™ X-100	300 µL (final conc. 0.3%)
1x PBS/pH 7.4	add to 10 mL

Blocking buffer II for immunohistochemical staining (10 mL)

goat serum	1 mL (final conc. 10%)
10% NaN$_3$	100 µL (final conc. 0.1%)
10% Triton™ X-100	100 µL (final conc. 0.1%)
1x PBS/pH 7.4	add to 10 mL

Mixture from VECTASTAIN® Elite ABC Kit (10 mL)

2% BSA	1 mL (final conc. 0.2%)
solution A from ABC Kit	10 µL
solution B from ABC Kit	10 µL
1x PBS/pH 7.4	add to 10 mL

3.7.3   Competitive inhibition

The specificity of the staining with anti-mTff1-1 and anti-rTff3-2, respectively, was tested by competition with the corresponding synthetic peptides, i.e., 1 mL antiserum (anti-mTff1-1 or anti-rTff3-2, diluted in blocking buffer) was pre-adsorbed with 10 µg corresponding synthetic peptide by shaking at 4°C overnight and then used for immunohistochemistry.

3.8   Stable transfection of RGM-1 cells

3.8.1   Construction of plasmid

3.8.1.1   Primer construction and reliable RT-PCR

The primers for the corresponding genes (human TFF1-3, GKN2) were designed for the complete coding sequences (CDs). Corresponding restriction sites were added to the 5'-end of both primers (forward and reverse). The primer pairs used in this study are listed in chapter 2.8. The PCR reaction was performed with HotStar HiFidelity DNA Polymerase Kit (Qiagen). HotStar HiFidelity DNA Polymerase possesses a 3'→5' exonuclease activity generally referred to as proofreading activity. It has been chemically modified to temporarily inactivate the polymerase activity, as well as the 3'→5' exonuclease activity of the enzyme. This prevents excessive degradation of both primers and template during PCR setup and the initial PCR cycles, providing highly sensitive and reliable high-fidelity PCR. The products generated using HotStar HiFidelity DNA Polymerase can be used directly in TA- or UA- cloning procedures. Following the manufacturer's instructions, 2 µL cDNA from human tissue (stomach for TFF1, TFF2 and GKN2; colon for TFF3) was used in a 20 µL PCR reaction. After shortly mixing and brief centrifugation, PCR amplification without mineral oil was then performed in the programmable thermo Robocycler with lid heating.

Reliable RT-PCR reaction (20 µL)

cDNA (equivalent of 2mg/L RNA)	2 µL
5x HotStar HiFidelity PCR buffer*	4 µL
7.5 µM primer-mix (forward + reverse)	2 µL
HotStar HiFidelity DNA Polymerase (2.5 units/µL)	0.5 µL
RNase-free water	to 20 µL

*Contains 1.5 mM dNTPs and 7.5 mM MgSO$_4$.

Thermal cycling programs of reliable RT-PCR reaction

Step	Temperature (°C)	Time	Number of cycles
initial denaturation	95	5 min	1
denaturation	94	30 s	
annealing	60	45 s	35
extension	72	60 s	
final extension	72	10 min	1

3.8.1.2 TA cloning with pGEM®-T Easy Vector System I

Before cloning, 10 µL of each reliable RT-PCR amplicons were mixed with 1.8 µL 6x loading dye and analyzed by gel electrophoresis (see chapter 3.5.4). The remaining amplicons were then ligated into the pGEM-T® Easy Vector, a linearized vector with a single 3´-terminal thymidine at both strands. The T-overhangs at the insertion site of this vector greatly improve the efficiency of ligation of PCR products by preventing recircularization of the vector and providing a compatible overhang for PCR products generated by certain thermostable polymerases. Following the manufacturer's instructions of pGEM-T® Easy Vector System I kit (Promega GmbH), the 2x rapid ligation buffer, the pGEM-T® Easy vector, the T4 DNA Ligase and the PCR production were mixed (see below) and incubated for 15-30 min at room temperature, and competent E. *coli* cells were transformed with the ligation mix.

Ligation reaction (10 µL)
2x rapid ligation buffer	5 µL
pGEM®-T or pGEM®-T Easy Vector (50ng)	1 µL
T4 DNA ligase (400 units/µL)	1 µL
PCR product	2 µL
nuclease-free water	to 10 µL

3.8.1.3 Transformation of E. coli and white-blue screening

Preparation of competent E. *coli* cells (centrifuge Universal 30RF was used):

a) In a 5 mL centrifuge tube, 100 µL E. *coli* cells were added into 2 mL LB medium and shaked at 180 rev /min, 37°C, over night.

b) The overnight culture was transferred to 100 mL LB medium in an Erlenmeyer flask and shaked at 180 rev / min, 37°C for 1-2 h until the $OD_{600\,nm}$ ~ 0.45-0.55.

c) The sample was centrifuged at 3000 rpm at 4°C for 10 min. The cell pellet was resuspended in 10 mL 0.1 M $CaCl_2$ and kept on ice for 30 min.

d) After 5 min centrifugation at 1500 rpm 4°C, the cell pellet was resuspended in 5 mL ice cold 10% glycerol with 0.1 M $CaCl_2$.

e) The suspension was then aliquoted (100 µL each) in 1.5 ml eppendorf tube and kept at -80°C.

Transformation of competent E. *coli* cells consisted of following steps (plasmids carried the gene for ß-galactosidase, so the selection was done with help of the white-blue screening; centrifuge Universal 30RF was used):

a) During the incubation of the ligation, 100µL competent E. *coli* cells kept at -80°C were thawed on ice.

b) 10 µL ligation mixtures was added to 100 µL competent E. *coli* cells and gently

mixed, then incubated on ice for 10 min following a "heat-shock" for exactly 45 sec at 42°C in water bath.

c) The transformation mixture was kept on ice for another 10 min and then transferred into a 5 mL centrifuge tube with 1 mL SOC medium. The pipette tip was left in the tube.

d) The transformation mixture was shaked at 180 rev/min, 37°C for 1 h (tube cap was slightly opened).

e) Shortly before the next step, 40µl 5-Bromo-4-chloro-3-indolyl-beta-D-galactopyranoside (X-gal; light prevented) and 40µl Isopropyl β-D-1-thiogalactopyranoside (IPTG) was pipetted onto the LB agar containing plate, well mixed, spread with a sterile plastic loop and dried in air slightly.

f) After 1 h incubation, the ligation mixture was spread over tow LB agar containing plate from step (e). The LB agar plates were incubated at 37°C, overnight.

g) The positive clones (white colour, not blue) were picked with a pipette tip and each transferred to a 5 mL tube containing 2 mL LB medium with 100 µg / mL ampicillin.

h) The LB-ampicillin medium was incubated in the Innova® 4200 Incubator Shaker at 180 rev/min, 37°C, overnight.

i) The transformed colonies were identified by a colony PCR with a crude bacterial lysate serving as a template.

3.8.1.4 Plasmid DNA extraction from cell culture

From positively identified clonies, plasmid DNA was isolated with JetStar® plasmid mini prep kit (Genomed GmbH) following the manufacturer's instructions (centrifuge Universal 30RF was used) as following. The extracted plasmid DNA was used for either restriction digestion or cell transfection.

a) Each transformation mixture was transferred into a 2 mL Eppendorf tube and centrifuged at 4000 rpm for 10 min at room temperature.

b) The supernatant was discarded. 300 µL cell resuspending buffer E1 was added to each pellet and resuspended immediately with pipette.

c) Then, 300 µL lysis buffer E2 was added to the suspension, mixed and incubated for 5 min at room temperature.

d) 300 µL precipitation buffer E3 was added to the suspension, mixed and centrifuged at 13000 rpm for 5 min at room temperature.

e) The supernatant was transferred to a new 1.5 mL Eppendorf tube and 540µL isopropanol were added, shake briefly.

f) After centrifugation at 15000 rpm for 30 min at 4°C, the supernatant was discarded, 200 µL 70% ethanol (-20°C) was added to the pellet and vortexed.

g) After centrifugation at 15000 rpm for 5 min at 4°C, the supernatant was discarded. The plasmid pellet was air dried for approx. 30 min at room temperature and then dissolved in 30-50 µL distilled water.

3.8.1.5 DNA extraction from gel

The DNA band was excised with a clean sharp scalpel from the agarose gel and then extracted with QIAquick Gel Extraction Kit (Qiagen) following the manufacturer's

instructions (centrifuge Universal 30RF was used). Shortly, the excised DNA fragment was incubated with 3 volumes of buffer QG to 1 volume of gel (100 mg ~ 100 μL) at 50°C for ~10 min until the gel slice has completely dissolved. The colour of the mixture was yellow, indicating that pH was ≤7.5, which is the efficient range for the QIAquick membrane. One gel volume of isopropanol was added and mixed. The mixture was applied to the QIAquick column placed in a 2 mL collection tube to bind DNA. The flow-through was discarded and column was washed with 0.75 mL of buffer PE and centrifuged for 1 min at 15,000 rpm. The flow-through was discarded and column was centrifuged for an additional 1 min at 15,000 rpm to remove residual ethanol. Then the QIAquick column was placed into a clean 1.5 mL tube and 30 μL of buffer EB was dispensed directly onto the QIAquick membrane to completely elute the bound DNA. The concentration of plasmid DNA after every isolation procedure was measured by NanoDrop ND-1000 spectrophotometer (see chapter 3.5.1).

3.8.1.6   *Restriction digestion and ligation*

Different restriction enzymes were used in this study. As a general rule, the restriction digestion was carried out in 25 μL volume, using between 3-6 μL of the DNA (either the target fragments or vector plasmid). For each restriction enzyme the corresponding buffer was used. The concentration was of 1 unit per 1μg of target DNA. All restriction digestions were performed at 37°C for 2 h. The digested DNA were confirmed by gel electrophoresis with 5 μL 6x loading dye and the fragment of interest was excised from the agarose gel with a clean sharp scalpel, purified and isolated using QIAquick Gel Extraction Kit (see chapter 3.8.1.5), then used in the corresponding ligation reaction.

Restrictions digest (25μL)

10x buffer (corresponding to restriction enzyme)	2.5 μL
restriction enzyme (20 units/μL)	1 μL
target DNA (appro. 1-3 μg/μL)	3 - 6 μL
aqua dest. water	to 25 μL

In the ligation reaction, digested DNA fragment and vector plasmid were adjusted to the same concentration and incubated together in the presence of T4 DNA ligase (see below) at 4°C overnight. The ligation product was used for transformation of E. *coli*.

Ligation reaction (10 μL)

2x rapid ligation buffer	5 μL
digested DNA (target fragment; 0.1-1 μM)	1 μL
digested DNA (vector plasmid; 0.1-1 μM)	1 μL
T4 DNA ligase (400 units/μL)	1 μL
nuclease-free water	to 10 μL

3.8.2   Transfection of RGM-1 cells

The stable transfection of the RGM-1 cell line with the corresponding plasmid construction was performed using Lipofectamine® 2000 Transfection Reagent with a similar protocol as the siRNA transfection (chapter 3.2.2). Shortly, one day before transfection, RGM-1 cells were seeded in the 6-well plate at 2×10^6 cell density in 3 mL fully supplemented growth medium (plus 10% v/v FBS). This medium was replaced by 3 mL Opti-MEM® I reduced serum medium 4 h before transfection. Then cells were

transfected with 4 µg corresponding plasmid, respectively, using Lipofectamine® 2000 at 1 µg/mL. Different with siRNA transfection, after 4 hours, 10% v/v FBS was added to the transfection mix. At 8 hours after transfection, cells were washed replaced with the selective medium: fully supplemented including 10% v/v FBS and 0.5 mM G418-optimized selective antibiotic concentration. Cells were cultured for another 24-72 h with this selective medium until cell islets were formed. Cell islets were monitored under the microscope every day. The most distinctly separated cell isles were carefully separately trypsinized and transferred to separate wells of a 48-well plate using a 10 µL tip. With the selective medium, they were allowed to grow to confluence and those populations forming monolayers were transferred to 6-well plate, and then to a flask. After reaching confluence, the colony cells were analyzed by RT-PCR and Western blot. The primers and antibodies used are shown in chapter 2.

3.9 Statistical analyses

The statistical analyses were performed with the Excel 2003 programme using the Student's t-test. The error bars in the figures represent ± SD. Significant differences between the mean values of the different experimental groups are indicated by asterisks ($P \leq 0.05$: significance, one asterisk; $P \leq 0.01$: highly significance, two asterisks; $P \leq 0.001$: extremely high significance, three asterisks).

4   Results

This chapter presents the results of four connected projects all concerned with the functional aspects of TFFs *in vivo* and in *vitro*. As model systems, the GI tract and the CNS were used:

(a) studies of the gastric epithelial cell line RGM-1 (*in vitro*; 4.1.1);

(b) studies of a mouse model of ileitis after oral *T. gondii* infection (*in vivo*; 4.1.2);

(c) studies of a mouse model for encephalitis after i.p. *T.gondii* infection (*in vivo*; 4.2.1);

(d) studies of primary cell cultures from rat brain (*in vitro*; 4.2.2).

4.1   TFF analysis in the GI system

4.1.1 *Analysis of gastric epithelial RGM-1 cells after in vitro wounding*

4.1.1.1   Expression profiling of stationary and migratory RGM-1 cells

Expression profiles of migratory and stationary cells after *in vitro* wounding were analyzed in RGM-1 cells, a non-transformed gastric epithelial cell line well-established as an *in vitro* model for gastric restitution (Nakamura *et al.*, 1998; Osada *et al.*, 1999; Ragasa *et al.*, 2007).

In *in vitro* wounding experiments, the stationary and migratory cells were isolated respectively as described in chapter 3.2.4. Subsequently both cell populations were used for RT-PCR analysis (Figure 14A). The expression profiles of selected genes revealed differences between the migratory and stationary cells. β-actin used as an internal control for the integrity of the cDNA showed comparable expression in all samples. The corresponding semi-quantitative analysis (normalized against β-actin) is shown in Figure 14B.

As a gene representing the terminal differentiation of gastric surface mucous cells (Karam *et al.*, 2004; Hoffmann, 2012, 2013b), Tff1 was significantly up-regulated in migratory cells when compared with stationary cells. A significant up-regulation in migratory cells was also observed for the expression of Acta2/α-Sma, Ccna2 and Survivin/Birc5.

In contrast, the expression of Gkn2, Pgc, Muc16, Sdf-1/Cxcl12 and Lgr5 was significantly down-regulated in migratory cells; whereas Tff3 expression was variable with a tendency to be reduced in migratory cells.

Vim and β-actin showed comparable expression in stationary and migratory cells.
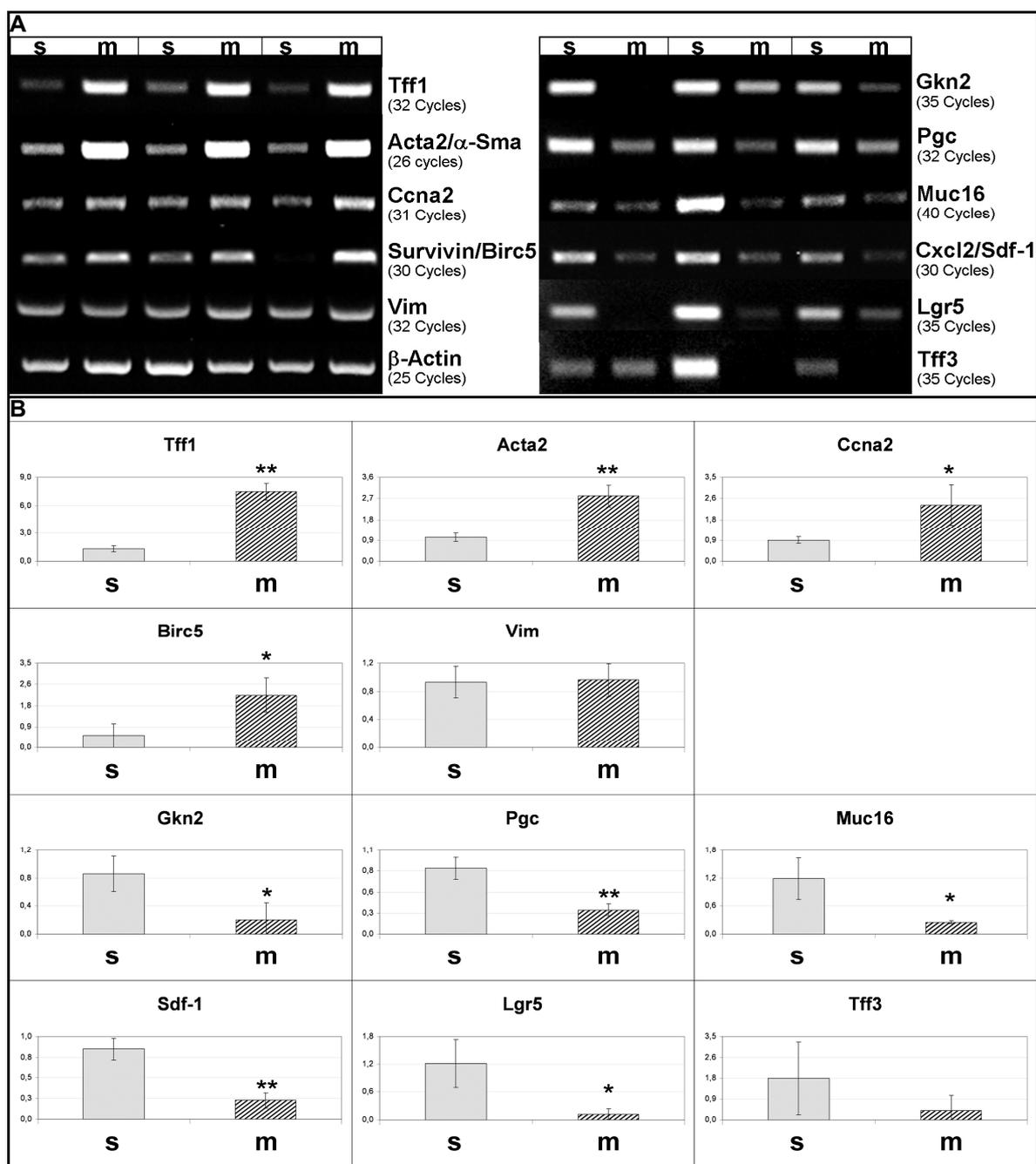
Figure 14: Expression profiling of stationary and migratory RGM-1 cells (RT-PCR analyses)
(A) Tff1, Acta2/α-Sma, cyclin A2 (Ccna2), survivin/Birc5, Vimentin (Vim), gastrokine 2 (Gkn2), Tff3, pepsinogen C (Pgc), mucin 16 (Muc16), stromal cell-derived factor-1 (Sdf1/Cxcl12) and leucine rich repeat containing G protein coupled receptor 5 (Lgr5) expression was monitored in RGM-1 cells 48 h after scratch wounding (three independent experiments). Both stationary (s) and migratory (m) cells were isolated and analyzed separately. The integrity of the cDNAs was tested by monitoring the transcripts for β-actin. The number of amplification cycles is given in parentheses. **(B)** The semi-quantitative evaluation of the corresponding transcript levels was normalized against β-actin (relative gene expression levels). The significance of the differences between stationary and migratory cells is indicated by asterisks.

Based on the elevated Tff1 transcript levels in the migratory RGM-1 cells, the expression of TFF1 peptide was also compared in stationary and migratory cells by immunofluorescence analysis. The repopulated zone of migratory cells and the zone of stationary cells were analyzed 24 h after scratch wounding (Figure 15A). Generally,

strongly Tff1 positive cells were mainly detected in the migratory zone. A semi-quantitative analysis of the relative Tff1 immunoreactivity per cell (for details of analysis, see chapter 3.7.1.3) clearly revealed that TFF1 staining is predominantly localized in migratory RGM-1 cells and that the difference is highly significant when compared with stationary cells (Figure 15B). The Tff1 immunofluorescence in the migratory cells is shown in Figure 15C, which indicates that TFF1 is probably localized in secretory granules.

The specificity of the antiserum anti-mTff1-1 was tested by Western blot analysis, which revealed that the antiserum detected Tff1 from both the mouse and the rat stomach and the immunoreactivity could be competitively inhibited by the synthetic peptide used for immunization (Figure 16).
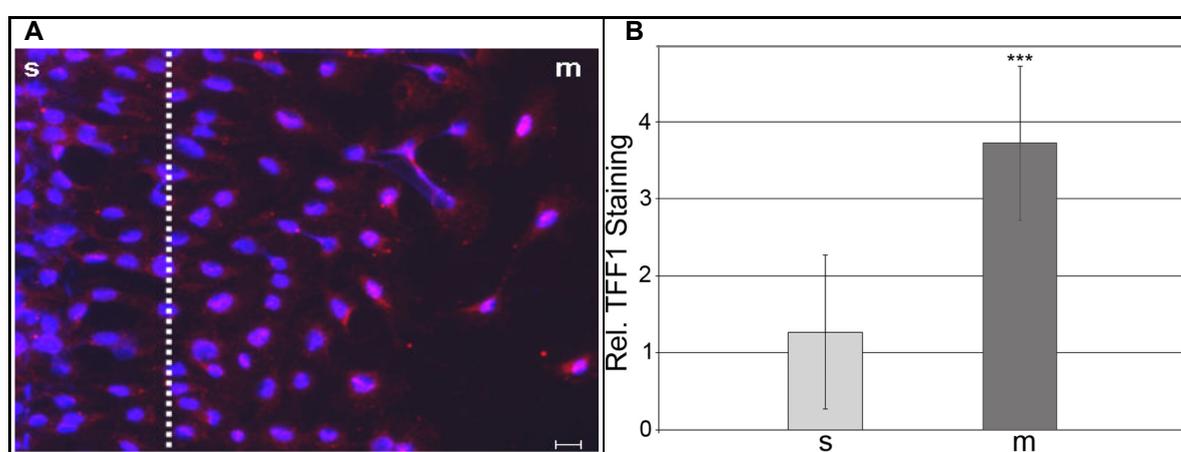
Figure 15: TFF1 peptide expression in the RGM-1 cells after 24 h wound healing
Scratch-wounded RGM-1 cells were allowed to migrate for 24 h. Immunofluorescence staining was performed with anti-mTff1-1 antiserum and Cy3-labeled secondary antibody (red); nuclei were counterstained with DAPI (blue). **(A)** Both the stationary (**s**) and the migratory (**m**) zones were imaged in one photo. The scratch wound is indicated by the white dotted line. **(B)** The relative Tff1 staining per cell is shown in stationary (**s**) and migratory cells (**m**). For each group 16 photographs from 5 different cover slips were analyzed. The difference between stationary and migratory cells is highly significant ($p < 1 \times 10^{-6}$). **(C)** Typical Tff1 immunofluorescence in migratory cells (Cy3 label, red). Nuclei appear in blue (DAPI). Scale bars: 20 µm
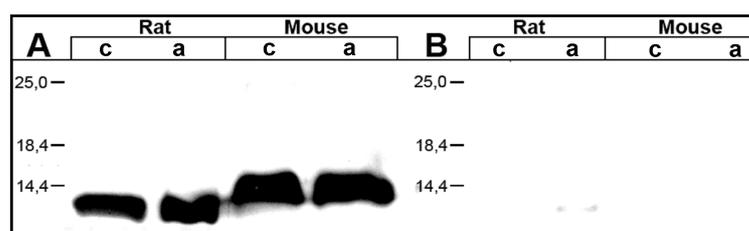
Figure 16: Western blot analysis for specificity test of anti-mTff1-1
SDS-PAGE under reducing conditions, subsequent Western blot analysis. **(A)** Extracts of the gastric corpus **(c)** and antrum **(a)** from the rat and the mouse, respectively, were analyzed using the affinity-purified anti-mTff1-1 antiserum. **(B)** Analysis after competition with the synthetic peptide FHPMAIENTQEEECPF. The molecular weight standard is shown on the left.

4.1.1.2   RNAi targeting Tff1 negatively influences migration of RGM-1 cells

Based on the clear differences in Tff1 expression levels between migratory and stationary RGM-1 cells (chapter 4.1.1.1), the further investigations were focussed on the function of TFF1 during the wound healing processes. The expression of Tff1 was mainly restricted to migratory RGM-1 cells (Figure 14, Figure 15) indicating that Tff1 may play a role in the cell migration. Moreover, a motogenic effect of TFF1 *in vitro* was reported previously (Marchbank *et al.*, 1998; Prest *et al.*, 2002; Buache *et al.*, 2011). Thus, it was tempting to test whether inhibition of Tff1 expression would affect migration of RGM-1 cells. Thus, Tff1 transcripts in RGM-1 cells were knocked down during the wound healing by siRNA.

RNAi experiments were carried out with three different RNAi duplexes targeting Tff1 (Tff1-siRNA1, Tff1-siRNA2, Tff1-siRNA3, see chapter 2.6). Following transfection with the siRNA duplexes or the negative control siRNA, respectively, RGM-1 cells were analyzed after *in vitro* scratch wounding by calculating the repopulated area after 24 h. The effects of three non-overlapping Tff1-siRNAs were tested with different concentrations, e.g. 62.5 nM and 125 nM (Figure 17).
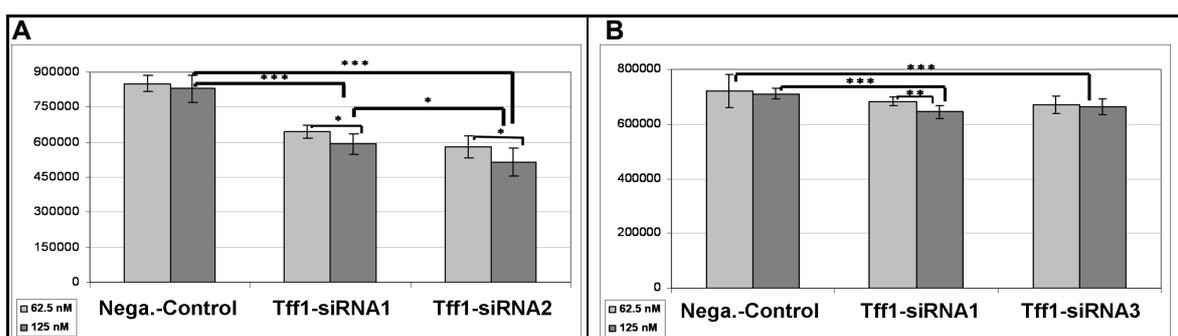
Figure 17: Concentration dependent siRNA duplexes efficiency test
RGM-1 cells treated either with stealth RNAi[TM] negative control or Tff1-siRNA1, 2, 3 were scratched and allowed to migrate in serum-free medium for 24 h. The wound areas of both the negative control group and the Tff1-siRNAs group were photographed 0 h and 24 h after the scratch at the exact same positions. Two concentrations of siRNA were tested: 62.5 nM and 125 nM. The re-populated areas calculated by their pixel numbers are shown. **(A)** Tff1-siRNA efficiency compared between Tff1-siRNA1 and Tff1-siRNA2. **(B)** Tff1-siRNA efficiency compared between Tff1-siRNA1 and Tff1-siRNA3.

All three siRNAs showed positive RNAi effects and the strongest knock-down effect was obtained with Tff1-siRNA2 at the concentration of 125 nM, which was further used for the subsequent wound healing experiments.

In the following studies, RGM-1 cells transfected with 125 nM Tff1-siRNA2 showed diminished migratory activity resulting in a smaller repopulated area when compared with the negative control and this effect was highly significant (Figure 18).

Furthermore, the cells transfected with 125 nM Tff1-siRNA2 were also analyzed by expression profiling of stationary and migratory cells (Figure 19). β-actin used as an internal control for the integrity of the cDNA showed comparable expression in all samples. The corresponding semi-quantitative analysis (normalized against β-actin) is shown in Figure 19B. As expected, Tff1 expression was suppressed in RGM-1 cells

transfected with Tff1-siRNA2 when compared with cells transfected with the negative control siRNA. Moreover, the expression level of Gkn2 was elevated in RGM-1 cells transfected with Tff1-siRNA2; whereas Acta2/α-SMA expression was reduced in these cells. Expression of β-actin was comparable in all samples.
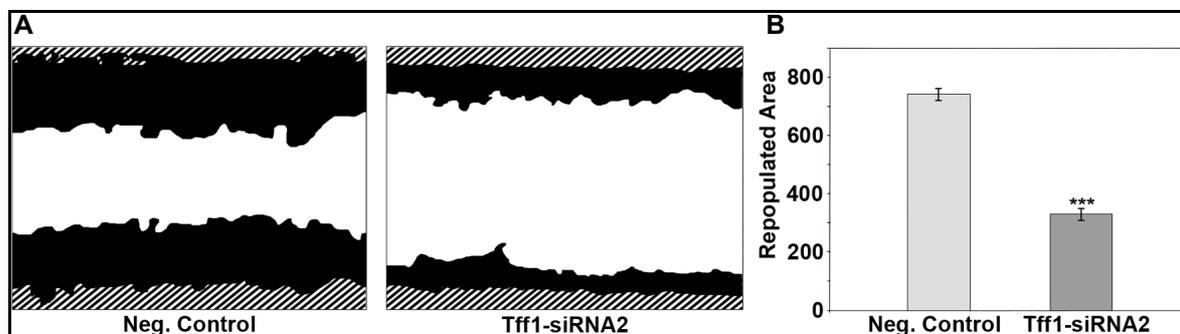
**Figure 18: RNA interference and analysis of cell migration rates**
RGM-1 cells treated either with 125 nM stealth RNAi[TM] negative control or 125 nM Tff1-siRNA2 were scratched and allowed to migrate in serum-free medium for 24 h. The wound areas of both the negative control group and the Tff1-siRNA2 group were photographed 0 h and 24 h after the scratch at the exact same positions. **(A)** In a typical experiment, the area of the re-populated zone covered with cells is schematically marked in black (24 h); whereas the stationary cells' zone is hatched (0 h); the non-populated area is shown in white. **(B)** The re-populated areas calculated by their pixel numbers are shown (for each group 46 photographs from 3 different experiments were analyzed). The difference between the negative control and Tff1-siRNA2 is highly significant (P= 3.62 x 10^{-6}).
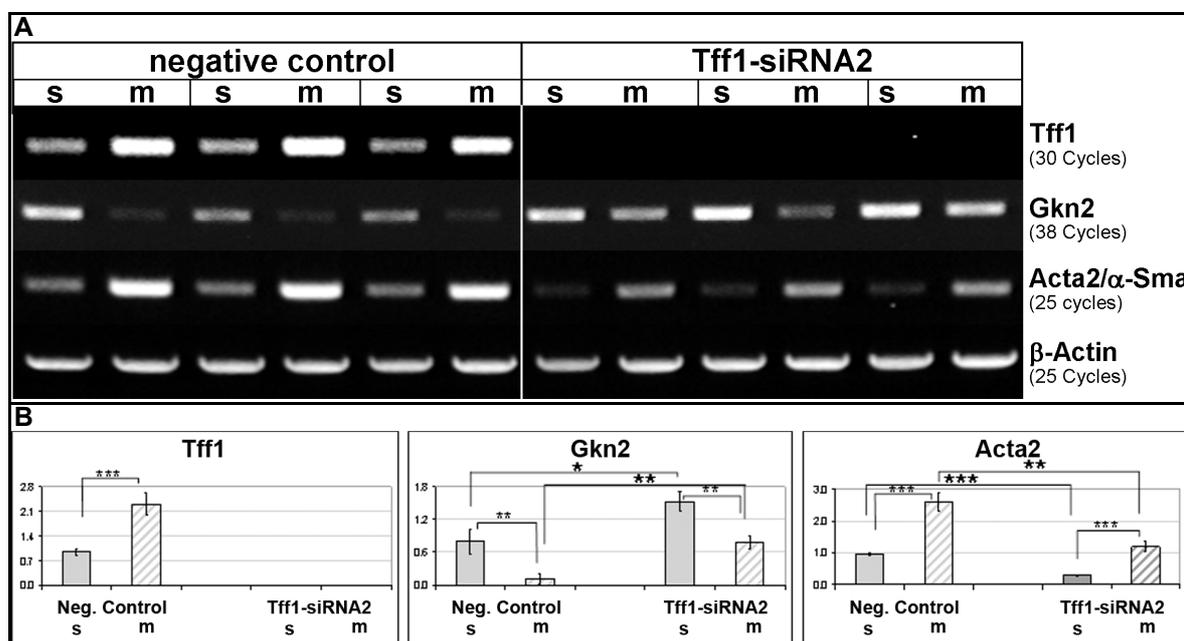
Figure 19: Expression profiling of stationary and migratory RGM-1 cells (RT-PCR analyses of RNAi experiment)
(A) RGM-1 cells were pre-treated with the stealth RNAi[TM] negative control or Tff1-siRNA2. Then, Tff1, gastrokine 2, and Acta2/α-Sma expression was monitored 24 h after scratch wounding (3 independent experiments). Both the stationary (s) and migratory (m) cells were isolated and analyzed separately. The integrity of the cDNAs was tested by monitoring the transcripts for β-actin. The number of amplification cycles is given in parentheses. **(B)** The semi-quantitative analysis of the corresponding transcript levels were normalized against β-actin (relative gene expression levels). The significance of the differences between stationary and migratory cells is indicated by asterisks.

4.1.2 Analysis of the mouse ileum after oral *T. gondii* infection (murine ileitis model*)*

4.1.2.1 Genotyping and infection of the mice

The role of TFF3 in the ileum during the inflammation and immune response was investigated here by studying Tff3^{KO} mice and their wild-type counterparts after oral infection with a type II strain of *T. gondii* (ME49).

Genotyping of mice used for the experiment was performed via tail blot (Figure 20). The corresponding primers were described before (see chapter 3.3.1). As expected, Tff3 expression was not detectable in Tff3^{KO} mice and the expression of the inserted *neo* gene was detected.
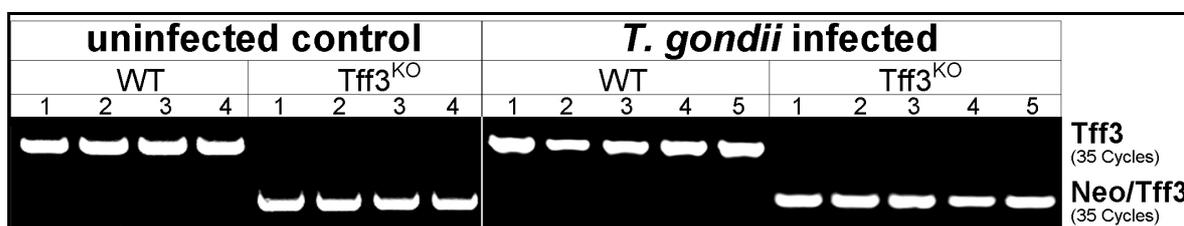
Figure 20: Tail blot analysis
The genotype of the experimental mice was determined by PCR analysis of the genomic DNA isolated from the tail of each mouse (both control and orally *T. gondii* infected group, respectively). The number of amplification cycles is given in parentheses.

Infection of the mice was as follows: 18 mice were divided into two groups: 8 mice (4x wild type and 4x Tff3^{KO}) for the uninfected control group and 10 mice (5x wild type and 5x Tff3^{KO}) for the *T. gondii* infected group. In the latter, 3 *T. gondii* cysts (ME49, type II strain) were orally administered per mouse (infection was performed by Dr. I. Dunay, IMMB, Magdeburg). The experimental infection was for 7 days and the mouse ileum was then obtained and analyzed.

4.1.2.2 Tff3^{KO} mice have a different immune response in the ileum after oral T. gondii infection

The gene expression profile of mouse ileum (after oral infection, with 3 *T. gondii* cysts for 7 days) was tested by RT-PCR (Figure 21A). β-actin used as an internal control for the integrity of the cDNA showed comparable expression in all samples. The corresponding semi-quantitative analysis (normalized against β-actin) is shown in Figure 21B.

Tff1 expression was hardly detectable in the ileum of uninfected mice; whereas there was an elevated expression after *T. gondii* infection (5/10 mice). In contrast, Tff3 was stably expressed in the wild type ileum of both control and infected groups. Tff2 was also found mainly in the uninfected control group. Interestingly, its expression level was decreased in Tff3^{KO} mice.

As typical Th1-associated cytokines after *T. gondii* infection, Ifnγ, Il-12αp35-2, Il-1β,

Il-10 and Tnfα were all induced in the infected group. Surprisingly, the up-regulation of these genes was significantly decreased in Tff3[KO] mice with exception of interleukin 10 (Il-10). This result indicates that the Tff3[KO] mice may have a different immune response in the ileum during the early stage of oral infection with *T. gondii*.
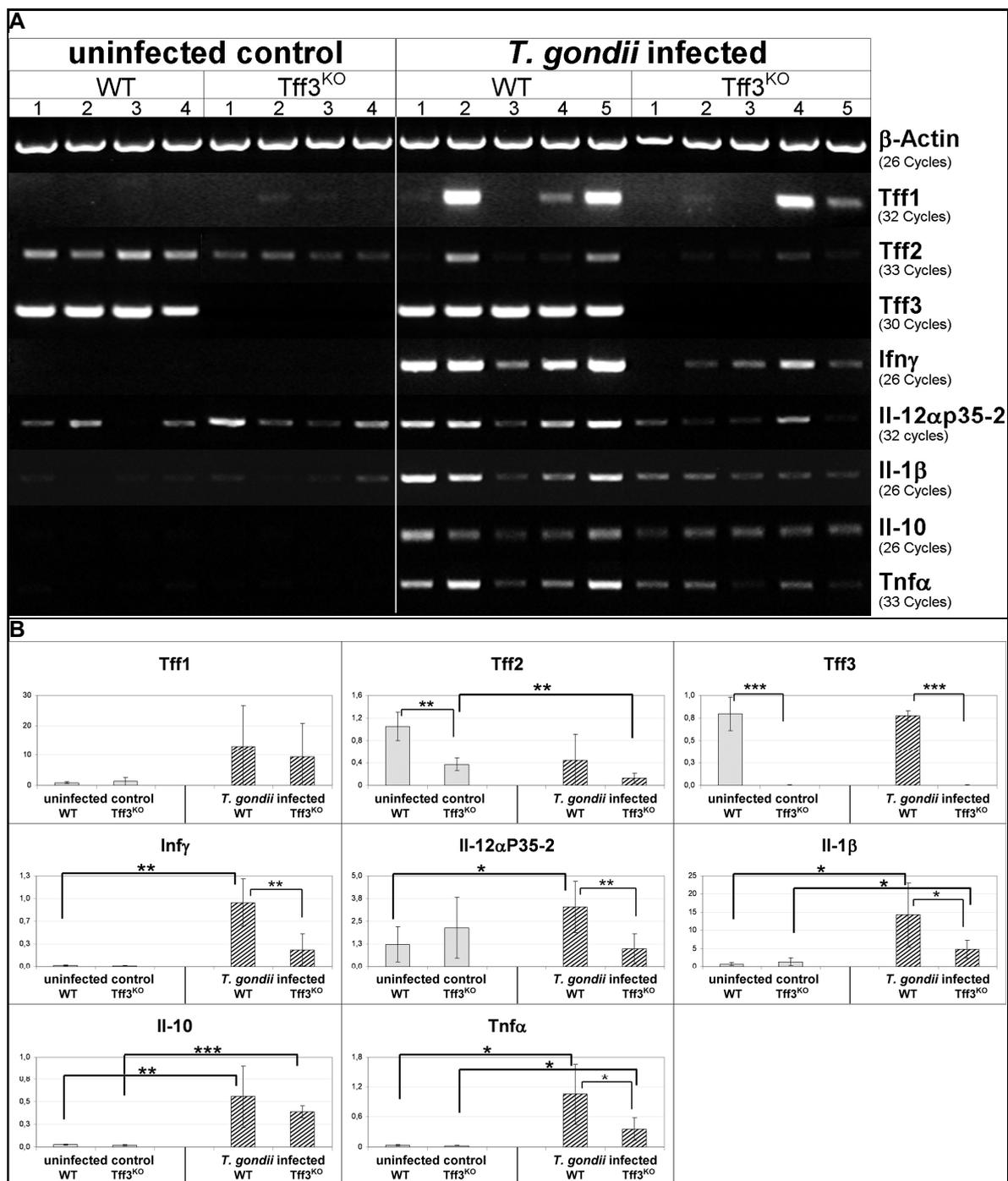
Figure 21: Expression profiling of the mouse ileum (RT-PCR analyses)
(A) Tff1, Tff2, Tff3, interferon gamma (Ifnγ), interleukin-12 subunit alpha isoform 2 (Il-12αp35-2), interleukin 1b (Il-1β), interleukin 10 (Il-10) and tumour necrosis factor α (Tnfα) expression was monitored in the ileum of mice with or without oral *T. gondii* infection (3 cysts for 7 days). The integrity of the cDNAs was tested by monitoring the transcripts for β-actin. The number of amplification cycles is given in parentheses. **(B)** The semi-quantitative analysis of the corresponding transcript levels (relative gene expression levels normalized against β-actin). The significance of the differences among groups is indicated by asterisks.

4.2 TFF expression in the CNS

4.2.1 Cerebral TFF expression after intraperitoneal *T. gondii* infection (murine *Toxoplasma* encephalitis model)

4.2.1.1 Genotyping and infection of the mice, infection efficiency test

Here, TFF expression was monitored in a mouse model of experimental *Toxoplasma* encephalitis (TE). Intraperitoneal infection with type II strain of *T. gondii* (DX) was performed with both Tff1^{KO} and Tff2^{KO} mice as well as their wild-type counterparts.

Genotyping of the mice used for the experiment was performed via tail blot (Figure 22). The corresponding primers were described before (see chapter 3.3.1). As expected, Tff1 expression was not detectable in Tff1^{KO} mice and the expression of the inserted *neo* gene was detected. Similarly in Tff2^{KO} mice, Tff2 expression was not detectable; instead, the inserted *neo* gene was detected.
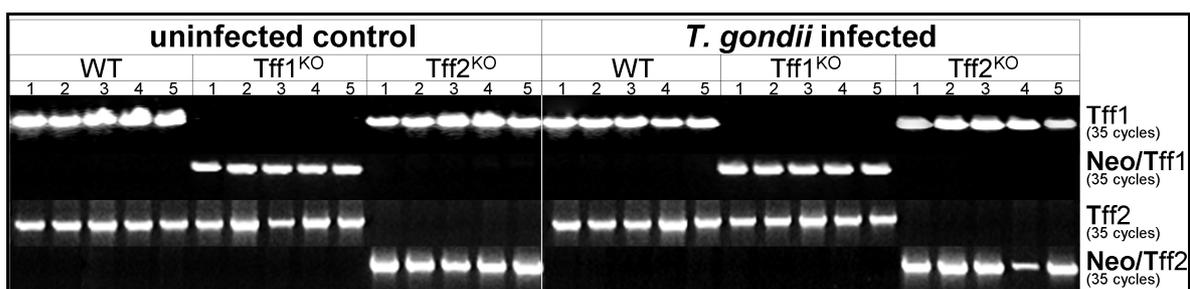
Figure 22: Tail blot analysis
The genotype of the experimental mice was determined by PCR analysis of the genomic DNA isolated from the tail of each mouse (both control and *T. gondii* infected (i.p.) group, respectively). The number of amplification cycles is given in parentheses.

Infection of the mice was as follows: 30 mice were divided into two groups: 15 mice (5x wild type, 5x Tff1^{KO} and 5x Tff2^{KO}) for the uninfected control group and 15 mice (5x wild type, 5x Tff1^{KO} and 5x Tff2^{KO}) for the *T. gondii* infected group. In the latter, 5 *T. gondii* cysts (DX, type II strain) were administered intraperitoneally per mouse (infection was performed by Dr. U. Händel, IMMB, Magdeburg). The experimental infection was for 4 weeks.

Invasion of the parasite was determined by PCR using the genomic DNA isolated from the heart of the experimental mice (Figure 23). The parasite DNA was detected targeting the *T. gondii* strain RH repeat region (Patrat-Delon *et al.*, 2010; GenBank® accession no. AF487550.1, corresponding primer pair: T.g/RHrep, see chapter 2.8). As expected, *T. gondii* DNA was detectable in the *T. gondii* infected mice only and not in the uninfected control mice.

Furthermore, the presence of parasites in the brain was also detected by immunohistochemistry (Figure 24) using an anti-*T. gondii* antibody (see chapter 2.3.2).

All sections from infected brains showed positive *T. gondii* staining (Figure 24B, D, F), whereas all sections from uninfected brains were negative (Figure 24A, C, E).
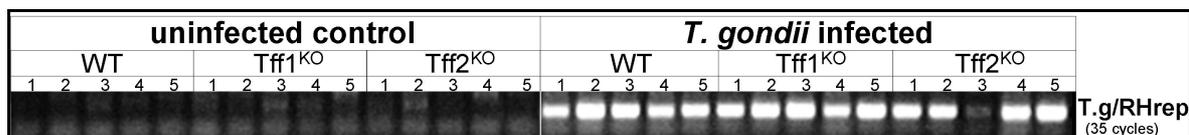
Figure 23: Parasite DNA test
The expression of *T. gondii* strain RH repeat region (T.g./RHrep) was tested by PCR. Genomic DNA was isolated from the heart of the mice (both control and *T. gondii* infected groups). The number of amplification cycles is given in parentheses.
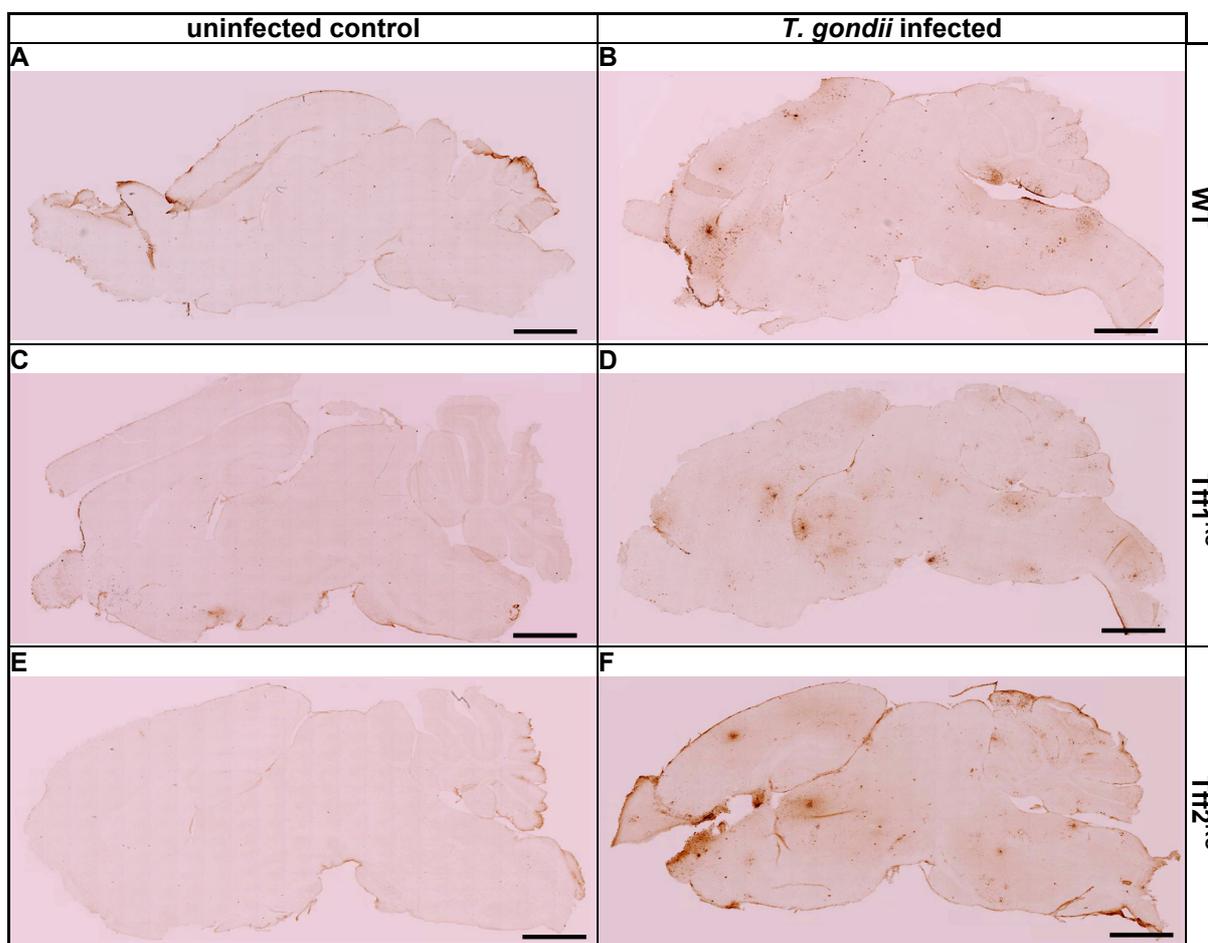
Figure 24: *T. gondii* localization in mouse brain (ABC stain)
Free floating staining of *T. gondii* in control (**A**: wild type, **C**: Tff1^{KO}, **E**: Tff2^{KO}) and infected (**B**: wild type, **D**: Tff1^{KO}, **F**: Tff2^{KO}) mice brain (i.p. infection with 5 *T. gondii* cysts for 11 days). Each overview presents a merge of about 300 single photos. All sections were stained and photographed under the same conditions. The staining in the meninges region was non-specific. Scale bars: 500 µm

4.2.1.2 TFF expression profiling in mouse brain after T. gondii infection: up-regulation of TFF1

The expression profiles for Tff1, Tff2 and Tff3 in different tissues were monitored via RT-PCR (Figure 25, on page 62). The brain was divided into the cerebellum and the

remaining brain (brain without cerebellum). The stomach was used as the internal control because of its well known Tff expression profile. β-actin used as an internal control for the integrity of the cDNA showed comparable expression levels in all samples. The corresponding semi-quantitative analysis (normalized against β-actin) is shown in Figure 25B. Generally, Tff1, Tff2 and Tff3 were detectable in stomach and differently expressed in brain.

In the uninfected control group, Tff1 was strongly expressed in the stomach as expected (except in Tff1^{KO} mice). Trace amounts of Tff1 were also detectable in the cerebellum and in the remaining brain (35 amplification cycles, data not shown). After *T. gondii* infection, Tff1 expression level in the infected group showed almost no change in the stomach but was significantly induced in the cerebellum and the remaining brain. Moreover, the up-regulation of Tff1 expression in the Tff2^{KO} mouse cerebellum and remaining brain was significantly higher than in wild type mice.

Aside from the expected expression of Tff2 in the stomach (except in Tff2^{KO} mice), Tff2 was also found in the brain with a significant up-regulation in Tff1^{KO} mice. However, Tff2 expression was not changed after *T. gondii* infection in both the brain and the the stomach. Of note, trace amounts of Tff2 were also detectable in the remaining brain with 35 amplification cycles (data not shown).

Tff3 expression was also detectable in both the stomach and the brain of all mice. In the brain, Tff3 was found to be expressed mainly in cerebellum and only in trace amounts in the remaining brain (signal was clearly detectable after 35 amplification cycles, data not shown). Interestingly, in the stomach the Tff3 expression level was higher in Tff2^{KO} mice when compared with the wild type mice. However, Tff3 expression was not affected by *T. gondii* infection in both the brain and the stomach (Figure 25B).

Following the up-regulation of Tff1 transcript levels in the brain (in wild type and Tff2^{KO} mice) after *T. gondii* infection (Figure 25), the TFF1 peptide was also localized by immunohistochemistry in the brain of wild type and Tff2^{KO} mice (Figure 26, on page 63). The section overview shows a relatively weak expression of the TFF1 peptide in brain sections of uninfected mice (wild type and Tff2^{KO}; Figure 26A, C), and a higher expression level in infected brain sections (Figure 26B, D).

Furthermore, the specificity of the immunostaining with anti-m-Tff1-1 antiserum was tested by competitive inhibition. In the uninfected wild type mouse brain, anti-m-Tff1-1 detected TFF1 peptide (Figure 27A, on page 63) and this staining could be competitively inhibited by the synthetic peptide used for immunization (Figure 27B).

The correctives of the RT-PCR products for Tff1 and Tff2 from mouse brain have been proven by cloning and sequencing. The results are presented in the Appendix III (on page iii).

Figure 25: Tff expression profiling of the mouse brain and stomach, respectively (RT-PCR analyses)
(A) Tff1, Tff2 and Tff3 expression was monitored in the mouse cerebellum, remaining brain and stomach with or without i.p. *T. gondii* infection (5 cysts, for 4 weeks). The integrity of the cDNAs was tested by monitoring the transcripts for β-actin. The number of amplification cycles is given in parentheses. **(B)** The semi-quantitative analysis of the corresponding transcript level was normalized against β-actin (relative gene expression levels). The significance of the differences among groups is indicated by asterisks.

Figure 26: Localization of TFF1 peptide in the mouse brain (IHC, ABC staining)
Brain sections from control (**A**: wild type, **C**: Tff2^{KO}) and *T. gondii* infected (**B**: wild type, **D**: Tff2^{KO}) mice (i.p., 5 cysts, for 4 weeks) were analyzed with affinity-purified anti-mTff1-1 antiserum. **A-D**: Each overview represents a merge of about 300 single photos. **a-d**: corresponding single photos of the cerebellum (**a-A, b-B, c-C, d-D**). All sections were stained and photographed under the same conditions. Scale bars: **A-D**: 500 µm, a-d: 150 µm.
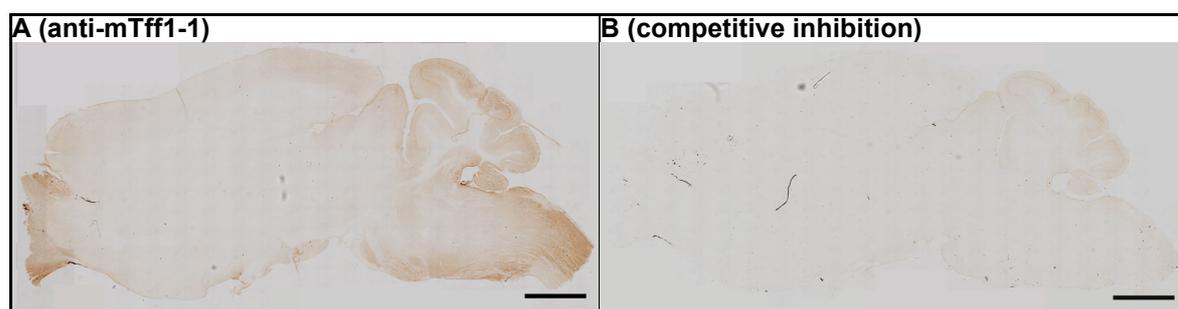
Figure 27: Specificity of the immunostaining with anti-m-Tff1-1 anti-serum (ABC staining)
Parallel brain sections from uninfected wild type mice were either stained with affinity-purified anti-mTff1-1 antiserum **(A)** or, after competition, with the synthetic peptide FHPMAIENTQEEECPF **(B)**. Each overview represents a merge of about 300 photos. All sections were stained and photographed under the same conditions. Scale bars: 500 µm.

4.2.1.3 Expression profiling in the cerebellum after T. gondii infection

RT-PCR and immunohistochemistry staining in the mouse brain showed that the Tffs were mainly expressed in the cerebellum. Thus this brain region was further investigated by systematic RT-PCR analyses.

The expression of the following cytokines involved in the immune response was analyzed: Iba1, Ifnγ, Tnfα, Il-12αp35-2, Il-1β, Il-2, Il-10 as well as two markers for T-cells, i.e., Cd4, Cd8 (Figure 28A, on page 65). β-actin used as an internal control for the integrity of the cDNA showed comparable expression in all samples. The expression of all studied genes was significantly up-regulated in the infected group, compared with the uninfected control group ($p<0.001$). The corresponding semi-quantitative evaluation (normalized against β-actin) is shown in Figure 28B (on page 65).

The expression of Iba-1, the typical marker for microglial cells particularly elevated in the activated status during the immune response (Ito *et al.*, 1998), was significantly induced after the infection. Interestingly, in the uninfected control group, Iba-1 expression was somewhat higher in Tff2^{KO} mice when compared with both wild type and Tff1^{KO} mice.

Cytokines involved in Th1 inflammation (Ifnγ, Tnfα, Il-12, Il-1β, Il2, and Il-10) and T-cell markers (Cd4, Cd8) were all significantly induced after *T. gondii* infection. Of note, expression of most cytokines is not significantly different when compared between wild type, Tff1^{KO} and Tff2^{KO} mice. Only Ifnγ showed a significantly higher expression of Ifnγ in the infected Tff2^{KO} mice when compared with both infected wild type and Tff1^{KO} mice. Furthermore, in the infected group, Cd8 also has a slightly higher expression level in the Tff2^{KO} mice when compared with both the wild type and the Tff1^{KO} mice.

According to the elevation of Iba1 transcript levels in the infected mouse brain (Figure 28), immunohistochemistry analysis of IBA-1 peptide was also performed in the wild type and Tff2^{KO} mouse brain (Figure 29, on page 66). Consistent with the RT-PCR results, the section overview showed a weak IBA-1 expression in uninfected brain sections (Figure 29A, C) but a much higher expression level in the infected brain sections (Figure 29B, D). The induction of IBA1 indicates an activation of microglial cells after *T. gondii* infection. However, the distribution of the IBA-1 and TFF1 peptides in the mouse brain is different (Figure 26, on page 63; Figure 29), which implies that TFF1 peptide is not expressed in microglial cells.
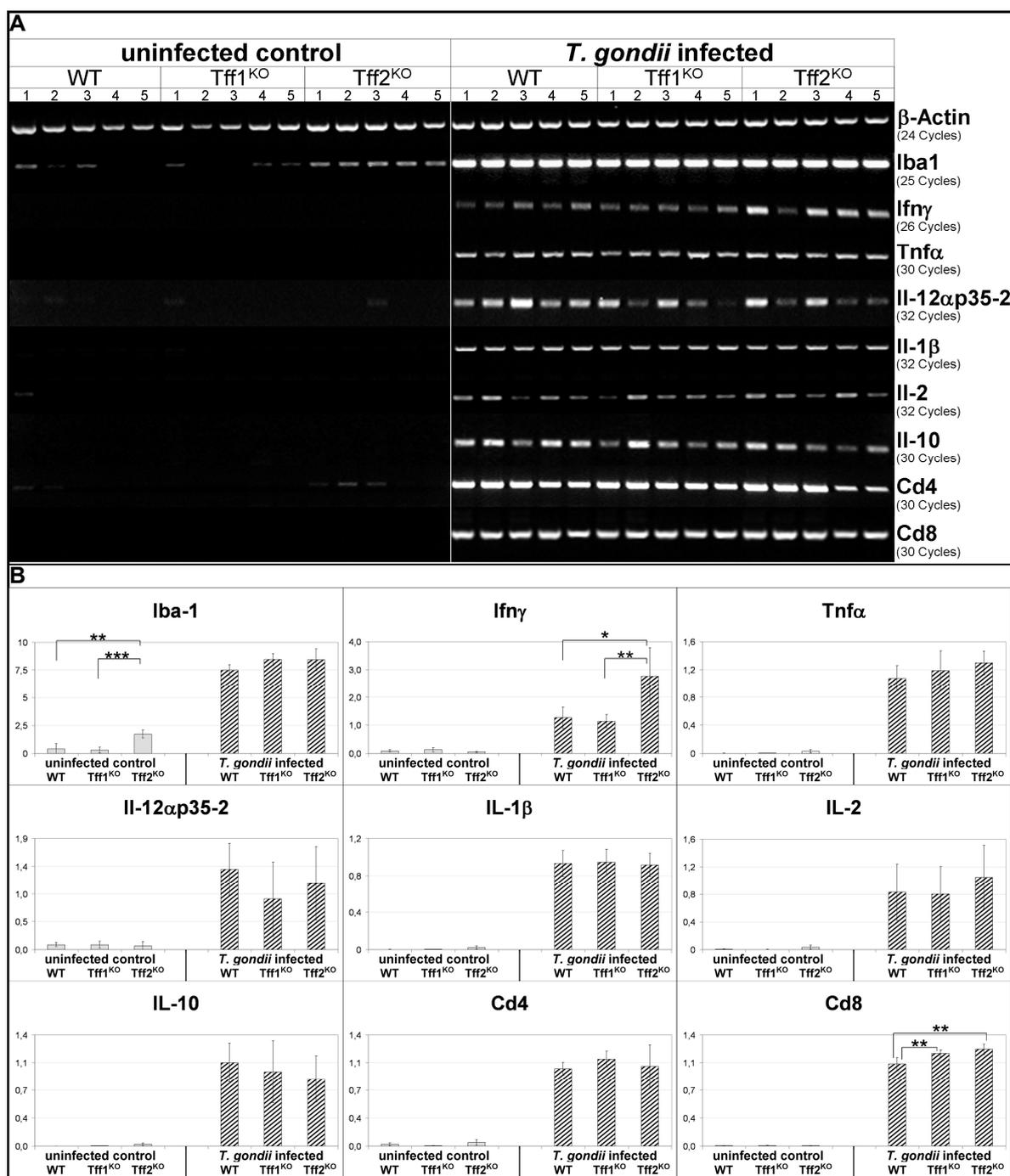
Figure 28: Expression of inflammatory genes in the mouse cerebellum (RT-PCR analyses)
(A) Ionized calcium binding adapter molecule 1 (Iba1), interferon gamma (Ifnγ), tumour necrosis factor α (Tnfα), interleukin-12 subunit alpha isoform 2 (Il-12αp35-2), interleukin 1b (Il-1β), interleukin 2 (Il-2), interleukin 10 (Il-10), Cd4 and Cd8 expression was monitored in the cerebellum (wild type, Tff1^{KO} and Tff2^{KO} mice) with or without i.p. *T. gondii* infection (5 cysts, for 4 weeks). The integrity of the cDNAs was tested by monitoring the transcripts for β-actin. The number of amplification cycles is given in parentheses. **(B)** The semi-quantitative analysis of the corresponding transcript levels was normalized against β-actin (relative gene expression levels). The significance of the differences is indicated by asterisks. The expression levels of all genes are significantly higher in the *T. gondii* infected mice when compared with the uninfected control group (p<0.001; this is not indicated with asterisks).

uninfected control	*T. gondii* infected
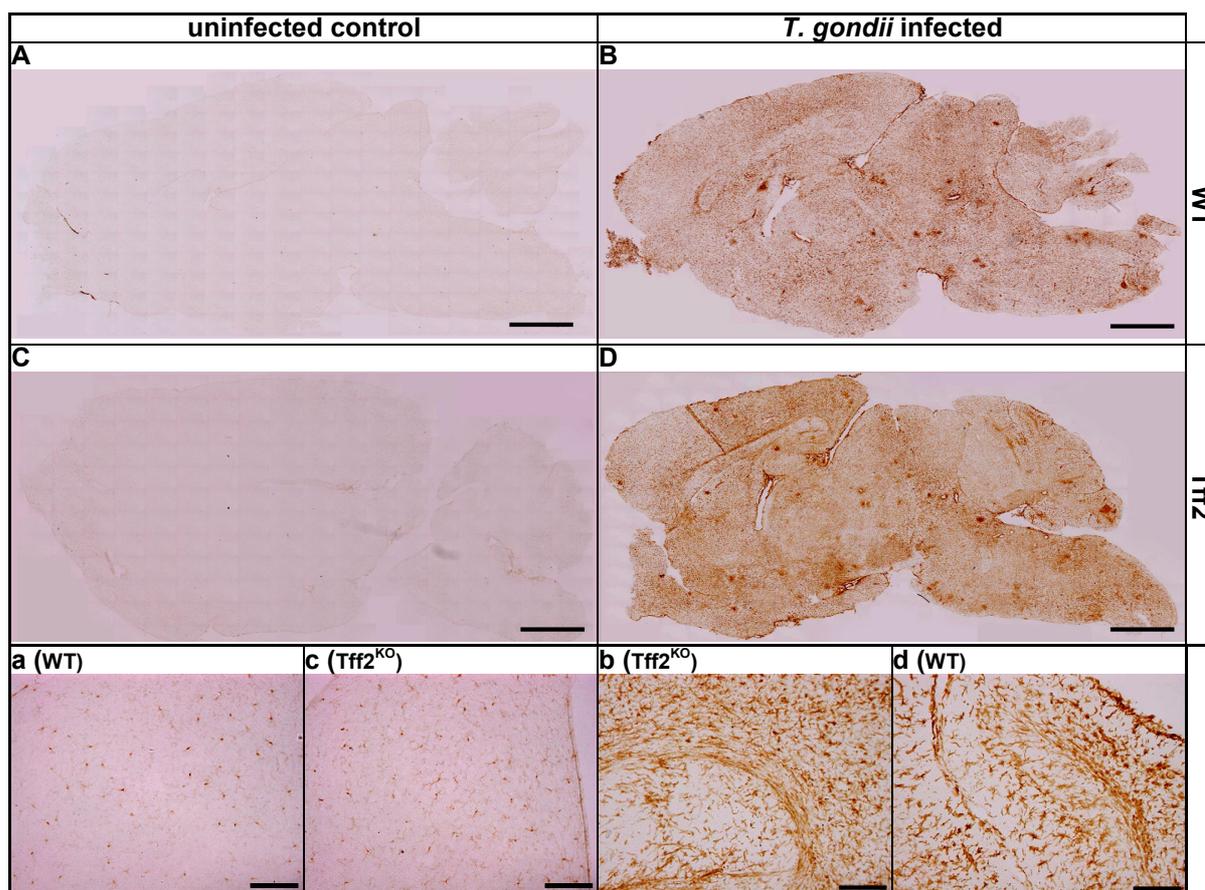
Figure 29: Localization of IBA-1 in mouse brain (IHC, ABC staining)
Brain sections from control (**A**: wild type, **C**: Tff2[KO]) and *T. gondii* infected (**B**: wild type, **D**: Tff2[KO]) mice were analyzed with anti-IBA-1 antibody. A-D: Each overview represents a merge of about 300 single photos. **a-d**: corresponding single photos of the cerebellum (**a**: from **A**; **b**: from **B**; **c**: from **C**; **d**: from **D**). All sections were stained and photographed under the same condition. Scale bars: A-D: 500 μm, a-d: 150 μm.

4.2.2 TFF expression in primary cell cultures from rat brain

The neural cell cultures from rat hippocampus or cortex and glial cell-enriched cultures from rat cortex (all cultures were provided by Dr. Stellmacher, IPT, Magdeburg), respectively, were tested for Tff expression. The following markers for the different cell types were used: IBA1 (Ito *et al.*, 1998) for microglial cells, GFAP for astrocytes (Eng *et al.*, 1971) and MAP2 for neurons (specifically in the perikarya and dendrites; Matus, 1991).

The RT-PCR expression profiles of these cell cultures are shown in Figure 30. β-actin used as an internal control for the integrity of the cDNA showed comparable expression in all samples. Tff1 and Tff2 expression was not detectable in all three cell cultures. The corrective of these two primer pairs were proved in chapter 3.1.1 (for Tff1) and by Znalesniak & Hoffmann (2010; for Tff2). In contrast, Tff3 was stably expressed. As expected, the expression of Gfap was detectable in all three cell cultures. Map2 expression was detectable in both of the neural cell cultures, but could hardly be found in the glial cell-enriched culture. The expression of Iba1 was much weaker in both of the neural cell cultures when compared with the glial cell-enriched culture.

neural cell cultures						glial cell-enriched cultures			
cortex			hippocampus						
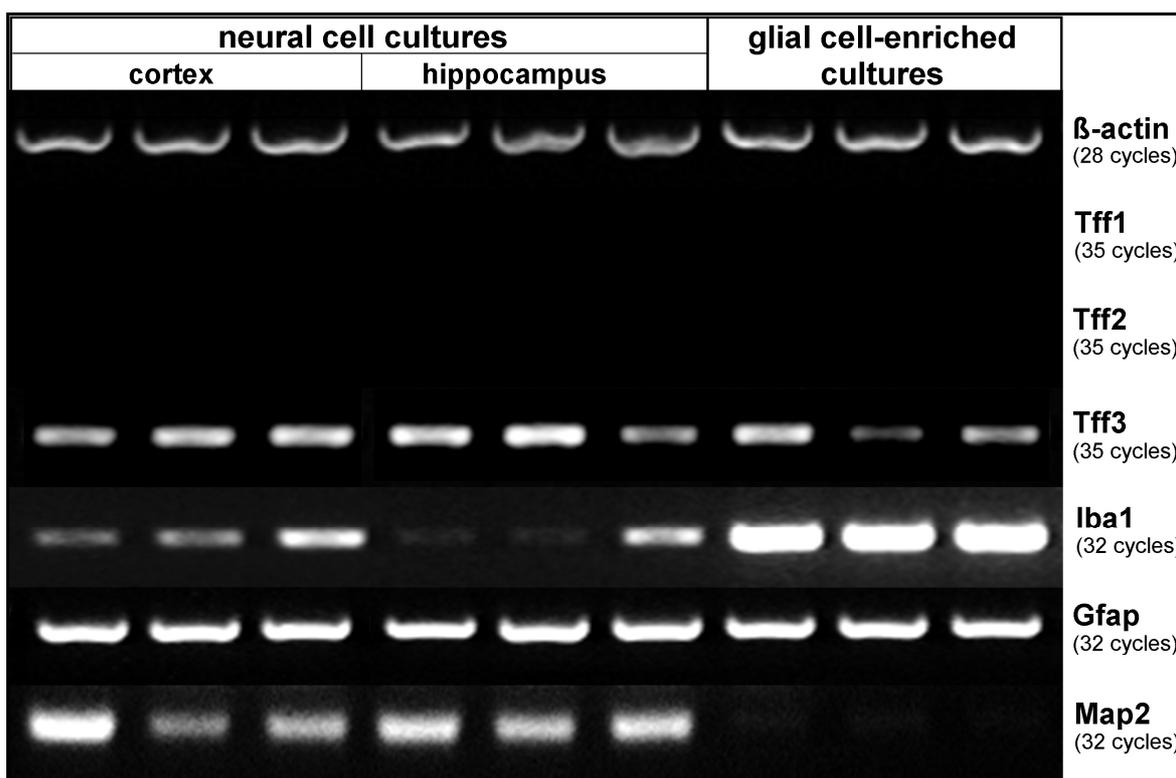
Figure 30: RT-PCR analyses of various primary cell cultures
Tff1, Tff2, Tff3, microtubule-associated protein 2 (Map2), glial fibrillary acidic protein (Gfap) and ionized calcium binding adaptor molecule 1 (Iba1) expression was monitored in rat primary cell cultures. Both neural (respectively from cortex and hippocampus) and glial cell-enriched cell cultures were isolated and analyzed separately. The integrity of the cDNAs was tested by monitoring the transcripts for β-actin. The number of amplification cycles is given in parentheses.

4.2.2.1 Localization of TFF3 peptide in neural cell cultures from the cortex or hippocampus

Based on the stable expression of TFF3 transcripts, the TFF3 peptide was also localized in the different cell cultures by immunofluorescence studies (Figure 31, on page 68; Figure 32, on page 69; Figure 34. on page 70).

In neural cell cultures from both cortex and hippocampus TFF3 was mainly detected in the neurons expressing MAP2 (Figure 31, Figure 34), but not in astrocytes marked by GFAP (Figure 32, Figure 34).

The double immunofluorescence staining in neural cell cultures of both the cortex and the hippocampus indicates that MAP2-positive neurons are also positively stained by TFF3 (Figure 31). However, some of the TFF3-positive cells were not found positively stained for Map2. These cells may represent glial cells. Thus, double immunofluorescence staining was performed with TFF3 and the astrocyte marker GFAP (Figure 32). The results clearly show that TFF3 is not localized in astrocytes (GFAP-positive cells).

Furthermore, a triple immunofluorescence staining of both cortex and hippocampus neural cell cultures was performed (Figure 34, on page 69). Here again, TFF3 is not expressed in astrocytes (GFAP positive cells). However, TFF3 is co-localized with IBA1

(typical of microglial cells) indicating that Tff3 may be expressed not only in neurons but also in microglial cells (Figure 34).

The specificity of the antiserum anti-r-Tff3-2 was also tested by immunofluorescence staining. In the neural cell cultures from both the cortex and hippocampus, anti-r-Tff3-2 could be competitively inhibited by the synthetic peptide used for immunization (Figure 33, on page 69).

4.2.2.2 Localization of Tff3 peptide in glial cell-enriched cultures from the cortex

To further investigate TFF3 expression in different glial cells, corresponding glial cell-enriched cultures were analyzed (Figure 35, on page 71). The antibodies anti-GFAP and anti-IBA1 clearly detected astrocytes and microglial cells, respectively, without any cross reactivity (Figure 35A). Tff3 was clearly expressed in microglial cells (IBA1 positive cells; Figure 35C) and no localization of TFF3 in astrocytes (GFAP positive cells) was found (Figure 35B, C). These results clearly indicate that in the glial cell-enriched cultures TFF3 is expressed in microglial cells but not in astrocytes.
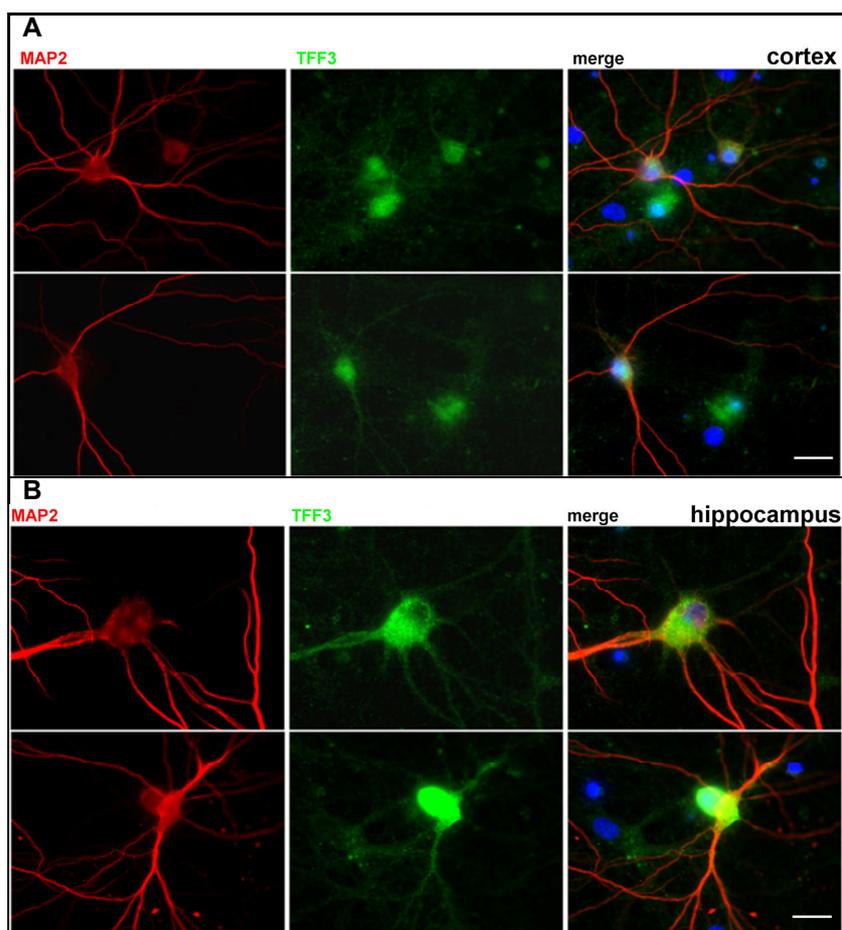
Figure 31: Double immunofluorescence studies of neural cell cultures (MAP2/red, TFF3/green)
Primary cell cultures from the cortex **(A)** or hippocampus **(B)**, respectively, were stained with anti-rTff3-2 antiserum and Alexa Fluor® 488-labeled secondary antibody (green, exposure time 7500 ms). Co-staining was with anti-MAP2 antibody and Cy3-labeled secondary antibody (red, exposure time 500 ms); nuclei were counter-stained with DAPI (blue). Scale bars: 20 μm.
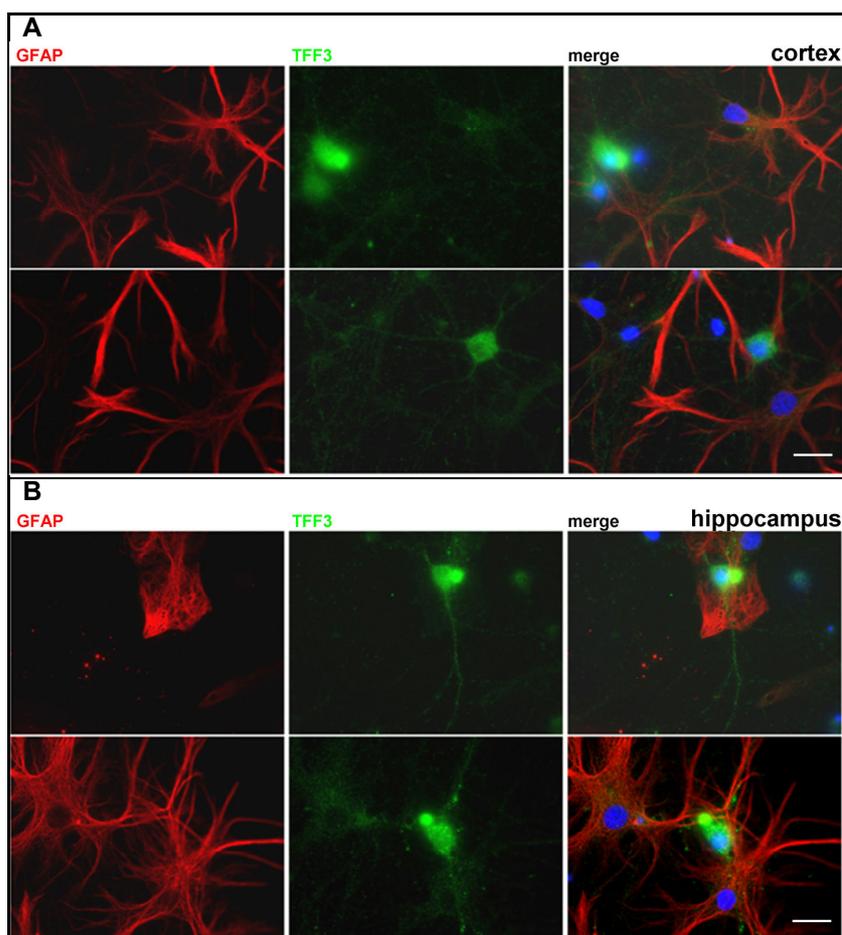
Figure 32: Double immunofluorescence studies of neural cell cultures (GFAP/red, TFF3/green)
Primary cell cultures from the cortex **(A)** or hippocampus **(B)**, respectively, were stained with anti-rTff3-2 antiserum and Alexa Fluor® 488-labeled secondary antibody (green, exposure time 7500 ms). Co-staining was with anti-GFAP antibody and Cy3-labeled secondary antibody (red, exposure time 500 ms); nuclei were counter-stained with DAPI (blue). Scale bars: 20 μm.
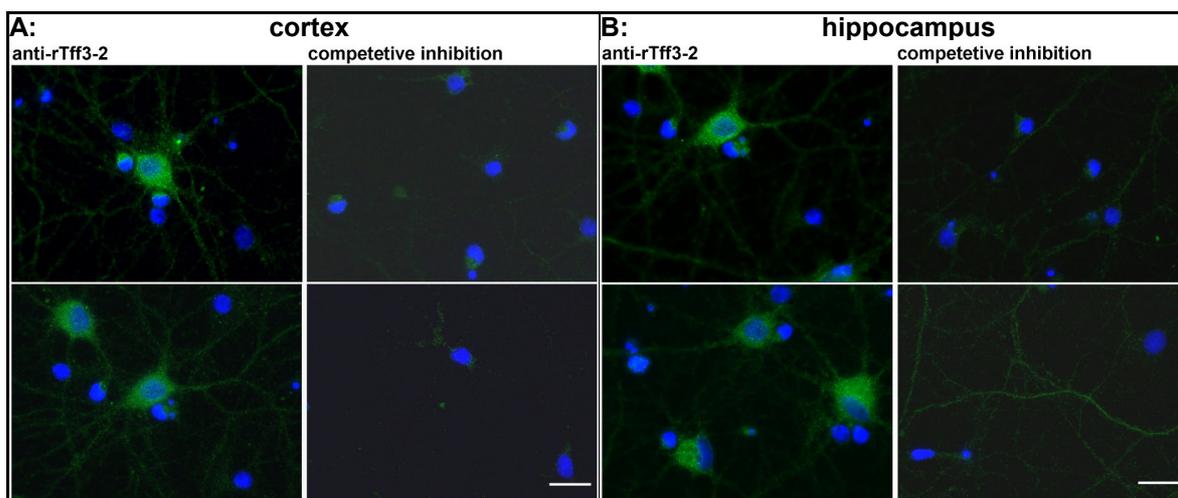
Figure 33: Specificity of immunofluorescence staining with anti-r-Tff3-2 antiserum (TFF3/green)
Cell cultures from the rat cortex **(A)** and hippocampus **(B)**, respectively, were either stained with anti-rTff3-2 antiserum or after competitive inhibition with the synthetic Tff3 peptide (whole rat Tff3 peptide sequence (1-59)), and then labeled with Alexa Fluor® 488-labeled secondary antibody (green, exposure time 7500 ms); nuclei were counter-stained with DAPI (blue). Scale bars: 20 μm.
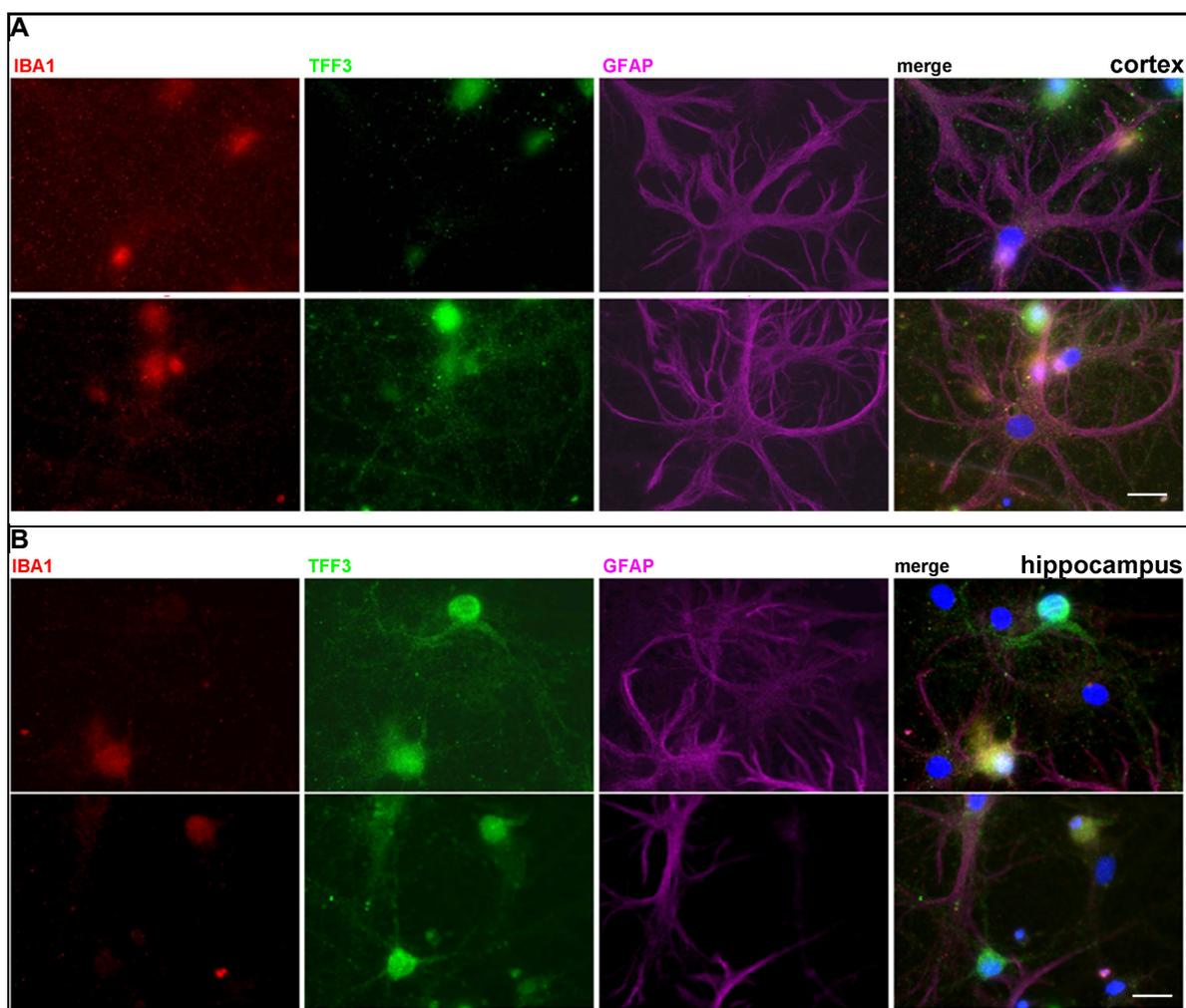
Figure 34: Triple immunofluorescence studies of neural cell cultures (IBA1/red, TFF3/green, GFAP/violet)
Primary cell cultures from the cortex **(A)** or hippocampus **(B)**, respectively, were stained with anti-rTff3-2 antiserum and Alexa Fluor® 488-labeled secondary antibody (green, exposure time 7500 ms). Co-staining was with anti-IBA1 and Cy3-labeled secondary antibody (red, exposure time 8000 ms), as well as anti-GFAP anti-body and DyLight™ 649-labeled secondary antibody (violet, exposure time 3000 ms). Nuclei were counterstained with DAPI (blue). Scale bars: 20 µm.
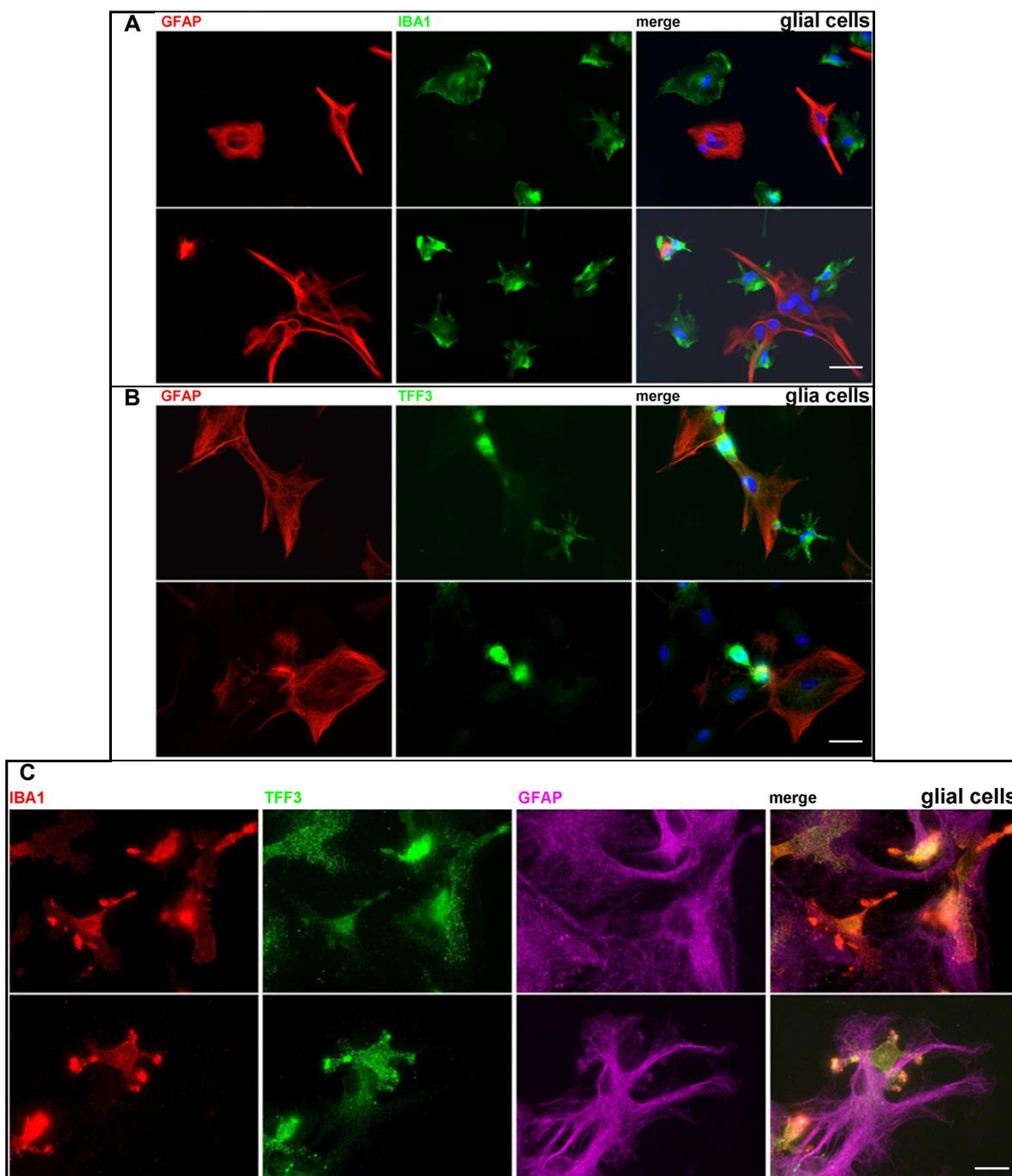
Figure 35: Immunofluorescence studies of glial cell-enriched cultures
Primary glial cell-enriched primary cultures from the cortex: **(A)** double staining with rabbit-anti-IBA1 anti-serum and Alexa Fluor® 488-labeled secondary antibody (**green**, exposure time 200 ms). Co-staining was with anti-GFAP antibody and Cy3-labeled secondary antibody (**red**, exposure time 500 ms); **(B)** double staining with anti-rTff3-2 antiserum and Alexa Fluor® 488-labeled secondary antibody (**green**, exposure time 2500 ms). Co-staining with anti-GFAP antibody and Cy3-labeled secondary antibody (**red**, exposure time 500 ms); **(C)** Triple staining with anti-rTff3-2 antiserum and Alexa Fluor®488-labeled secondary antibody (**green**, exposure time 3500 ms). Co-staining was with anti-IBA1 and Cy3-labeled secondary antibody (**red**, exposure time 3500 ms), as well as anti-GFAP antibody and DyLight™649-labeled secondary antibody (**violet**, exposure time 10000 ms). Nuclei were counterstained with DAPI (blue). Scale bars: 20 µm.

5　Discussion

5.1　TFFs in the GI system

5.1.1　TFF expression and function in RGM-1 cells (*in vitro*)

5.1.1.1　Increased Tff1 synthesis in migratory cells during wound healing processes

The migration of epithelial cells is the major component of the mucosal restitution occurring in the early phase of the mucosal repair (Silen & Ito, 1985; Hoffmann, 2013b). The enhancing effect of the TFF1 peptide on cell migration has been shown in various gastric-, intestinal-, oral-, bronchial-, and corneal-epithelial cells (Playford *et al.*, 1995; Hoffmann *et al.*, 2001; Hoffmann & Jagla, 2002; Prest *et al.*, 2002). Previous studies demonstrated that TFF1 expression is up-regulated after the mucosal injury (Rio *et al.*, 1991; Wright *et al.*, 1992; Taupin & Podolsky, 2003), and after the total wounding (multi scratch assay) in the transformed human bronchial epithelial cell line (BEAS-2B) and human lung adenocarcinoma epithelial cell line (A549; Znalesniak, 2013). TFF1 expression is also strongly up-regulated after treatment with TNFα in *in vitro* models of gastric epithelial inflammation in a dose-dependent manner (Koike *et al.*, 2007).

In this study, Tff1 expression was shown to be increased in migratory RGM-1 cells during wound healing processes. As a secretory product of terminally differentiated gastric surface mucous cells (Kouznetsova *et al.*, 2004), the up-regulated expression of Tff1 in migratory cells is unusual, because normally migratory cells lose the markers of terminal differentiation (Znalesniak *et al.*, 2009). However, this result has been clearly shown on both transcriptional (Figure 14) and protein levels (Figure 15). Of note, the antiserum anti-mTff1-1 used here recognized also Tff1 from rat stomach on a Western blot analysis and the specificity was demonstrated by competitive inhibition with the synthetic peptide used as antigen (Figure 16).

Furthermore, the expression levels of Tff1 and Gkn2 were not parallel but rather contrary in stationary versus migratory RGM-1 cells (Figure 14, Figure 19). The co-expression of these two genes was expected, because human TFF1 has been reported form disulfide-linked heterodimers with GKN2 (Westley *et al.*, 2005; Kouznetsova *et al.*, 2007b). Moreover, as expected, the Tff1-Gkn2 heterodimer was detectable in the rat and mouse stomach tissue (data not shown). One explanation for the discrepancy would be that in RGM-1 cells Tff1 exists in other, different molecular forms (e. g., monomers, homodimers). This assumption is supported by analysis of human TFF1 after gel filtration of antral extracts, which gave clear indications for the existence of additional forms of TFF1 (e.g., TFF1 monomer, TFF1 dimer) in normal human gastric mucosa (Newton *et al.*, 2000) and where the TFF1 was found not only as a TFF1-GKN2 heterodimer but also in small amounts as monomers or homodimers (Kouznetsova *et al.*, 2007b).

The reciprocal regulation of Tff1 and Tff3 expression in stationary and migratory RGM-1 cells respectively (Figure 14) might be due to the fact that they are not co-expressed in the gastric mucosa *in vivo*. In human, TFF1 expression is detectable in terminally differentiated surface mucous cells of both the corpus and the antrum; whereas TFF3 is preferentially expressed in deeper lying surface mucous cells of the gastric antrum (i.e. the proliferative zone) and is hardly detectable in the corpus (Kouznetsova *et al.*, 2004, 2007a, 2011). This different origin might also explain the rather variable expression of Tff3 in RGM-1 cells. Additionally, TFF1 and TFF3 have probably different molecular functions. Gastric TFF3 presumably forms TFF3-FCGBP heteromers, which are mucus components (Albert *et al.*, 2010; Kouznetsova *et al.*, 2011), whereas gastric TFF1 is mainly not associated with mucus (Kouznetsova *et al.*, 2007b).

Furthermore, TFF1 has been reported to suppress the TNFα–mediated NF-κB activation and play an important role in regulating the NF-κB–mediated inflammatory response in the multistep gastric tumorigenesis cascades (Koike *et al.*, 2007). Moreover, the loss of TFF1 is associated with activation of NF-κB–mediated inflammation and gastric neoplasia in mice and humans (Soutto *et al.*, 2011). In this study, the migratory RGM-1 cells showed the tendency to induce the expression of several inflammation related genes, such as Tgfα, Tgfβ1, Tgfβ2 (data not shown). Thus, the up-regulation of TFF1 in migratory RGM-1 cells could indicate a suppressive role of TFF1 in inflammatory processes during the restitution/wound healing. Additionally, in mammary cells, TFF1 exhibited both *in vitro* and *in vivo* anti-tumour-effects (Buache *et al.*, 2011). Therefore, the induction of Tff1 during restitution in RGM-1 cells might prevent excessive cell invasion as well.

Several genes (Acta2/α-Sma, Ccna2 and survivin/Birc5) are also significantly up-regulated in migratory RGM-1 cells after *in vitro* wounding (Figure 14). As a hallmark of myofibroblast differentiation, α-SMA is essential for connective tissue remodelling during wound healing (Tomasek *et al.*, 2002). Generally, the expression of α-SMA is typical of migratory cells and is associated with the generation of increased contractile forces and stress fibre formation (Masszi *et al.*, 2003; Znalesniak *et al.*, 2009; Znalesniak & Hoffmann, 2010).

Cyclin A2 plays a key role in cell cycle regulation by controlling both the S phase (DNA replication) and the G2/M transition (cell growth and protein synthesis/mitosis) in association with Cdk2 and Cdk1, respectively; furthermore, it also negatively controls cell motility by promoting RhoA activation (Arsic *et al.*, 2012). Thus, up-regulation of cyclin A2 expression in migratory RGM-1 cells is not expected to enhance cell motility, but is rather due to progression of migratory cells through the cell cycle (Watanabe *et al.*, 1994; Zahm *et al.*, 1997).

Survivin is expressed predominantly in gastric surface mucous cells and plays a role in mucosal integrity and protection of the gastric mucosa against injury (Chiou *et al.*, 2003). It is a chromosomal passenger protein (Altieri, 2003) and is shown to inhibit apoptosis, to regulate cell division and enhances cell migration and invasion (McKenzie *et al.*, 2010; McKenzie & Grossman, 2012). Furthermore, it was reported to

be expressed only during mitosis (Waligórska-Stachura *et al.*, 2012) and the suppression of survivin in RGM-1 cells was shown to increase the cell damage to injury by indomethacin (Chiou *et al.*, 2005). Thus, the up-regulated expression of survivin in migratory cells is perfectly in line with its inhibitor function of apoptosis and regulation of the cell cycle, because cell migration is coupled to a suppression of apoptosis (Cho & Klemke, 2000).

In contrast, the significant down-regulation of the transcript levels of Pgc (typical of mucous neck and antral gland cells; Kouznetsova *et al.*, 2011) and Gkn2 (secretory peptide of human gastric surface mucous cells) in migratory RGM-1 cells is typical of genes characteristic of terminal differentiation (Znalesniak *et al.*, 2009; Znalesniak & Hoffmann, 2010). Of note, many other known gastric differentiation markers, e.g. gastric lipase (LipF), lysozyme (Lyz) and Tff2 (Hoffmann, 2012, 2013b) were either not detectable or present in trace amounts only (data not shown).

Moreover, Sdf-1 expression level was also down-regulated in migratory RGM-1 cells. This secretory α-chemokine is typically expressed in normal intestinal villus epithelium (Agace *et al.*, 2000). It contributes to mucosal wound healing by enhancing restitution together with its receptor Cxcr4 (Smith *et al.*, 2005) and is important for the active recruitment of stem cells during repair of damaged tissue (Kucia *et al.*, 2005). The down-regulation of Sdf-1 in migratory RGM-1 cell is comparable with the situation in the non-transformed intestinal epithelial cell lines IEC-18 (Znalesniak *et al.*, 2009) and IEC-6 where Sdf-1 promotes restitution (Smith *et al.*, 2005).

The EMT is a physiological process in which epithelial cells acquire the motile and invasive characteristics of mesenchymal cells (Hay, 1995, 2005; Savagner *et al.*, 2005; Moreno-Bueno *et al.*, 2008) and has been reported to generate cells with properties of stem cells (Mani *et al.*, 2008). As a stem cell marker, Lgr5 is characteristic for the population of gastric stem cells that are located mainly at the base of antral glands but not fundic glands (Barker *et al.*, 2010; Kouznetsova *et al.*, 2011; Hoffmann, 2012). Thus the expression of Lgr5 in RGM-1 cells is indicative of the undifferentiated character of this non-transformed cell line and might somehow also be involved in its regeneration source. Moreover, the down-regulation of Lgr5 expression in migratory cells is reminiscent to the down-regulation of the stem cell marker Musashi-1 in migratory IEC-18 cells (Znalesniak *et al.*, 2009), and speaks against the acquisition of stem cell characteristics in these migratory cells. As a consequence, this also suggests that migratory RGM-1 cells do not undergo the EMT. Furthermore, the typical EMT markers, E-cadherin and N-cadherin showed unstable or non-significant alterations in migratory cells compared with stationary cells (data not shown), which is in line with the reports on the IEC-18 cell line (Znalesniak & Hoffmann, 2010; Znalesniak, 2013). Besides, the RGM1 cells show mostly coherent cell migration with few individual pioneer cells moving at the migration front (Figure 4). Therefore the down-regulation of E-cadherin expression is not expected, as the cells do not loose their cell-cell contacts with exception of pioneer cells at the migratory front. This is consistent with previous studies, which show that EMT is not complete in the restitution/wound healing process (Schäfer & Werner, 2008; Znalesniak *et al.*, 2009).

The lack of clear EMT in migratory RGM-1 cells is also supported by the expression of vimentin, which is comparable in stationary and migratory cells. Moreover, the elevated expression of cyclin A2 in migratory cells is another indication against EMT because cyclin A2 is reported to be instrumental in preventing EMT (Bendris *et al.*, 2012). However, the significant down-regulation of Muc16 in migratory cells could point towards a partial EMT because the knockdown of Muc16 (also known as cancer antigen 125 (CA125)) in ovarian cancer cells has been reported to alter epithelial and mesenchymal markers, cell motility and migration (Comamala *et al.*, 2011). Furthermore, up-regulation of α-SMA, which is a typical mesenchymal marker (Kalluri & Weinberg, 2009), could also be a sign for a partial EMT in migratory RGM-1 cells.

5.1.1.2 *Tff1 plays a role in restitution in vitro*

In a functional test of Tff1 during restitution process, RGM-1 cells were transfected with the Tff1-siRNA in the scratch wounding assays. As shown in Figure 17, the *in vitro* restitution was impaired by all three siRNA duplexes and this effect increased with the concentration of the siRNA duplexes. Tff1 expression was dramatically reduced in these cells as expected (Figure 19). The significant down-regulation of α-SMA expression in Tff1-siRNA2-transfected cells indicates that the differentiation of RGM-1 cells into a migratory phenotype was negatively affected by Tff1-siRNA2 (Figure 19).

Insufficient endogenous Tff1 in RGM-1 cells strongly decreased their migration (Figure 18). This result is in agreement with that of TFF1 knockdown experiments using shRNA analyzing the migration of MCF-7 (human breast adenocarcinoma cell line) and ZR75.1 (human breast carcinoma cell line) cells in transwell chambers (Buache *et al.*, 2011). Therefore, Tff1 is a motogenic factor, which probably has a function *in vivo* during restitution of the gastric mucosa by SMCs and during self-renewal. Particularly, a possible up-regulation of TFF1 synthesis in migratory SMCs *in vivo* would be an ideal mechanism to specifically enhance restitution only where topologically needed and to minimize eventual negative side effects of TFF1 such as cell scattering and invasiveness.

In summary, the up-regulation of Tff1 expression in migratory RGM-1 cells after the wounding indicates that secretory Tff1 directly supports cell migration by an autocrine/paracrine mechanism. This is consistent with the observation by Znalesniak *et al.* (2009) that migratory IEC-18 cells up-regulated the expression of genes that support cell migration in many ways, such as plasminogen activator inhibitor-1 (Pai-1), transforming growth factor α (Tgfα), heparin-binding EGF-like growth factor (Hb-Egf), ornithine decarboxylase (Odc), and α-Sma. Moreover, the reduced migration after knockdown of Tff1 by RNAi demonstrates the important role of Tff1 during the restitution process. In addition, Tff1 may also play a role in regulating the inflammatory response through suppression NF-κB–mediated inflammation.

5.1.2 Tff3 plays a role in the intestinal immune response *in vivo* after oral *T. gondii* infection

There are numerous *in vivo* studies indicating the protective and healing effects of TFF peptides in the GI tract (Hoffmann & Jagla, 2002; Kjellev, 2009; Hoffmann, 2013a). Some studies also reported a function in the modulation of the immune response, especially for TFF2 (Baus-Loncar *et al.*, 2005a, 2005b). TFF2 and TFF3 are found not only in the gastric mucosa, but also in lymphoid tissues and can stimulate the migration of monocytes (Cook *et al.*, 1999; Kurt-Jones *et al.*, 2007). Some *in vitro* studies are indicative for a possible function of TFF2 and TFF3 in the recruitment of leukocytes during mucosal inflammation (Graness *et al.*, 2002).

To further test the possible function of TFF3 in the immune responses, a mouse model for the *T. gondii* induced type 1 immunity was used including the Tff3^{KO} and corresponding wild type mice. The significant down-regulation of Th1 involved cytokines induced by *T. gondii* parasite, e.g., Ifnγ, Il-12αp35-2, IL-1β, Il-10 and Tnfα in the Tff3^{KO} mouse ileum indicates that the absence of Tff3 reduced the immune response and the intestinal inflammation in the mouse ileum (Figure 21). Both Ifnγ and Il-12, as well as Tnfα, which is essential for the activation of macrophages, are critical for the *T. gondii* induced inflammation and immune response (Denkers & Gazzinelli, 1998; Stafford *et al.*, 2002). Here, the significantly reduced up-regulation of these cytokines clearly demonstrated a depleted immune reaction in the Tff3^{KO} mice ileum after *T. gondii* infection. Moreover, Il-1β is required for the production of Ifn-γ by NK cells (Hunter *et al.*, 1995), so it might be speculated that Tff3 could play a role in the reaction of NK cells after *T. gondii* infection based on the down-regulation of both Ifn-γ and Il-1β when in the absent of Tff3.

This conclusion is in line with the hematoxylin and eosin (H&E) staining (Figure 36; performed by Dr. I. Dunay (IMMB) and PD Dr. T. Kalinski (IPA), Magdeburg), as well as with the CD4 immunostaining (data not shown, performed by PD Dr. T. Kalinski) in both infected Tff3^{KO} and corresponding wild type mice ileum. In the ileum of Tff3^{KO} mice, the H&E staining revealed a more preserved epithelial structure and a significantly increased villi height (Figure 36). Furthermore, a semi-quantitative evaluation of CD4 immunostaining showed a significant decrease of CD4 expression (data not shown; both data were provided by PD Dr. T. Kalinski).

In summary, this study demonstrates the function of Tff3 as a positive regulator in the immune response after *T. gondii* infection. Interestingly, in contrast, Tff2 peptide was reported to antagonize IL-12 release from DCs and macrophages and to negatively regulate type 1 immunity against *T. gondii* in the intestine after the oral infection (McBerry *et al.*, 2012). Several groups have also reported that application of recombinant TFF peptides, especially TFF2, can reduce inflammatory indices in animal models of colitis (Tran *et al.*, 1999; Giraud, 2000; Soriano-Izquierdo *et al.*, 2004). Thus, TFF2 and TFF3 might have different roles in the intestinal immune system.
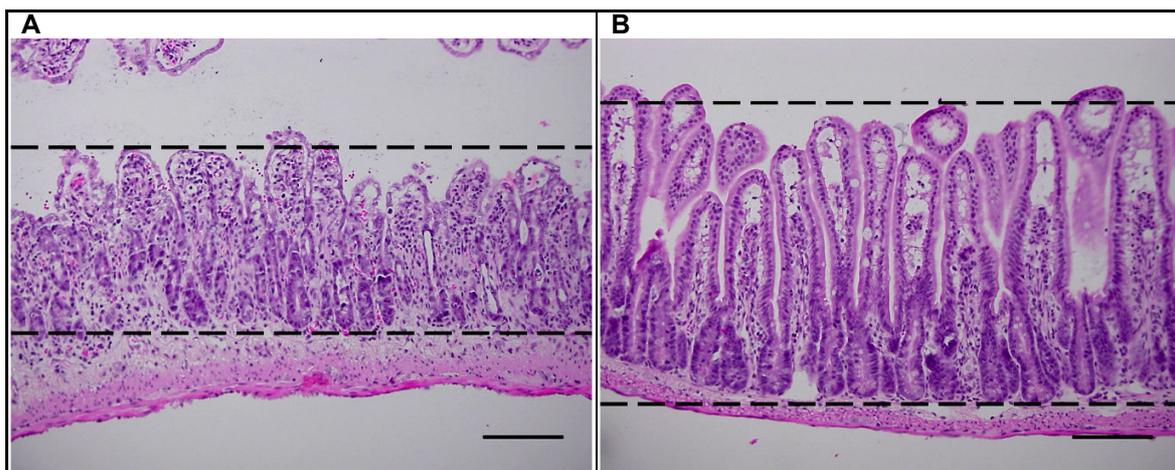
Figure 36: H&E staining of mouse ileum after *T. gondii* infection
Typical H&E staining of mouse ileum after the oral infection with *T. gondii* (3 cysts, for 7 days). **(A)** Ileum section of wild type mice, **(B)** ileum section of Tff3[KO] mice. The villi height is indicated by dashed lines. The histological staining showed here was performed by Dr. I. Dunay. All sections were stained and photographed under the same conditions. Scale bars: 50 µm

TFF3 is typically secreted by intestinal goblet cells (together with MUC2). Recently, MUC2 was reported to have an immunoregulatory function in the gut by mitigating the inflammatory response in DCs (Belkaid & Grainger, 2013; Shan *et al.*, 2013). Thus, a role of TFF3 for the intestinal immune response is within the limits of expectation, i.e., by regulating the response of DCs.

Of note, the different immune responses in the ileum of Tff3[KO] mice when compared with the corresponding wild type mice appeared only in the early stage (7 days) after very low-dose (3 cysts) oral infection with *T. gondii*. In a comparison test (data not shown), an extended duration of infection (up to 11 days) and an increased number of cysts (up to 10 cysts) eliminated the effect of Tff3 on intestinal inflammation. Moreover, infection with different cyst numbers and duration resulted also in different immune responses in the mouse brain. The expression of inflammation markers, such as Ifnγ, Il-12, IL-1β and Tnfα, was not distinctly changed in the brain 7 days after the oral infection with 3 cysts; whereas these markers were significantly up-regulated 11 days after the oral infection with a higher dose (10 cysts; data not shown). This is an indication for the different extent of *T. gondii* infection throughout the body under different conditions. Furthermore, Tff3 might play a role in the immune response of the ileum only at the very early stage of *T. gondii* infection, before the parasites reach the brain.

Additionally, the expression of Tff2 mRNA was down-regulated in Tff3[KO] mice (Figure 21). This is in line with a previous study, which demonstrates reduced Tff2 expression in gastric antrum of Tff3[KO] mice, suggesting a intercalated regulation of the TFF transcripts (Taupin *et al.*, 1999).

5.2   TFFs in the CNS system

5.2.1 Cerebral TFF expression in a mouse model of *Toxoplasma* encephalitis

5.2.1.1   Expression profile of Tffs in the mouse brain after T. gondii infection

Although previous studies showed expression of TFF peptides in the murine brain, the precise localization and function of TFF peptides in the CNS is still largely unclear. In order to better understand the expression of TFFs in the brain during inflammatory conditions, a gene expression analysis was performed using a mouse model of TE. In line with previous reports, the transcripts of Tffs, especially Tff1 and Tff3, were found to be predominantly expressed in the cerebellum (Figure 25). The immunostaining of mouse brain slices (Figure 26) revealed a localization of Tff1 in the cerebellum (especially in the granular layer and probably also in Purkinje cells). These results indicate a neuronal expression of Tff1 in the mouse brain and are consistent with the expression pattern shown in the rat brain (Hirota *et al.*, 1995; Jensen *et al.*, 2013). A tendency of decreased staining of Purkinje cells (number, form) was observed in *T. gondii* infected brain slides (Figure 26a-d), which is consistent with a previous study demonstrating that the Purkinje cell layer was markedly affected in the form of disfiguring and focal loss of cells with apoptotic and necrotic changes after the *T. gondii* infection (El-Sagaff *et al.*, 2005). In line with this, many studies demonstrated a decrease in Purkinje cells (number, volume or density) after various infections (Jamroz *et al.*, 2009; Shi *et al.*, 2009; Wallace *et al.*, 2010; Sugiura *et al.*, 2011; Campeau *et al.*, 2013). Moreover, both the results from RT-PCR analysis (Tff1 expressed predominately in cerebellum) and immunostaining (increased Tff1 expression in the mouse brain after *T. gondii* infection) were comparable with *in situ* hybridization studies performed by Dr. E. Znalesniak (IMMC, Magdeburg; personal communication).

Of special note, Tff2 transcription was significantly increased in the brain of Tff1^{KO} mice (Figure 25). Here, for the first time, the different expression of Tff2 transcripts has been identified in the brain of Tff1^{KO} mice when compared with wild type mice. In contrast, the expression of Tff2 in the stomach does not show a significant difference between Tff1^{KO} and wild type mice. Conversely, other studies reported that, a lack of TFF1 induced dramatic inhibition of TFF2 expression in the stomach (Karam *et al.*, 2004; Tomasetto & Rio, 2005). The mechanism of how the lack of Tff1 regulates the increased expression of Tff2 in the brain is still unclear. As an immediate early gene, TFF2 is capable of regulating its own expression through activation of the TFF2 promoter (Bulitta *et al.*, 2002); the TFF2 promoter can also be activated in response to stimulation with both TFF2 and TFF3 peptides (Taupin *et al.*, 1999). Some factors were demonstrated to regulate Tff2 expression through the Tff2 promoter. For example, the zinc finger transcription factor Sp3, which was reported to be associated with the TFF1 promoter in MCF-7 cells together with Sp1 (Sun *et al.*, 2005), was also bound to the TFF2 promoter and acted as a negative regulator that attenuated the transcriptional

activity of the TFF2 gene (Liu *et al.*, 2012). Moreover, the upstream stimulating factor (USF) acts as a positive regulator targeted at the Tff2 promoter (Al-azzeh *et al.*, 2002). A GAG motif could be responsible for mediating promoter activation in response to TFF2 stimulation (Bulitta *et al.*, 2002) and a CCAAT sequence as a cell line-specific cis-acting regulatory element may contribute to the high level expression of TFF2 in MCF-7 cells (Chi *et al.*, 2004). Additionally, *H pylori* infection increases DNA methylation at the Tff2 promoter, which reduces the antral expression of Tff2 (Peterson *et al.*, 2010). Furthermore, administration of aspirin induces activated protein kinase C and eventually modifies (directly or indirectly) transcription factors acting on elements of the 5'-flanking region of TFF2, resulting in the up-regulation of TFF2 transcription (Azarschab *et al.*, 2001)**.**

To be mentioned, the immunostaining of *T. gondii* parasites in the untreated control brain slides also shows some slight positive signals at the marginal zones, i.e., the meninges (Figure 24 A, C, E). This staining is probably non-specific because *T. gondii* was reported to be found predominantly in the grey matter of the mouse brain (Ferguson & Hutchison, 1987). Moreover, the location of these slight signals was not reproducible on parallel slides. This also points to a non-specific staining of the meninges.

5.2.1.2   *Tffs may play a role in the CNS for the immune response*

IBA1, as typical marker for microglia, is particularly elevated in the activated status of the microglial cells during the immune response (Ito *et al.*, 1998, 2001). The up-regulation of Iba1 in the brain after *T. gondii* infection (Figure 28, Figure 29) is a clear indication for the activation of microglial cells, which are specialized macrophages acting as the first and main form of active immune defence to protect neurons in the CNS (Brodal, 2010). This result is consistent with previous *in vitro* studies, which indicate that the tachyzoites can invade microglia of the mouse brain after the *T. gondii* infection (Fischer *et al.*, 1997). Interestingly, in the uninfected group, the expression level of Iba1 in the cerebellum is significantly higher in Tff2^{KO} mice when compared with the wild type (Figure 28, Figure 29). Thus demonstrates that the absence of Tff2 positively regulates the inflammation in the cerebellum. This is in line with studies that show a higher baseline level of intestinal inflammation markers, e.g., Il-1β, in Tff2^{KO} mice (Kurt-Jones *et al.*, 2007). Moreover, there are reports demonstrating that TFF2 antagonizes Il-12 release from DCs and macrophages and negatively regulates type 1 immunity in the intestine after the oral infection with *T. gondii* (McBerry *et al.*, 2012).

A significant up-regulation of the IL-12–mediated type 1 inflammatory cytokine Ifnγ as well as Cd8 (typical of cytotoxic T-cells and DCs) was observed in the cerebellum of Tff2^{KO} mice when compared with wild type mice. This is again an indication for a function of Tff2 in the immune response of the CNS as a negative regulator of the type 1 cytokine release from T lymphocytes and DCs in the *T. gondii* pathogenesis (Figure 28).

Furthermore, the up-regulated Tff1 expression (on both transcript and protein levels, Figure 25, Figure 26) in the mouse brain, particularly in the cerebellum, after *T. gondii* infection is a first hint that Tff1 might also be involved in inflammatory processes of the brain. Based on the localization-studies presented in Figure 25 (Tff1) and Figure 28 (Iba1), no co-expression was detectable off hand. Iba1 is a typical microglial protein (Ito *et al.*, 1998), whereas Tff1 is probably of neuronal origin (Lein *et al.*, 2007; Jensen *et al.*, 2013).

In conclusion, the results of this study strengthen the connection between Tff2 and the immune system in the CNS and are also consistent with the published data indicating that Tff2 acts as a negative regulatory factor of the immune responses. In the CNS, Tff2 appears to function as an anti-inflammatory peptide which also plays a role after i.p. *T. gondii* infection. Furthermore, the up-regulation of Tff1 particularly in the cerebellum after *T. gondii* infection is currently enigmatic and might also be an indication for a function during inflammatory processes. However, further investigations are required to clarify the function of TFF1. For example, an *in vitro* model of inflammation based on primary cell cultures from Tff1-deficient mice brain could be established. The examination of inflammatory parameters in the blood and liquor cerebrospinalis during the inflammatory processes in wild type and Tff1^{KO} mice would also be helpful for the understanding of the function of Tff1 in the immune system.

5.2.2 TFF3 is expressed in primary cell cultures of rat brain

In the past, TFFs have been demonstrated to be expressed in the CNS and a function as neuropeptides has been proposed. However, the precise cellular origin of TFFs in the brain has not been determined unambiguously (Hoffmann *et al.*, 2001; Hoffmann & Jagla, 2002). In this study, immunofluorescence analysis on rat brain primary cell cultures clearly showed the neuronal expression of TFF3 based on the co-localization with MAP2 (neuron marker; Figure 30). In contrast, astrocytes, defined by their GFAP immune reactivity, clearly did not show any specific staining for TFF3 (Figure 32). As a neuropeptide, TFF3 expression revealed changes during postnatal cerebellar development (Hinz *et al.*, 2004). Moreover, the neuronal expression of TFF3 could be the reason for various functions in the CNS: such as a fear modulating effect, a function for hearing, motoric skills and learning and memory. Tff3 showed differential dose dependent behavioural effects when injected into the basolateral nucleus of the rat amygdala: an anxiolytic effect at a low dose and an anxiogenic effect at a higher dose (Schwarzberg *et al.*, 1999). Furthermore, a lack of Tff3 resulted in hearing impairment and accelerated presbyacusis (Lubka *et al.*, 2008). TFF3 is also concerned with behavioural effect, such as various motoric skills (Blaschke, 2010). Also an effect on learning and memory has been described in the mouse after i.p. administration of TFF3 (Shi *et al.*, 2012).

Another major result of this study is that TFF3 is synthesized by microglial cells as well (co-localization with IBA1). Microglia is an integral part of the immune system. The co-localization of TFF3 probably indicates that TFF3 may act also as a regulator of the

immune response in the CNS (Figure 33, Figure 35). This would be related to the previous result demonstrating function of Tff3 in the immune response of the intestine after *T. gondii* infection (see chapter 5.1.2). To elucidate a possible role of TFFs in immune response, also a Lipopolysaccharides (LPS) administration model for neural inflammation was applied. A similar model has been described previously *in vivo* (mouse model) and *in vitro* (e.g., primary mixed glial cell cultures, microglia cell lines N9; Candelario-Jalil *et al.*, 2007; Qin *et al.*, 2007; Lu *et al.*, 2010). The up-regulation of Ifnγ, Il-10 and Tnfα was observed 24h after incubation with various concentrations (500/1000/1500/2000 ng/mL) of LPS, which is indicative for the inflammatory processes in the cells. However, no appreciable change of the Tff3 expression was found in all cell cultures after the LPS treatment. Furthermore, the LPS challenge did not induce Tff1 or Tff2 (data not shown).

The dissociated primary neural or glial cell cultures are prevalent and crucial research tools allowing access to individual cells for studies. In spite of the advantages, *in vitro* cell culture has also limitations in reproducing the natural environment. Therefore, the lack of expression of Tff1 or Tff2 in the primary cultures from cortex or hippocampus could result from the absence of adequate dynamic interactions.

5.3 Future prospects

The results from this study present the base for future investigations concerning the function of TFFs, particularly in the immune system and the CNS. TFF3, as a constituent of the mucus, was shown to have a function in regulating the intestinal immune response. Thus, it will be interesting to clarify the mechanism of how TFF3 activates DCs and to test whether TFF3 plays a role in chronic inflammatory diseases of the gut. Furthermore, it will be challenging to study the function of TFF3 as a secretory product of neurons as well as of microglial cells in the brain. Moreover, to analyze the nature of the complementary regulation of TFF1 and TFF2 in the brain and the functional consequences are interesting goals.

6   Summary / Zusammenfassung

Summary

The trefoil factor family peptides (TFF1, -2 and -3) are mainly expressed by mucous epithelial cells and are predominantly found in the gastrointestinal (GI) tract as exocrine products. TFFs are expressed also in the central nervous system (CNS). Previous studies demonstrated protective and healing effects of all three TFF peptides after various mucosal damages in the GI tract and also their participation in immune responses and inflammatory processes. TFFs show various behavioural effects in the CNS as well. Generally, this study was designed to gain more insights into the expression and function of TFFs in the GI tract and the CNS considering four different aspects:

(1) The migration of epithelial cells is the major component of mucosal restitution occurring in the early phase of mucosal repair. Here, in an *in vitro* model of gastric restitution (scratch wounding of the non-transformed cell line RGM-1), separated stationary and migratory cells were compared. Surprisingly, Tff1 (a differentiation marker for gastric surface mucous cells) was significantly up-regulated in migratory RGM-1 cells. Furthermore a knock-down of Tff1 by the means of RNA interference significantly diminished migration of RGM-1 cells. This clearly points to a motogenic function of TFF1 during restitution.

(2) Gene expression was investigated in a mouse model of induced ileitis after low-dose oral *Toxoplasma gondii* (*T. gondii*) infection. A comparison between Tff3^{KO} and wild type mice revealed that the inflammatory response is significantly reduced in Tff3^{KO} mice. Thus, the mucus constituent Tff3 seems to play an essential role in activating dendritic cells after *T. gondii* infection.

(3) In order to gain new insights into the expression and role of TFFs in the CNS during inflammatory conditions, different Tff^{KO} mice and wild type mice were compared in a model of induced encephalitis after i.p. *T. gondii* infection. Here, Tff1 was significantly up-regulated particularly in the cerebellum after *T. gondii* infection. Of note, the up-regulation of Tff1 was even higher in Tff2^{KO} mice. Furthermore, genes typical of inflammation showed no different regulation between Tff1^{KO}, Tff2^{KO} and wild type mice after *T. gondii* infection implying that Tff1 plays no direct role in this process. However, a significant up-regulation of interferon-γ in the cerebellum was higher in Tff2^{KO} mice when compared with Tff1^{KO} and wild type mice indicating a function of Tff2 in the immune response of the CNS as a negative regulator.

(4) In order to elucidate which type of cells (neurons, astrocytes and microglial cells) express TFFs, primary cell cultures from the rat cortex or hippocampus were investigated. Double immunofluorescence analysis together with MAP2 clearly showed the neuronal expression of TFF3. In contrast, astrocytes (GFAP positive cells) showed no specific TFF3 staining. Furthermore, TFF3 was synthesized by microglial cells as well, based on its co-localization with IBA1. Thus, TFF3 is a typical neuropeptide, which could also act as a regulator of the immune response in the CNS.

Zusammenfassung

Die Peptide der *trefoil factor family* (TFF1, -2 und -3) werden überwiegend von mukösen Epithelzellen exprimiert und sind hauptsächlich im gastrointestinalen (GI) Trakt als exokrine Produkte zu finden. Außerdem werden TFFs im zentralen Nervensystem (ZNS) exprimiert. Frühere Studien haben protektive und heilende Effekte von allen drei TFFs nach verschiedenen Schäden an mukösen Epithelien im GI-Trakt gezeigt sowie eine Beteiligung von TFFs bei der Immunantwort und Entzündungsprozessen nachgewiesen. Außerdem zeigen TFFs verhaltensbiologische Effekte nach Applikation in das ZNS. Daher wurde die vorliegende Arbeit darauf ausgelegt neue Erkenntnisse über die Expression und Funktion von TFFs im GI-Trakt und ZNS unter Berücksichtigung von vier verschiedenen Modellsystemen zu erlangen:

(1) Die Migration von Epithelzellen ist die Hauptkomponente der mukosalen Restitution, die in der frühen Phase der mukosalen Reparatur stattfindet. Dementsprechend wurde ein *in vitro*-Modell für die Restitution des Magens (*scratch assay* von nicht-transformierten gastrischen epithelialen RGM1-Zellen) benutzt, um stationäre und migrierenden Zellen zu vergleichen. Dabei zeigte sich eine signifikante Hochregulierung von Tff1 (ein Marker für die Differenzierung von Oberflächenepithelzellen) in migrierenden RGM1-Zellen. Ferner bewirkte ein *Knockdown* von Tff1 durch RNA-Interferenz eine deutliche Verringerung der Migration von RGM1-Zellen, was auf eine motogene Funktion von Tff1 während der Restitution hindeutet.

(2) Ein Maus-Modell für induzierte Ileitis nach gering dosierter oraler *Toxoplasma gondii*-Infektion wurde für Gen-Expressions-Untersuchungen verwendet. Der Vergleich von Tff3^{KO}- mit Wildtyp-Mäusen ergab eine signifikante Reduzierung der Entzündungsantwort. Dies weist darauf hin, dass Tff3 als Bestandteil des Mukus eine entscheidende Rolle bei der Aktivierung von dendritischen Zellen nach einer Infektion mit *T. gondii* zukommt.

(3) Um die Expression und Funktion von TFFs im ZNS unter entzündlichen Bedingen zu analysieren wurden mit Hilfe eines Maus-Modells für induzierte Enzephalitis (nach intraperitonealer *T. gondii*-Infektion) verschiedene Tff^{KO}- mit Wildtyp-Mäusen verglichen. Es zeigte sich eine signifikante Hochregulierung von Tff1 nach Infektion mit *T. gondii*, insbesondere im Cerebellum, die in Tff2^{KO}- Mäusen bemerkenswerterweise am höchsten war. Hinzu kommt, dass charakteristische Entzündungsgene keine Unterschiede in der Regulation zwischen Tff^{KO}-, Tff2^{KO}- und Wildtyp-Mäusen nach Infektion mit *T. gondii* aufwiesen. Dies könnte darauf hindeuten, dass Tff1 keinen unmittelbaren Einfluss auf die Entzündungsreaktion hat. Dennoch wurde eine signifikante Hochregulierung von Interferon-γ im Cerebellum von Tff2^{KO}-Mäusen im Vergleich zu Tff1^{KO}- und Wildtyp-Mäusen beobachtet, was ein Hinweis für die Aufgabe von Tff2 als negativer Regulator bei der Immunantwort des ZNS sein könnte.

(4) Um aufzuklären, welche Zell-Typen (Neuronen, Astrozyten und Mikrogliazellen) TFFs exprimieren, wurden Primärzellkulturen des Ratten-Cortex bzw. Hippocampus untersucht. Doppel-Immunofluoreszenz-Analysen mit MAP2 zeigten deutlich die neuronale Expression von TFF3, wohingegen Astrozyten (GFAP-positive Zellen) keine

spezifische TFF3-Färbung zeigten. Weiterhin wurde nachgewiesen, dass TFF3, beruhend auf der Co-Lokalisation mit IBA1, von Mikrogliazellen synthetisiert wird. Folglich könnte TFF3 als Neuropeptid außerdem als Regulator bei der Immunantwort des ZNS agieren.

7   References

Agace, W.W., Amara, A., Roberts, a I., Pablos, J.L., Thelen, S., Uguccioni, M., Li, X.Y., Marsal, J., Arenzana-Seisdedos, F., Delaunay, T., Ebert, E.C., Moser, B., & Parker, C.M. (2000) Constitutive expression of stromal derived factor-1 by mucosal epithelia and its role in HIV transmission and propagation. *Curr. Biol. CB*, **10**, 325–328.

Al-azzeh, E., Dittrich, O., Vervoorts, J., Blin, N., Gött, P., & Lüscher, B. (2002) Gastroprotective peptide trefoil factor family 2 gene is activated by upstream stimulating factor but not by c-Myc in gastrointestinal cancer cells. *Gut*, **51**, 685–690.

Albert, T.K., Laubinger, W., Müller, S., Hanisch, F., Kalinski, T., Meyer, F., & Hoffmann, W. (2010) Human intestinal TFF3 forms disulfide-linked heteromers with the mucus-associated FCGBP protein and is released by hydrogen sulfide. *J. Proteome Res.*, **9**, 3108–3117.

Alison, M.R., Chinery, R., Poulsom, R., Ashwood, P., Longcroft, J.M., & Wright, N.A. (1995) Experimental ulceration leads to sequential expression of spasmolytic polypeptide, intestinal trefoil factor, epidermal growth factor and transforming growth factor alpha mRNAs in rat stomach. *J. Pathol.*, **175**, 405–414.

Allen, A. & Pearson, J.P. (1993) Mucus glycoproteins of the normal gastrointestinal tract. *Eur. J. Gastroenterol. Hepatol.*, **5**, 193–199.

Altieri, D.C. (2003) Survivin in apoptosis control and cell cycle regulation in cancer. *Prog. Cell Cycle Res.*, **5**, 447–452.

Arsic, N., Bendris, N., Peter, M., Begon-Pescia, C., Rebouissou, C., Gadéa, G., Bouquier, N., Bibeau, F., Lemmers, B., & Blanchard, J.M. (2012) A novel function for Cyclin A2: control of cell invasion via RhoA signaling. *J. Cell Biol.*, **196**, 147–162.

Atuma, C. (2000) Gastrointestinal Mucosal Protective Mechanisms (Ph.D. Thesis), Department of Physiology, Uppsala University, Sweden.

Azarschab, P., Al-Azzeh, E., Kornberger, W., & Gött, P. (2001) Aspirin promotes TFF2 gene activation in human gastric cancer cell lines. *FEBS Lett.*, **488**, 206–210.

Balda, M.S. & Matter, K. (2009) Tight junctions and the regulation of gene expression. *Biochim. Biophys. Acta*, **1788**, 761–767.

Barker, N. & Clevers, H. (2010) Leucine-rich repeat-containing G-protein-coupled receptors as markers of adult stem cells. *Gastroenterology*, **138**, 1681–1696.

Barker, N., Huch, M., Kujala, P., van de Wetering, M., Snippert, H.J., van Es, J.H., Sato, T., Stange, D.E., Begthel, H., van den Born, M., Danenberg, E., van den Brink, S., Korving, J., Abo, A., Peters, P.J., Wright, N., Poulsom, R., & Clevers, H. (2010) Lgr5(+ve) stem cells drive self-renewal in the stomach and build long-lived gastric units in vitro. *Cell Stem Cell*, **6**, 25–36.

Barker, N., van Es, J.H., Kuipers, J., Kujala, P., van den Born, M., Cozijnsen, M., Haegebarth, A., Korving, J., Begthel, H., Peters, P.J., & Clevers, H. (2007) Identification of stem cells in small intestine and colon by marker gene Lgr5. *Nature*, **449**, 1003–1007.

Bartel, D.P. (2004) MicroRNAs: genomics, biogenesis, mechanism, and function. *Cell*, **116**, 281–297.

Bates, P.A. (2006) Housekeeping by Leishmania. *Trends Parasitol.*, **22**, 447–448.

Baus-Loncar, M., Kayademir, T., Takaishi, S., & Wang, T. (2005a) Trefoil factor family 2 deficiency and immune response. *Cell. Mol. Life Sci.*, **62**, 2947–2955.

Baus-Loncar, M., Schmid, J., Lalani, E.-N., Rosewell, I., Goodlad, R.A., Stamp, G.W.H., Blin, N., & Kayademir, T. (2005b) Trefoil factor 2 (TFF2) deficiency in murine digestive tract influences the immune system. *Cell. Physiol. Biochem.*, **16**, 31–42.

Beck, P.L., Wong, J.F., Li, Y., Swaminathan, S., Xavier, R.J., Devaney, K.L., & Podolsky, D.K. (2004) Chemotherapy- and radiotherapy-induced intestinal damage is regulated by intestinal trefoil factor. *Gastroenterology*, **126**, 796–808.

Beck, S., Schmitt, H., Shizuya, H., Blin, N., & Gött, P. (1996) Cloning of contiguous genomic fragments from human chromosome 21 harbouring three trefoil peptide genes. *Hum. Genet.*, **98**, 233–235.

Belkaid, Y. & Grainger, J. (2013) Mucus coat, a dress code for tolerance. *Science*, **342**, 432–433.

Bendris, N., Arsic, N., Lemmers, B., & Blanchard, J.M. (2012) Cyclin A2, Rho GTPases and EMT. *Small GTPases*, **3**, 225–228.

Bernstein, E., Caudy, A.A., Hammond, S.M., & Hannon, G.J. (2001) Role for a bidentate ribonuclease in the initiation step of RNA interference. *Nature*, **409**, 363–366.

Black, M.W. & Boothroyd, J.C. (2000) Lytic cycle of Toxoplasma gondii. *Microbiol. Mol. Biol. Rev.*, **64**, 607–623.

Blackwell, J.M., Roberts, C.W., & Alexander, J. (1993) Influence of genes within the MHC on mortality and brain cyst development in mice infected with Toxoplasma gondii: kinetics of immune regulation in BALB H-2 congenic mice. *Parasite Immunol.*, **15**, 317–324.

Blaschke, K. (2010) Vergleichende neurobiologische Untersuchungen von TFF3-defizienten Mäusen und Wildtyptieren (Ph.D. Thesis), medizinischen Fakultät der Otto-von-Guericke-Universität Magdeburg.

Bliss, S.K., Butcher, B.A., & Denkers, E.Y. (2000) Rapid recruitment of neutrophils containing prestored IL-12 during microbial infection. *J. Immunol.*, **165**, 4515–4521.

Böcker, W., Denk, H., Heitz, P.U., & Moch, H. (2008) *Pathologie*, 4th edn. Böcker, W. (Edt.), Urban & Fischer in Elsevier, Munich, Jena.

Bossenmeyer-Pourié, C., Kannan, R., Ribieras, S., Wendling, C., Stoll, I., Thim, L., Tomasetto, C., & Rio, M.-C. (2002) The trefoil factor 1 participates in gastrointestinal cell differentiation by delaying G1-S phase transition and reducing apoptosis. *J. Cell Biol.*, **157**, 761–770.

Brodal, P. (2010) *The Central Nervous System*, 4th edn. Oxford University Press, Oslo, Norway (Google eBook).

Buache, E., Etique, N., Alpy, F., Stoll, I., Muckensturm, M., Reina-San-Martin, B., Chenard, M.P., Tomasetto, C., & Rio, M.C. (2011) Deficiency in trefoil factor 1 (TFF1) increases tumorigenicity of human breast cancer cells and mammary tumor development in TFF1-knockout mice. *Oncogene*, **30**, 3261–3273.

Bulitta, C.J., Fleming, J. V, Raychowdhury, R., Taupin, D., Rosenberg, I., & Wang, T.C. (2002) Autoinduction of the trefoil factor 2 (TFF2) promoter requires an upstream cis-acting element. *Biochem. Biophys. Res. Commun.*, **293**, 366–374.

Campeau, J.L., Wu, G., Bell, J.R., Rasmussen, J., & Sim, V.L. (2013) Early increase and late decrease of purkinje cell dendritic spine density in prion-infected organotypic mouse cerebellar cultures. *PLoS One*, **8**, e81776.

Candelario-Jalil, E., de Oliveira, A.C.P., Gräf, S., Bhatia, H.S., Hüll, M., Muñoz, E., & Fiebich, B.L. (2007) Resveratrol potently reduces prostaglandin E2 production and free radical formation in lipopolysaccharide-activated primary rat microglia. *J. Neuroinflamm.*, **4**, 25.

Caplen, N.J., Parrish, S., Imani, F., Fire, A., & Morgan, R. a (2001) Specific inhibition of gene expression by small double-stranded RNAs in invertebrate and vertebrate systems. *Proc. Natl. Acad. Sci. U. S. A.*, **98**, 9742–9747.

Carstea, E.D., Hough, S., Wiederholt, K., & Welch, P.J. (2005) State-of-the-art modified RNAi compounds for therapeutics. *IDrugs Investig. drugs J.*, **8**, 642–647.

Chadwick, M.P., May, F.E., & Westley, B.R. (1995) Production and comparison of mature single-domain "trefoil" peptides pNR-2/pS2 Cys58 and pNR-2/pS2 Ser58. *Biochem. J.*, **308**, 1001–1007.

Chadwick, M.P., Westley, B.R., & May, F.E. (1997) Homodimerization and hetero-oligomerization of the single-domain trefoil protein pNR-2/pS2 through cysteine 58. *Biochem. J.*, **327**, 117–123.

Chen, Y., Lu, Y., De Plaen, I.G., Wang, L., & Tan, X. (2000) Transcription factor NF-kappaB signals antianoikic function of trefoil factor 3 on intestinal epithelial cells. *Biochem. Biophys. Res. Commun.*, **274**, 576–582.

Chi, A.L., Lim, S., & Wang, T.C. (2004) Characterization of a CCAAT-enhancer element of trefoil factor family 2 (TFF2) promoter in MCF-7 cells. *Peptides*, **25**, 839–847.

Chinery, R., Bates, P.A., De, A., & Freemont, P.S. (1995) Characterisation of the single copy trefoil peptides intestinal trefoil factor and pS2 and their ability to form covalent dimers. *FEBS Lett.*, **357**, 50–54.

Chinery, R., Williamson, J., & Poulsom, R. (1996) The gene encoding human intestinal trefoil factor (TFF3) is located on chromosome 21q22.3 clustered with other members of the trefoil peptide family. *Genomics*, **32**, 281–284.

Chiou, S., Tanigawa, T., Akahoshi, T., Abdelkarim, B., Jones, M.K., & Tarnawski, A.S. (2005) Survivin: a novel target for indomethacin-induced gastric injury. *Gastroenterology*, **128**, 63–73.

Chiou, S.-K., Moon, W.S., Jones, M.K., & Tarnawski, A.S. (2003) Survivin expression in the stomach: implications for mucosal integrity and protection. *Biochem. Biophys. Res. Commun.*, **305**, 374–379.

Cho, S.Y. & Klemke, R.L. (2000) Extracellular-regulated kinase activation and CAS/Crk coupling regulate cell migration and suppress apoptosis during invasion of the extracellular matrix. *J. Cell Biol.*, **149**, 223–236.

Chomczynski, P. & Sacchi, N. (1987) Single-step method of RNA isolation by acid guanidinium thiocyanate-phenol-chloroform extraction. *Anal. Biochem.*, **162**, 156–159.

Chwieralski, C.E., Schnurra, I., Thim, L., & Hoffmann, W. (2004) Epidermal growth factor and trefoil factor family 2 synergistically trigger chemotaxis on BEAS-2B cells via different signaling cascades. *Am. J. Respir. Cell Mol. Biol.*, **31**, 528–537.

Comamala, M., Pinard, M., Thériault, C., Matte, I., Albert, A., Boivin, M., Beaudin, J., Piché, A., & Rancourt, C. (2011) Downregulation of cell surface CA125/MUC16 induces epithelial-to-mesenchymal transition and restores EGFR signalling in NIH:OVCAR3 ovarian carcinoma cells. *Br. J. Cancer*, **104**, 989–999.

Cook, G.A., Familari, M., Thim, L., & Giraud, A.S. (1999) The trefoil peptides TFF2 and TFF3 are expressed in rat lymphoid tissues and participate in the immune response. *FEBS Lett.*, **456**, 155–159.

Cotran, R.S., Kumar, V., T. Collins, S., L. Robbins, B., & Schmitt, R. (2004) *Robbins Pathologic Basis of Disease*, 7th edn. Gruliow, R (Edt.), Saunders, Philadelphia.

Coussens, L.M. & Werb, Z. (2002) Inflammation and cancer. *Nature*, **420**, 860–867.

D'Andrea, A., Rengaraju, M., Valiante, N.M., Chehimi, J., Kubin, M., Aste, M., Chan, S.H., Kobayashi, M., Young, D., & Nickbarg, E. (1992) Production of natural killer cell stimulatory factor (interleukin 12) by peripheral blood mononuclear cells. *J. Exp. Med.*, **176**, 1387–1398.

De, A., Brown, D.G., Gorman, M.A., Carr, M., Sanderson, M.R., & Freemont, P.S. (1994) Crystal structure of a disulfide-linked "trefoil" motif found in a large family of putative growth factors. *Proc. Natl. Acad. Sci. U. S. A.*, **91**, 1084–1088.

De Fougerolles, A., Vornlocher, H., Maraganore, J., & Lieberman, J. (2007) Interfering with disease: a progress report on siRNA-based therapeutics. *Nat. Rev. Drug Discov.*, **6**, 443–453.

De Wever, O., Pauwels, P., De Craene, B., Sabbah, M., Emami, S., Redeuilh, G., Gespach, C., Bracke, M., & Berx, G. (2008) Molecular and pathological signatures of epithelial-mesenchymal transitions at the cancer invasion front. *Histochem. Cell Biol.*, **130**, 481–494.

Deckert, M., Sedgwick, J.D., Fischer, E., & Schlüter, D. (2006) Regulation of microglial cell responses in murine Toxoplasma encephalitis by CD200/CD200 receptor interaction. *Acta Neuropathol.*, **111**, 548–558.

Denkers, E.Y. & Gazzinelli, R.T. (1998) Regulation and function of T-cell-mediated immunity during Toxoplasma gondii infection. *Clin. Microbiol. Rev.*, **11**, 569–588.

Dignass, A., Lynch-Devaney, K., Kindon, H., Thim, L., & Podolsky, D.K. (1994) Trefoil peptides promote epithelial migration through a transforming growth factor beta-independent pathway. *J. Clin. Invest.*, **94**, 376–383.

Dubey, J.P. (2008) The history of Toxoplasma gondii--the first 100 years. *J. Eukaryot. Microbiol.*, **55**, 467–475.

Dubey, J.P., Lindsay, D.S., & Speer, C. a (1998) Structures of Toxoplasma gondii tachyzoites, bradyzoites, and sporozoites and biology and development of tissue cysts. *Clin. Microbiol. Rev.*, **11**, 267–299.

Dubey, J.P., Miller, N.L., & Frenkel, J.K. (1970) The Toxoplasma gondii oocyst from cat feces. *J. Exp. Med.*, **132**, 636–662.

Dunay, I.R., Damatta, R. a, Fux, B., Presti, R., Greco, S., Colonna, M., & Sibley, L.D. (2008) Gr1(+) inflammatory monocytes are required for mucosal resistance to the pathogen Toxoplasma gondii. *Immunity*, **29**, 306–317.

Dunay, I.R., Fuchs, A., & Sibley, L.D. (2010) Inflammatory monocytes but not neutrophils are necessary to control infection with Toxoplasma gondii in mice. *Infect. Immun.*, **78**, 1564–1570.

Dunay, I.R. & Sibley, L.D. (2010) Monocytes mediate mucosal immunity to Toxoplasma gondii. *Curr. Opin. Immunol.*, **22**, 461–466.

Dürer, U., Hartig, R., Bang, S., Thim, L., & Hoffmann, W. (2007) TFF3 and EGF induce different migration patterns of intestinal epithelial cells in vitro and trigger increased internalization of E-cadherin. *Cell. Physiol. Biochem.*, **20**, 329–346.

Elbashir, S.M., Harborth, J., Lendeckel, W., Yalcin, A., Weber, K., & Tuschl, T. (2001) Duplexes of 21-nucleotide RNAs mediate RNA interference in cultured mammalian cells. *Nature*, **411**, 494–498.

El-Sagaff, S., Salem, H.S., Nichols, W., Tonkel, A.K., & Abo-Zenadah, N.Y.A. (2005) Cell death pattern in cerebellum neurons infected with Toxoplasma gondii. *J. Egypt. Soc. Parasitol.*, **35**, 809–818.

Emami, S., Rodrigues, S., Rodrigue, C.M., Le Floch, N., Rivat, C., Attoub, S., Bruyneel, E., & Gespach, C. (2004) Trefoil factor family (TFF) peptides and cancer progression. *Peptides*, **25**, 885–898.

Eng, L.F., Vanderhaeghen, J.J., Bignami, A., & Gerstl, B. (1971) An acidic protein isolated from fibrous astrocytes. *Brain Res.*, **28**, 351–354.

Etienne-Manneville, S. (2008) Polarity proteins in migration and invasion. *Oncogene*, **27**, 6970–6980.

Farrell, J.J., Taupin, D., Koh, T.J., Chen, D., Zhao, C., Podolsky, D.K., & Wang, T.C. (2002) TFF2/SP-deficient mice show decreased gastric proliferation, increased acid secretion, and increased susceptibility to NSAID injury. *J. Clin. Invest.*, **109**, 193–204.

Feil, W., Lacy, E.R., Wong, Y.M., Burger, D., Wenzl, E., Starlinger, M., & Schiessel, R. (1989) Rapid epithelial restitution of human and rabbit colonic mucosa. *Gastroenterology*, **97**, 685–701.

Ferguson, D.J. & Hutchison, W.M. (1987) The host-parasite relationship of Toxoplasma gondii in the brains of chronically infected mice. *Virchows Arch. A.*, **411**, 39–43.

Feustel, S.M., Meissner, M., & Liesenfeld, O. (2012) Toxoplasma gondii and the blood-brain barrier. *Virulence*, **3**, 182–192.

Fire, A., Xu, S., Montgomery, M.K., Kostas, S.A., Driver, S.E., & Mello, C.C. (1998) Potent and specific genetic interference by double-stranded RNA in Caenorhabditis elegans. *Nature*, **391**, 806–811.

Fischer, H.G., Nitzgen, B., Reichmann, G., Gross, U., & Hadding, U. (1997) Host cells of Toxoplasma gondii encystation in infected primary culture from mouse brain. *Parasitol. Res.*, **83**, 637–641.

FitzGerald, A.J., Pu, M., Marchbank, T., Westley, B.R., May, F.E.B., Boyle, J., Yadollahi-Farsani, M., Ghosh, S., & Playford, R.J. (2004) Synergistic effects of systemic trefoil factor family 1 (TFF1) peptide and epidermal growth factor in a rat model of colitis. *Peptides*, **25**, 793–801.

Fox, J.G. & Wang, T.C. (2007) Inflammation, atrophy, and gastric cancer. *J. Clin. Invest.*, **117**, 60–69.

Frenkel, J.K., Dubey, J.P., & Miller, N.L. (1970) Toxoplasma gondii in cats: fecal stages identified as coccidian oocysts. *Science*, **167**, 893–896.

Friedl, P. (2004) Prespecification and plasticity: shifting mechanisms of cell migration. *Curr. Opin. Cell Biol.*, **16**, 14–23.

Friedl, P. & Wolf, K. (2010) Plasticity of cell migration: a multiscale tuning model. *J. Cell Biol.*, **188**, 11–19.

Fu, T., Kalbacher, H., & Hoffmann, W. (2013) TFF1 is differentially expressed in stationary and migratory rat gastric epithelial cells (RGM-1) after in vitro wounding: influence of TFF1 RNA interference on cell migration. *Cell. Physiol. Biochem.*, **32**, 997–1010.

Gajhede, M., Petersen, T.N., Henriksen, A., Petersen, J.F., Dauter, Z., Wilson, K.S., & Thim, L. (1993) Pancreatic spasmolytic polypeptide: first three-dimensional structure of a member of the mammalian trefoil family of peptides. *Structure*, **1**, 253–262.

Gazzinelli, R.T., Eltoum, I., Wynn, T.A., & Sher, A. (1993a) Acute cerebral toxoplasmosis is induced by in vivo neutralization of TNF-alpha and correlates with the down-regulated expression of inducible nitric oxide synthase and other markers of macrophage activation. *J. Immunol.*, **151**, 3672–3681.

Gazzinelli, R.T., Hieny, S., Wynn, T.A., Wolf, S., & Sher, A. (1993b) Interleukin 12 is required for the T-lymphocyte-independent induction of interferon gamma by an intracellular parasite and induces resistance in T-cell-deficient hosts. *Proc. Natl. Acad. Sci. U. S. A.*, **90**, 6115–6119.

Gazzinelli, R.T., Wysocka, M., Hayashi, S., Denkers, E.Y., Hieny, S., Caspar, P., Trinchieri, G., & Sher, A. (1994) Parasite-induced IL-12 stimulates early IFN-gamma synthesis and resistance during acute infection with Toxoplasma gondii. *J. Immunol.*, **153**, 2533–2543.

Giraud, A.S. (2000) X. Trefoil peptide and EGF receptor/ligand transgenic mice. *Am. J. Physiol. Gastrointest. Liver Physiol.*, **278**, G501–6.

Göke, M.N., Cook, J.R., Kunert, K.S., Fini, M.E., Gipson, I.K., & Podolsky, D.K. (2001) Trefoil peptides promote restitution of wounded corneal epithelial cells. *Exp. Cell Res.*, **264**, 337–344.

Goslin, K., Asmussen, H., & Banker, G. (1998) *Culturing Nerve Cells*, 2nd edn. The MIT Press, London, UK.

Gött, P., Beck, S., Machado, J.C., Carneiro, F., Schmitt, H., & Blin, N. (1996) Human trefoil peptides: genomic structure in 21q22.3 and coordinated expression. *Eur. J. Hum. Genet. EJHG*, **4**, 308–315.

Graness, A., Chwieralski, C.E., Reinhold, D., Thim, L., & Hoffmann, W. (2002) Protein kinase C and ERK activation are required for TFF-peptide-stimulated bronchial epithelial cell migration and tumor necrosis factor-alpha-induced interleukin-6 (IL-6) and IL-8 secretion. *J. Biol. Chem.*, **277**, 18440–18446.

Grivennikov, S.I., Greten, F.R., & Karin, M. (2010) Immunity, inflammation, and cancer. *Cell*, **140**, 883–899.

Grønbaek, H., Vestergaard, E.M., Hey, H., Nielsen, J.N., & Nexø, E. (2006) Serum trefoil factors in patients with inflammatory bowel disease. *Digestion*, **74**, 33–39.

Grünert, S., Jechlinger, M., & Beug, H. (2003) Diverse cellular and molecular mechanisms contribute to epithelial plasticity and metastasis. *Nat. Rev. Mol. Cell Biol.*, **4**, 657–665.

Guizzetti, M. & Costa, L.G. (1996) Inhibition of muscarinic receptor-stimulated glial cell proliferation by ethanol. *J. Neurochem.*, **67**, 2236–2245.

Guppy, N.J., El-Bahrawy, M.E., Kocher, H.M., Fritsch, K., Qureshi, Y. a, Poulsom, R., Jeffery, R.E., Wright, N. a, Otto, W.R., & Alison, M.R. (2012) Trefoil factor family peptides in normal and diseased human pancreas. *Pancreas*, **41**, 888–896.

Hammond, S.M., Bernstein, E., Beach, D., & Hannon, G.J. (2000) An RNA-directed nuclease mediates post-transcriptional gene silencing in Drosophila cells. *Nature*, **404**, 293–296.

Hanby, A.M., Poulsom, R., Elia, G., Singh, S., Longcroft, J.M., & Wright, N.A. (1993) The expression of the trefoil peptides pS2 and human spasmolytic polypeptide (hSP) in "gastric metaplasia" of the proximal duodenum: implications for the nature of "gastric metaplasia". *J. Pathol.*, **169**, 355–360.

Händel, U., Brunn, A., Drögemüller, K., Müller, W., Deckert, M., & Schlüter, D. (2012) Neuronal gp130 expression is crucial to prevent neuronal loss, hyperinflammation, and lethal course of murine Toxoplasma encephalitis. *Am. J. Pathol.*, **181**, 163–173.

Hansson, G.C. (2012) Role of mucus layers in gut infection and inflammation. *Curr. Opin. Microbiol.*, **15**, 57–62.

Hauser, F., Poulsom, R., Chinery, R., Rogers, L.A., Hanby, A.M., Wright, N.A., & Hoffmann, W. (1993) hP1.B, a human P-domain peptide homologous with rat intestinal trefoil factor, is expressed also in the ulcer-associated cell lineage and the uterus. *Proc. Natl. Acad. Sci. U. S. A.*, **90**, 6961–6965.

Havelaar, A.H., Kemmeren, J.M., & Kortbeek, L.M. (2007) Disease burden of congenital toxoplasmosis. *Clin. Infect. Dis.*, **44**, 1467–1474.

Hay, E.D. (1995) An overview of epithelio-mesenchymal transformation. *Acta Anat.*, **154**, 8–20.

Hay, E.D. (2005) The mesenchymal cell, its role in the embryo, and the remarkable signaling mechanisms that create it. *Dev. Dyn.*, **233**, 706–720.

He, L. & Hannon, G.J. (2004) MicroRNAs: small RNAs with a big role in gene regulation. *Nat. Rev. Genet.*, **5**, 522–531.

Helander, H.F. (1981) The cells of the gastric mucosa. *Int. Rev. Cytol.*, **70**, 217–289.

Higashiyama, M., Doi, O., Kodama, K., Yokuchi, H., Inaji, H., & Tateishi, R. (1996) Estimation of serum level of pS2 protein in patients with lung adenocarcinoma. *Anticancer Res.*, **16**, 2351–2355.

Hinz, M., Schwegler, H., Chwieralski, C.E., Laube, G., Linke, R., Pohle, W., & Hoffmann, W. (2004) Trefoil factor family (TFF) expression in the mouse brain and pituitary: changes in the developing cerebellum. *Peptides*, **25**, 827–832.

Hirota, M., Awatsuji, H., Furukawa, Y., & Hayashi, K. (1994a) Cytokine regulation of PS2 gene expression in mouse astrocytes. *Biochem. Mol. Biol. Int.*, **33**, 515–520.

Hirota, M., Awatsuji, H., Sugihara, Y., Miyashita, S., Furukawa, Y., & Hayashi, K. (1995) Expression of pS2 gene in rat brain. *Biochem. Mol. Biol. Int.*, **35**, 1079–1084.

Hirota, M., Miyashita, S., Hayashi, H., Furukawa, Y., & Hayashi, K. (1994b) pS2 gene especially expressed in the late G1/S phase of mouse astrocytes. *Neurosci. Lett.*, **171**, 49–51.

Ho, S.B., Shekels, L.L., Toribara, N.W., Kim, Y.S., Lyftogt, C., Cherwitz, D.L., & Niehans, G.A. (1995) Mucin gene expression in normal, preneoplastic, and neoplastic human gastric epithelium. *Cancer Res.*, **55**, 2681–2690.

Hoffmann, W. (2004) Trefoil factor family (TFF) peptides: regulators of mucosal regeneration and repair, and more. *Peptides*, **25**, 727–730.

Hoffmann, W. (2005) Trefoil factors TFF (trefoil factor family) peptide-triggered signals promoting mucosal restitution. *Cell. Mol. Life Sci.*, **62**, 2932–2938.

Hoffmann, W. (2006) *TFF (Trefoil Factor Family) Peptides.* 1st edn. *in Handbook of Biologically Active Peptides.* Kastin A. (Edt.), Elsevier, San Diego, CA, pp 1147-1154.

Hoffmann, W. (2007) TFF (trefoil factor family) peptides and their potential roles for differentiation processes during airway remodeling. *Curr. Med. Chem.*, **14**, 2716–2719.

Hoffmann, W. (2008) Regeneration of the gastric mucosa and its glands from stem cells. *Curr. Med. Chem.*, **15**, 3133–3144.

Hoffmann, W. (2009) Trefoil factor family (TFF) peptides and chemokine receptors: a promising relationship. *J. Med. Chem.*, **52**, 6505–6510.

Hoffmann, W. (2012) Stem cells, self-renewal and cancer of the gastric epithelium. *Curr. Med. Chem.*, **19**, 5975–5983.

Hoffmann, W. (2013a) *TFF Peptides*, 2nd edn. *in Handbook of Biologically Active Peptides.* Kastin A. (Edt.), Elsevier Inc., Baton Rouge, LA, pp 1338-1345.

Hoffmann, W. (2013b) Self-renewal of the gastric epithelium from stem and progenitor cells. *Front. Biosci. (Schol. Ed.)*, **S5**, 720–731.

Hoffmann, W. & Hauser, F. (1993) The P-domain or trefoil motif: a role in renewal and pathology of mucous epithelia? *Trends Biochem. Sci.*, **18**, 239–243.

Hoffmann, W. & Jagla, W. (2002) Cell type specific expression of secretory TFF peptides: colocalization with mucins and synthesis in the brain. *Int. Rev. Cytol.*, **213**, 147–181.

Hoffmann, W., Jagla, W., & Wiede, A. (2001) Molecular medicine of TFF-peptides: from gut to brain. *Histol. Histopathol.*, **16**, 319–334.

Houghton, J., Stoicov, C., Nomura, S., Rogers, A.B., Carlson, J., Li, H., Cai, X., Fox, J.G., Goldenring, J.R., & Wang, T.C. (2004) Gastric cancer originating from bone marrow-derived cells. *Science*, **306**, 1568–1571.

Howe, D.K. & Sibley, L.D. (1995) Toxoplasma gondii comprises three clonal lineages: correlation of parasite genotype with human disease. *J. Infect. Dis.*, **172**, 1561–1566.

Huber, M.A., Azoitei, N., Baumann, B., Grünert, S., Sommer, A., Pehamberger, H., Kraut, N., Beug, H., & Wirth, T. (2004) NF- κ B is essential for epithelial- mesenchymal transition and metastasis in a model of breast cancer progression. *J. Clin. Invest.*, **114**, 569–581.

Hunter, C.A., Chizzonite, R., & Remington, J.S. (1995) IL-1 beta is required for IL-12 to induce production of IFN-gamma by NK cells. A role for IL-1 beta in the T cell-independent mechanism of resistance against intracellular pathogens. *J. Immunol.*, **155**, 4347–4354.

Hunter, C.A., Subauste, C.S., Van Cleave, V.H., & Remington, J.S. (1994) Production of gamma interferon by natural killer cells from Toxoplasma gondii-infected SCID mice: regulation by interleukin-10, interleukin-12, and tumor necrosis factor alpha. *Infect. Immun.*, **62**, 2818–2824.

Hutchison, W.M., Dunachie, J.F., Siim, J.C., & Work, K. (1970) Coccidian-like nature of Toxoplasma gondii. *Br. Med. J.*, **1**, 142–144.

InvivoGen (2003) siRNA design guidelines. http://www.sirnawizard.com/guidelines.php

Ito, D., Imai, Y., Ohsawa, K., Nakajima, K., Fukuuchi, Y., & Kohsaka, S. (1998) Microglia-specific localisation of a novel calcium binding protein, Iba1. *Brain Res. Mol. Brain Res.*, **57**, 1–9.

Ito, D., Tanaka, K., Suzuki, S., Dembo, T., & Fukuuchi, Y. (2001) Enhanced expression of Iba1, ionized calcium-binding adapter molecule 1, after transient focal cerebral ischemia in rat brain. *Stroke.*, **32**, 1208–1215.

Itoh, H., Tomita, M., Uchino, H., Kobayashi, T., Kataoka, H., Sekiya, R., & Nawa, Y. (1996) cDNA cloning of rat pS2 peptide and expression of trefoil peptides in acetic acid-induced colitis. *Biochem. J.*, **318 (Pt 3)**, 939–944.

Ivanov, A.I., Nusrat, A., & Parkos, C.A. (2005) Endocytosis of the apical junctional complex: mechanisms and possible roles in regulation of epithelial barriers. *BioEssays*, **27**, 356–365.

Jagla, W., Wiede, A., Dietzmann, K., Rutkowski, K., & Hoffmann, W. (2000) Co-localization of TFF3 peptide and oxytocin in the human hypothalamus. *FASEB J.*, **14**, 1126–1131.

Jakowlew, S.B., Breathnach, R., Jeltsch, J.-M., Masiakowski, P., & Chambon, P. (1984) Sequence of the pS2 mRNA induced by estrogen in the human breast cancer cell line MCF-7. *Nucleic Acids Res.*, **12**, 2861–2878.

Jamroz, E., Adamek, D., Paprocka, J., Adamowicz, M., Marszał, E., & Wevers, R. a (2009) CDG type Ia and congenital cytomegalovirus infection: two coexisting conditions. *J. Child Neurol.*, **24**, 13–18.

Jechlinger, M., Grunert, S., Tamir, I.H., Janda, E., Lüdemann, S., Waerner, T., Seither, P., Weith, A., Beug, H., & Kraut, N. (2003) Expression profiling of epithelial plasticity in tumor progression. *Oncogene*, **22**, 7155–7169.

Jensen, P., Heimberg, M., Ducray, A.D., Widmer, H.R., & Meyer, M. (2013) Expression of trefoil factor 1 in the developing and adult rat ventral mesencephalon. *PLoS One*, **8**, e76592.

Johansson, M.E. V, Ambort, D., Pelaseyed, T., Schütte, A., Gustafsson, J.K., Ermund, A., Subramani, D.B., Holmén-Larsson, J.M., Thomsson, K. a, Bergström, J.H., van der Post, S., Rodriguez-Piñeiro, A.M., Sjövall, H., Bäckström, M., & Hansson, G.C. (2011) Composition and functional role of the mucus layers in the intestine. *Cell. Mol. Life Sci.*, **68**, 3635–3641.

Johnson, A.M. (1984) Strain-dependent, route of challenge-dependent, murine susceptibility to toxoplasmosis. *Z. Parasitenkd.*, **70**, 303–309.

Jørgensen, K.H., Thim, L., & Jacobsen, H.E. (1982) Pancreatic spasmolytic polypeptide (PSP): I. Preparation and initial chemical characterization of a new polypeptide from porcine pancreas. *Regul. Pept.*, **3**, 207–219.

Kalluri, R. & Weinberg, R.A. (2009) The basics of epithelial-mesenchymal transition. *J. Clin. Invest.*, **119**, 1420–1428.

Karam, S.M., Tomasetto, C., & Rio, M.-C. (2004) Trefoil factor 1 is required for the commitment programme of mouse oxyntic epithelial progenitors. *Gut*, **53**, 1408–1415.

Kim, D.H. & Rossi, J.J. (2007) Strategies for silencing human disease using RNA interference. *Nat. Rev. Genet.*, **8**, 173–184.

Kindon, H., Pothoulakis, C., Thim, L., Lynch-Devaney, K., & Podolsky, D.K. (1995) Trefoil peptide protection of intestinal epithelial barrier function: cooperative interaction with mucin glycoprotein. *Gastroenterology*, **109**, 516–523.

Kinoshita, K., Taupin, D.R., Itoh, H., & Podolsky, D.K. (2000) Distinct pathways of cell migration and antiapoptotic response to epithelial injury: structure-function analysis of human intestinal trefoil factor. *Mol. Cell. Biol.*, **20**, 4680–4690.

Kjellev, S. (2009) The trefoil factor family - small peptides with multiple functionalities. *Cell. Mol. Life Sci.*, **66**, 1350–1369.

Kobayashi, I., Kawano, S., Tsuji, S., Matsui, H., Nakama, A., Sawaoka, H., Masuda, E., Takei, Y., Nagano, K., Fusamoto, H., Ohno, T., Fukutomi, H., & Kamada, T. (1996) RGM1, a cell line derived from normal gastric mucosa of rat. *In Vitro Cell. Dev. Biol. Anim.*, **32**, 259–261.

Kobayashi, M., Fitz, L., Ryan, M., Hewick, R.M., Clark, S.C., Chan, S., Loudon, R., Sherman, F., Perussia, B., & Trinchieri, G. (1989) Identification and purification of natural killer cell stimulatory factor (NKSF), a cytokine with multiple biologic effects on human lymphocytes. *J. Exp. Med.*, **170**, 827–845.

Koike, T., Shimada, T., Fujii, Y., Chen, G., Tabei, K., Namatame, T., Yamagata, M., Tajima, A., Yoneda, M., Terano, A., & Hiraishi, H. (2007) Up-regulation of TFF1 (pS2) expression by TNF-alpha in gastric epithelial cells. *J. Gastroenterol. Hepatol.*, **22**, 936–942.

Kouznetsova, I., Gerlach, K.L., Zahl, C., & Hoffmann, W. (2010) Expression analysis of human salivary glands by laser microdissection: differences between submandibular and labial glands. *Cell. Physiol. Biochem.*, **26**, 375–382.

Kouznetsova, I., Kalinski, T., Meyer, F., & Hoffmann, W. (2011) Self-renewal of the human gastric epithelium: new insights from expression profiling using laser microdissection. *Mol. Biosyst.*, **7**, 1105–1112.

Kouznetsova, I., Kalinski, T., Peitz, U., Mönkemüller, K.E., Kalbacher, H., Vieth, M., Meyer, F., Roessner, A., Malfertheiner, P., Lippert, H., & Hoffmann, W. (2007a) Localization of TFF3 peptide in human esophageal submucosal glands and gastric cardia: differentiation of two types of gastric pit cells along the rostro-caudal axis. *Cell Tissue Res.*, **328**, 365–374.

Kouznetsova, I., Laubinger, W., Kalbacher, H., Kalinski, T., Meyer, F., Roessner, A., & Hoffmann, W. (2007b) Biosynthesis of gastrokine-2 in the human gastric mucosa: restricted spatial expression along the antral gland axis and differential interaction with TFF1, TFF2 and mucins. *Cell. Physiol. Biochem.*, **20**, 899–908.

Kouznetsova, I., Peitz, U., Vieth, M., Meyer, F., Vestergaard, E.M., Malfertheiner, P., Roessner, A., Lippert, H., & Hoffmann, W. (2004) A gradient of TFF3 (trefoil factor family 3) peptide synthesis within the normal human gastric mucosa. *Cell Tissue Res.*, **316**, 155–165.

Kucia, M., Reca, R., Miekus, K., Wanzeck, J., Wojakowski, W., Janowska-Wieczorek, A., Ratajczak, J., & Ratajczak, M.Z. (2005) Trafficking of normal stem cells and metastasis of cancer stem cells involve similar mechanisms: pivotal role of the SDF-1-CXCR4 axis. *Stem Cells*, **23**, 879–894.

Kurt-Jones, E.A., Cao, L., Sandor, F., Rogers, A.B., Whary, M.T., Nambiar, P.R., Cerny, A., Bowen, G., Yan, J., Takaishi, S., Chi, A.L., Reed, G., Houghton, J., Fox, J.G., & Wang, T.C. (2007) Trefoil family factor 2 is expressed in murine gastric and immune cells and controls both gastrointestinal inflammation and systemic immune responses. *Infect. Immun.*, **75**, 471–480.

Lalani, E.N., Williams, R., Jayaram, Y., Gilbert, C., Chaudhary, K.S., Siu, L.S., Koumarianou, A., Playford, R., & Stamp, G.W. (1999) Trefoil factor-2, human spasmolytic polypeptide, promotes branching morphogenesis in MCF-7 cells. *Lab. Invest.*, **79**, 537–546.

Leaphart, C.L., Qureshi, F., Cetin, S., Li, J., Dubowski, T., Baty, C., Batey, C., Beer-Stolz, D., Guo, F., Murray, S.A., & Hackam, D.J. (2007) Interferon-gamma inhibits intestinal restitution by preventing gap junction communication between enterocytes. *Gastroenterology*, **132**, 2395–2411.

Lee, J.M., Dedhar, S., Kalluri, R., & Thompson, E.W. (2006) The epithelial-mesenchymal transition: new insights in signaling, development, and disease. *J. Cell Biol.*, **172**, 973–981.

Lefebvre, O., Chenard, M.-P., Masson, R., Linares, J., Dierich, A., LeMeur, M., Wendling, C., Tomasetto, C., Chambon, P., & Rio, M.-C. (1996) Gastric mucosa abnormalities and tumorigenesis in mice lacking the pS2 trefoil protein. *Science*, **274**, 259–262.

Lefebvre, O., Wolf, C., Kédinger, M., Chenard, M.-P., Tomasetto, C., Chambon, P., & Rio, M.-C. (1993) The mouse one P-domain (pS2) and two P-domain (mSP) genes exhibit distinct patterns of expression. *J. Cell Biol.*, **122**, 191–198.

Lein, E.S., Hawrylycz, M.J., Ao, N., Ayres, M., Bensinger, A., *et al.* (2007) Genome-wide atlas of gene expression in the adult mouse brain. *Nature*, **445**, 168–176.

Lemercinier, X., Muskett, F.W., Cheeseman, B., McIntosh, P.B., Thim, L., & Carr, M.D. (2001) High-resolution solution structure of human intestinal trefoil factor and functional insights from detailed structural comparisons with the other members of the trefoil family of mammalian cell motility factors. *Biochemistry*, **40**, 9552–9559.

Liesenfeld, O. (2002) Oral infection of C57BL/6 mice with Toxoplasma gondii: a new model of inflammatory bowel disease? *J. Infect. Dis.*, **185**, S96–101.

LifeTechnologies (2003) siRNA Design Guidelines | Technical Bulletin #506, http://www.lifetechnologies.com/de/de/home/references/ambion-tech-support/rnai-sirna/general-articles/-sirna-design-guidelines.html

Liu, C., Fan, Y., Dias, A., Esper, L., Corn, R.A., Bafica, A., Machado, F.S., & Aliberti, J. (2006) Cutting edge: dendritic cells are essential for in vivo IL-12 production and development of resistance against Toxoplasma gondii infection in mice. *J. Immunol.*, **177**, 31–35.

Liu, J., Wang, X., Cai, Y., Zhou, J., Guleng, B., Shi, H., & Ren, J. (2012) The regulation of trefoil factor 2 expression by the transcription factor Sp3. *Biochem. Biophys. Res. Commun.*, **427**, 410–414.

Lu, X., Ma, L., Ruan, L., Kong, Y., Mou, H., Zhang, Z., Wang, Z., Wang, J.M., & Le, Y. (2010) Resveratrol differentially modulates inflammatory responses of microglia and astrocytes. *J. Neuroinflamm.*, **7**, 46.

Lubka, M., Müller, M., Baus-Loncar, M., Hinz, M., Blaschke, K., Hoffmann, W., Pfister, M., Löwenheim, H., Pusch, C.M., Knipper, M., & Blin, N. (2008) Lack of Tff3 peptide results in hearing impairment and accelerated presbyacusis. *Cell. Physiol. Biochem.*, **21**, 437–444.

Luft, B.J., Conley, F., Remington, J.S., Laverdiere, M., Wagner, K.F., Levine, J.F., Craven, P.C., Strandberg, D.A., File, T.M., Rice, N., & Meunier-Carpentier, F. (1983) Outbreak of central-nervous-system toxoplasmosis in western Europe and North America. *Lancet*, **1**, 781–784.

Luqmani, Y., Bennett, C., Paterson, I., Corbishley, C.M., Rio, M.C., Chambon, P., & Ryall, G. (1989) Expression of the pS2 gene in normal, benign and neoplastic human stomach. *Int. J. Cancer*, **44**, 806–812.

Machado, J.C., Carneiro, F., Ribeiro, P., Blin, N., & Sobrinho-Simões, M. (1996) pS2 protein expression in gastric carcinoma. An immunohistochemical and immunoradiometric study. *Eur. J. cancer*, **32A**, 1585–1590.

Machado, J.C., Nogueira, A.M., Carneiro, F., Reis, C.A., & Sobrinho-Simões, M. (2000) Gastric carcinoma exhibits distinct types of cell differentiation: an immunohistochemical study of trefoil peptides (TFF1 and TFF2) and mucins (MUC1, MUC2, MUC5AC, and MUC6). *J. Pathol.*, **190**, 437–443.

Madsen, J., Nielsen, O., Tornøe, I., Thim, L., & Holmskov, U. (2007) Tissue localization of human trefoil factors 1, 2, and 3. *J. Histochem. Cytochem. Off. J. Histochem. Soc.*, **55**, 505–513.

Mani, S. a, Guo, W., Liao, M.-J., Eaton, E.N., Ayyanan, A., Zhou, A.Y., Brooks, M., Reinhard, F., Zhang, C.C., Shipitsin, M., Campbell, L.L., Polyak, K., Brisken, C., Yang, J., & Weinberg, R. a (2008) The epithelial-mesenchymal transition generates cells with properties of stem cells. *Cell*, **133**, 704–715.

Marchbank, T., Westley, B.R., May, F.E., Calnan, D.P., & Playford, R.J. (1998) Dimerization of human pS2 (TFF1) plays a key role in its protective/healing effects. *J. Pathol.*, **185**, 153–158.

Mashimo, H., Wu, D.-C., Podolsky, D.K., & Fishman, M.C. (1996) Impaired defense of intestinal mucosa in mice lacking intestinal trefoil factor. *Science*, **274**, 262–265.

Masiakowski, P., Breathnach, R., Bloch, J., Gannon, F., Krust, A., & Chambon, P. (1982) Cloning of cDNA sequences of hormone-regulated genes from the MCF-7 human breast cancer cell line. *Nucleic Acids Res.*, **10**, 7895–7903.

Masszi, A., Di Ciano, C., Sirokmány, G., Arthur, W.T., Rotstein, O.D., Wang, J., McCulloch, C.A.G., Rosivall, L., Mucsi, I., & Kapus, A. (2003) Central role for Rho in TGF-beta1-induced alpha-smooth muscle actin expression during epithelial-mesenchymal transition. *Am. J. Physiol. Renal Physiol.*, **284**, F911–24.

Matranga, C., Tomari, Y., Shin, C., Bartel, D.P., & Zamore, P.D. (2005) Passenger-strand cleavage facilitates assembly of siRNA into Ago2-containing RNAi enzyme complexes. *Cell*, **123**, 607–620.

Matsuda, K., Yamauchi, K., Matsumoto, T., Sano, K., Yamaoka, Y., & Ota, H. (2008) Quantitative analysis of the effect of Helicobacter pylori on the expressions of SOX2, CDX2, MUC2, MUC5AC, MUC6, TFF1, TFF2, and TFF3 mRNAs in human gastric carcinoma cells. *Scand. J. Gastroenterol.*, **43**, 25–33.

Matus, A. (1991) Microtubule-associated proteins and neuronal morphogenesis. *J. Cell Sci. Suppl.*, **15**, 61–67.

May, F.E.B., Griffin, S.M., & Westley, B.R. (2009) The trefoil factor interacting protein TFIZ1 binds the trefoil protein TFF1 preferentially in normal gastric mucosal cells but the co-expression of these proteins is deregulated in gastric cancer. *Int. J. Biochem. Cell Biol.*, **41**, 632–640.

McBerry, C., Egan, C.E., Rani, R., Yang, Y., Wu, D., Boespflug, N., Boon, L., Butcher, B., Mirpuri, J., Hogan, S.P., Denkers, E.Y., Aliberti, J., & Herbert, D.R. (2012) Trefoil factor 2 negatively regulates type 1 immunity against Toxoplasma gondii. *J. Immunol.*, **189**, 3078–3084.

McCormack, S.A., Viar, M.J., & Johnson, L.R. (1992) Migration of IEC-6 cells: a model for mucosal healing. *Am. J. Physiol.*, **263**, G426–35.

McKenzie, J. a & Grossman, D. (2012) Role of the apoptotic and mitotic regulator survivin in melanoma. *Anticancer Res.*, **32**, 397–404.

McKenzie, J. a, Liu, T., Goodson, A.G., & Grossman, D. (2010) Survivin enhances motility of melanoma cells by supporting Akt activation and α5 integrin upregulation. *Cancer Res.*, **70**, 7927–7937.

Mead, P.S., Slutsker, L., Dietz, V., McCaig, L.F., Bresee, J.S., Shapiro, C., Griffin, P.M., & Tauxe, R. V (1999) Food-related illness and death in the United States. *Emerg. Infect. Dis.*, **5**, 607–625.

Medzhitov, R. (2008) Origin and physiological roles of inflammation. *Nature*, **454**, 428–435.

Miller, C.M., Boulter, N.R., Ikin, R.J., & Smith, N.C. (2009) The immunobiology of the innate response to Toxoplasma gondii. *Int. J. Parasitol.*, **39**, 23–39.

Miyashita, S., Nomoto, H., Konishi, H., & Hayashi, K. (1994) Estimation of pS2 protein level in human body fluids by a sensitive two-site enzyme immunoassay. *Clin. Chim. Acta.*, **228**, 71–81.

Moreno-Bueno, G., Portillo, F., & Cano, a (2008) Transcriptional regulation of cell polarity in EMT and cancer. *Oncogene*, **27**, 6958–6969.

Moyer, R.A., Wendt, M.K., Johanesen, P.A., Turner, J.R., & Dwinell, M.B. (2007) Rho activation regulates CXCL12 chemokine stimulated actin rearrangement and restitution in model intestinal epithelia. *Lab. Invest.*, **87**, 807–817.

Munoz, M., Liesenfeld, O., & Heimesaat, M.M. (2011) Immunology of Toxoplasma gondii. *Immunol. Rev.*, **240**, 269–285.

Muskett, F.W., May, F.E.B., Westley, B.R., & Feeney, J. (2003) Solution structure of the disulfide-linked dimer of human intestinal trefoil factor (TFF3): the intermolecular orientation and interactions are markedly different from those of other dimeric trefoil proteins. *Biochemistry*, **42**, 15139–15147.

Nakamura, E., Takahashi, S., Matsui, H., & Okabe, S. (1998) Interleukin-1beta inhibits growth factor-stimulated restoration of wounded rat gastric epithelial cell monolayers. *Dig. Dis. Sci.*, **43**, 476–484.

Newton, J.L., Allen, A., Westley, B.R., & May, F.E. (2000) The human trefoil peptide, TFF1, is present in different molecular forms that are intimately associated with mucus in normal stomach. *Gut*, **46**, 312–320.

Nicolle, C. & Manceaux, L. (1908) Sur une infection a corps de Leishman (ou organismes voisons) du gondi. *C R Acad Sci*, **147**, 736.

Nogueira, A.M., Machado, J.C., Carneiro, F., Reis, C.A., Gött, P., & Sobrinho-Simões, M. (1999) Patterns of expression of trefoil peptides and mucins in gastric polyps with and without malignant transformation. *J. Pathol.*, **187**, 541–548.

Nollet, F., Berx, G., & van Roy, F. (1999) The role of the E-cadherin/catenin adhesion complex in the development and progression of cancer. *Mol. Cell Biol. Res. Commun.*, **2**, 77–85.

Nunez, A.M., Jakowlev, S., Briand, J.P., Gaire, M., Krust, A., Rio, M.-C., & Chambon, P. (1987) Characterization of the estrogen-induced pS2 protein secreted by the human breast cancer cell line MCF-7. *Endocrinology*, **121**, 1759–1765.

Nusrat, A., Delp, C., & Madara, J.L. (1992) Intestinal epithelial restitution. Characterization of a cell culture model and mapping of cytoskeletal elements in migrating cells. *J. Clin. Invest.*, **89**, 1501–1511.

Orlando, R.C., Lacy, E.R., Tobey, N.A., & Cowart, K. (1992) Barriers to paracellular permeability in rabbit esophageal epithelium. *Gastroenterology*, **102**, 910–923.

Osada, T., Watanabe, S., Tanaka, H., Hirose, M., Miyazaki, A., & Sato, N. (1999) Effect of mechanical strain on gastric cellular migration and proliferation during mucosal healing: role of Rho dependent and Rac dependent cytoskeletal reorganisation. *Gut*, **45**, 508–515.

Ota, H., Hayama, M., Momose, M., El-Zimaity, H.M.T., Matsuda, K., Sano, K., Maruta, F., Okumura, N., & Katsuyama, T. (2006) Co-localization of TFF2 with gland mucous cell mucin in gastric mucous cells and in extracellular mucous gel adherent to normal and damaged gastric mucosa. *Histochem. Cell Biol.*, **126**, 617–625.

Patrat-Delon, S., Gangneux, J.-P., Lavoué, S., Lelong, B., Guiguen, C., le Tulzo, Y., & Robert-Gangneux, F. (2010) Correlation of parasite load determined by quantitative PCR to clinical outcome in a heart transplant patient with disseminated toxoplasmosis. *J. Clin. Microbiol.*, **48**, 2541–2545.

Paulsen, F.P., Woon, C.-W., Varoga, D., Jansen, A., Garreis, F., Jäger, K., Amm, M., Podolsky, D.K., Steven, P., Barker, N.P., & Sel, S. (2008) Intestinal trefoil factor/TFF3 promotes re-epithelialization of corneal wounds. *J. Biol. Chem.*, **283**, 13418–13427.

Paunel-Görgülü, A.N., Franke, A.G., Paulsen, F.P., & Dünker, N. (2011) Trefoil factor family peptide 2 acts pro-proliferative and pro-apoptotic in the murine retina. *Histochem. Cell Biol.*, **135**, 461–473.

Perry, J.K., Kannan, N., Grandison, P.M., Mitchell, M.D., & Lobie, P.E. (2008) Are trefoil factors oncogenic? *Trends Endocrinol. Metab.*, **19**, 74–81.

Peterson, A.J., Menheniott, T.R., O'Connor, L., Walduck, A.K., Fox, J.G., Kawakami, K., Minamoto, T., Ong, E.K., Wang, T.C., Judd, L.M., & Giraud, A.S. (2010) Helicobacter pylori infection promotes methylation and silencing of trefoil factor 2, leading to gastric tumor development in mice and humans. *Gastroenterology*, **139**, 2005–2017.

Peyron, F., Lobry, J.R., Musset, K., Ferrandiz, J., Gomez-Marin, J.E., Petersen, E., Meroni, V., Rausher, B., Mercier, C., Picot, S., & Cesbron-Delauw, M.-F. (2006) Serotyping of Toxoplasma gondii in chronically infected pregnant women: predominance of type II in Europe and types I and III in Colombia (South America). *Microbes Infect.*, **8**, 2333–2340.

Piggott, N.H., Henry, J.A., May, F.E., & Westley, B.R. (1991) Antipeptide antibodies against the pNR-2 oestrogen-regulated protein of human breast cancer cells and detection of pNR-2 expression in normal tissues by immunohistochemistry. *J. Pathol.*, **163**, 95–104.

Playford, R.J., Marchbank, T., Chinery, R., Evison, R., Pignatelli, M., Boulton, R. a, Thim, L., & Hanby, a M. (1995) Human spasmolytic polypeptide is a cytoprotective agent that stimulates cell migration. *Gastroenterology*, **108**, 108–116.

Playford, R.J., Marchbank, T., Goodlad, R. a, Chinery, R. a, Poulsom, R., & Hanby, a M. (1996) Transgenic mice that overexpress the human trefoil peptide pS2 have an increased resistance to intestinal damage. *Proc. Natl. Acad. Sci. U. S. A.*, **93**, 2137–2142.

Podolsky, D.K., Lynch-Devaney, K., Stow, J.L., Oates, P., Murgue, B., DeBeaumont, M., Sands, B.E., & Mahida, Y.R. (1993) Identification of human intestinal trefoil factor. Goblet cell-specific expression of a peptide targeted for apical secretion. *J. Biol. Chem.*, **268**, 6694–6702.

Polshakov, V.I., Williams, M.A., Gargaro, A.R., Frenkiel, T.A., Westley, B.R., Chadwick, M.P., May, F.E., & Feeney, J. (1997) High-resolution solution structure of human pNR-2/pS2: a single trefoil motif protein. *J. Mol. Biol.*, **267**, 418–432.

Poulsen, S.S., Kissow, H., Hare, K., Hartmann, B., & Thim, L. (2005) Luminal and parenteral TFF2 and TFF3 dimer and monomer in two models of experimental colitis in the rat. *Regul. Pept.*, **126**, 163–171.

Poulsom, R. (1996) Trefoil peptides. *Baillieres. Clin. Gastroenterol.*, **10**, 113–134.

Prest, S.J., May, F.E.B., & Westley, B.R. (2002) The estrogen-regulated protein, TFF1, stimulates migration of human breast cancer cells. *FASEB J.*, **16**, 592–594.

Probst, J.C., Skutella, T., Müller-Schmid, A., Jirikowski, G.F., & Hoffmann, W. (1995) Molecular and cellular analysis of rP1.B in the rat hypothalamus: in situ hybridization and immunohistochemistry of a new P-domain neuropeptide. *Brain Res. Mol. Brain Res.*, **33**, 269–276.

Probst, J.C., Zetzsche, T., Weber, M., Theilemann, P., Skutella, T., Landgraf, R., & Jirikowski, G.F. (1996) Human intestinal trefoil factor is expressed in human hypothalamus and pituitary: evidence for a novel neuropeptide. *FASEB J.*, **10**, 1518–1523.

Qin, L., Wu, X., Block, M.L., Liu, Y., Breese, G.R., Hong, J.-S., Knapp, D.J., & Crews, F.T. (2007) Systemic LPS causes chronic neuroinflammation and progressive neurodegeneration. *Glia*, **55**, 453–462.

Quigley, E.M. & Turnberg, L.A. (1987) pH of the microclimate lining human gastric and duodenal mucosa in vivo. Studies in control subjects and in duodenal ulcer patients. *Gastroenterology*, **92**, 1876–1884.

Radke, J.R. & White, M.W. (1998) A cell cycle model for the tachyzoite of Toxoplasma gondii using the Herpes simplex virus thymidine kinase. *Mol. Biochem. Parasitol.*, **94**, 237–247.

Radtke, F. & Clevers, H. (2005) Self-renewal and cancer of the gut: two sides of a coin. *Science*, **307**, 1904–1909.

Ragasa, R., Nakamura, E., Marrone, L., Yanaka, S., Hayashi, S., Takeuchi, K., & Hagen, S.J. (2007) Isothiocyanate inhibits restitution and wound repair after injury in the stomach: ex vivo and in vitro studies. *J. Pharmacol. Exp. Ther.*, **323**, 1–9.

Regalo, G., Wright, N. A, & Machado, J.C. (2005) Trefoil factors: from ulceration to neoplasia. *Cell. Mol. Life Sci.*, **62**, 2910–2915.

Reymond, A., Marigo, V., Yaylaoglu, M.B., Leoni, A., Ucla, C., Scamuffa, N., Caccioppoli, C., Dermitzakis, E.T., Lyle, R., Banfi, S., Eichele, G., Antonarakis, S.E., & Ballabio, A. (2002) Human chromosome 21 gene expression atlas in the mouse. *Nature*, **420**, 582–586.

Ribieras, S., Tomasetto, C., & Rio, M.-C. (1998) The pS2/TFF1 trefoil factor, from basic research to clinical applications. *Biochim. Biophys. Acta*, **1378**, F61–77.

Rinnert, M., Hinz, M., Buhtz, P., Reiher, F., Lessel, W., & Hoffmann, W. (2010) Synthesis and localization of trefoil factor family (TFF) peptides in the human urinary tract and TFF2 excretion into the urine. *Cell Tissue Res.*, **339**, 639–647.

Rio, M.-C., Bellocq, J.P., Daniel, J.Y., Tomasetto, C., Lathe, R., Chenard, M.P., Batzenschlager, A., & Chambon, P. (1988a) Breast cancer-associated pS2 protein: synthesis and secretion by normal stomach mucosa. *Science*, **241**, 705–708.

Rio, M.C., Chenard, M.P., Wolf, C., Marcellin, L., Tomasetto, C., Lathe, R., Bellocq, J.P., & Chambon, P. (1991) Induction of pS2 and hSP genes as markers of mucosal ulceration of the digestive tract. *Gastroenterology*, **100**, 375–379.

Rio, M.C., Lepage, P., Diemunsch, P., Roitsch, C., & Chambon, P. (1988b) [Primary structure of human protein pS2]. *C. R. Acad. Sci. III.*, **307**, 825–831.

Rösler, S., Haase, T., Claassen, H., Schulze, U., Schicht, M., Riemann, D., Brandt, J., Wohlrab, D., Müller-Hilke, B., Goldring, M.B., Sel, S., Varoga, D., Garreis, F., & Paulsen, F.P. (2010) Trefoil

factor 3 is induced during degenerative and inflammatory joint disease, activates matrix metalloproteinases, and enhances apoptosis of articular cartilage chondrocytes. *Arthritis Rheum.*, **62**, 815–825.

Ruchaud-Sparagano, M.-H., Westley, B.R., & May, F.E.B. (2004) The trefoil protein TFF1 is bound to MUC5AC in human gastric mucosa. *Cell. Mol. Life Sci.*, **61**, 1946–1954.

Sabin, A.B. & Olitsky, P.K. (1937) Toxoplasma and obligate intracellular parasitism. *Science*, **85**, 336–338.

Saitoh, T., Mochizuki, T., Suda, T., Aoyagi, Y., Tsukada, Y., Narisawa, R., & Asakura, H. (2000) Elevation of TFF1 gene expression during healing of gastric ulcer at non-ulcerated sites in the stomach: semiquantification using the single tube method of polymerase chain reaction. *J. Gastroenterol. Hepatol.*, **15**, 604–609.

Saraiva, M. & O'Garra, A. (2010) The regulation of IL-10 production by immune cells. *Nat. Rev. Immunol.*, **10**, 170–181.

Savagner, P., Kusewitt, D.F., Carver, E. a, Magnino, F., Choi, C., Gridley, T., & Hudson, L.G. (2005) Developmental transcription factor slug is required for effective re-epithelialization by adult keratinocytes. *J. Cell. Physiol.*, **202**, 858–866.

Schäfer, M. & Werner, S. (2008) Cancer as an overhealing wound: an old hypothesis revisited. *Nat. Rev. Mol. Cell Biol.*, **9**, 628–638.

Scholven, J., Taras, D., Sharbati, S., Schön, J., Gabler, C., Huber, O., Meyer zum Büschenfelde, D., Blin, N., & Einspanier, R. (2009) Intestinal expression of TFF and related genes during postnatal development in a piglet probiotic trial. *Cell. Physiol. Biochem.*, **23**, 143–156.

Schwarzberg, H., Kalbacher, H., & Hoffmann, W. (1999) Differential behavioral effects of TFF peptides: injections of synthetic TFF3 into the rat amygdala. *Pharmacol. Biochem. Behav.*, **62**, 173–178.

Seib, T., Blin, N., Hilgert, K., Seifert, M., Theisinger, B., Engel, M., Dooley, S., Zang, K.-D., & Welter, C. (1997) The three human trefoil genes TFF1, TFF2, and TFF3 are located within a region of 55 kb on chromosome 21q22.3. *Genomics*, **40**, 200–202.

Shan, M., Gentile, M., Yeiser, J.R., Walland, a C., Bornstein, V.U., Chen, K., He, B., Cassis, L., Bigas, A., Cols, M., Comerma, L., Huang, B., Blander, J.M., Xiong, H., Mayer, L., Berin, C., Augenlicht, L.H., Velcich, A., & Cerutti, A. (2013) Mucus enhances gut homeostasis and oral tolerance by delivering immunoregulatory signals. *Science*, **342**, 447–453.

Shi, H.-S., Yin, X., Song, L., Guo, Q.-J., & Luo, X.-H. (2012) Neuropeptide Trefoil factor 3 improves learning and retention of novel object recognition memory in mice. *Behav. Brain Res.*, **227**, 265–269.

Shi, L., Smith, S.E.P., Malkova, N., Tse, D., Su, Y., & Patterson, P.H. (2009) Activation of the maternal immune system alters cerebellar development in the offspring. *Brain. Behav. Immun.*, **23**, 116–123.

Sibley, L.D., Mordue, D.G., Su, C., Robben, P.M., & Howe, D.K. (2002) Genetic approaches to studying virulence and pathogenesis in Toxoplasma gondii. *Philos. Trans. R. Soc. Lond. B. Biol. Sci.*, **357**, 81–88.

Silen, W. & Ito, S. (1985) Mechanisms for rapid re-epithelialization of the gastric mucosal surface. *Annu. Rev. Physiol.*, **47**, 217–229.

Singh, S., Poulsom, R., Hanby, andrew M., Rogers, len A., Wright, nicholas A., Sheppard, michael C., & Langman, M.J. (1998) Expression of oestrogen receptor and oestrogen-inducible genes pS2 and ERD5 in large bowel mucosa and cancer. *J. Pathol.*, **184**, 153–160.

Siu, L.-S., Romanska, H., Abel, P.D., Baus-Loncar, M., Kayademir, T., Stamp, G.W.H., & Lalani, E.-N. (2004) TFF2 (trefoil family factor2) inhibits apoptosis in breast and colorectal cancer cell lines. *Peptides*, **25**, 855–863.

Smith, J.M., Johanesen, P.A., Wendt, M.K., Binion, D.G., & Dwinell, M.B. (2005) CXCL12 activation of CXCR4 regulates mucosal host defense through stimulation of epithelial cell migration and

promotion of intestinal barrier integrity. *Am. J. Physiol. Gastrointest. Liver Physiol.*, **288**, G316–26.

Sonnemann, K.J. & Bement, W.M. (2011) Wound repair: toward understanding and integration of single-cell and multicellular wound responses. *Annu. Rev. Cell Dev. Biol.*, **27**, 237–263.

Soriano-Izquierdo, A., Gironella, M., Massaguer, A., May, F.E.B., Salas, A., Sans, M., Poulsom, R., Thim, L., Piqué, J.M., & Panés, J. (2004) Trefoil peptide TFF2 treatment reduces VCAM-1 expression and leukocyte recruitment in experimental intestinal inflammation. *J. Leukoc. Biol.*, **75**, 214–223.

Soutto, M., Belkhiri, A., Piazuelo, M.B., Schneider, B.G., Peng, D., Jiang, A., Washington, M.K., Kokoye, Y., Crowe, S.E., Zaika, A., Correa, P., Peek, R.M., & El-Rifai, W. (2011) Loss of TFF1 is associated with activation of NF-κB-mediated inflammation and gastric neoplasia in mice and humans. *J. Clin. Invest.*, **121**, 1753–1767.

Splendore, A. (1908) Un nuovo protozoa parassita deconigli incontrato nelle lesioni anatomiche d'une malattia che ricorda in molti punti il Kala-azar dell'uoma. Nota preliminare pel. *Rev Soc Sci Sao Paulo*, **3**, 109–112.

Stafford, J.L., Neumann, N.F., & Belosevic, M. (2002) Macrophage-mediated innate host defense against protozoan parasites. *Crit. Rev. Microbiol.*, **28**, 187–248.

Sturm, A. & Dignass, A.U. (2008) Epithelial restitution and wound healing in inflammatory bowel disease. *World J. Gastroenterol.*, **14**, 348–353.

Subauste, C. (2012) Animal models for Toxoplasma gondii infection. *Curr. Protoc. Immunol.*, **Chapter 19**, Unit 19.3.1–23.

Suemori, S., Lynch-Devaney, K., & Podolsky, D.K. (1991) Identification and characterization of rat intestinal trefoil factor: tissue- and cell-specific member of the trefoil protein family. *Proc. Natl. Acad. Sci. U. S. A.*, **88**, 11017–11021.

Sugiura, N., Uda, A., Inoue, S., Kojima, D., Hamamoto, N., Kaku, Y., Okutani, A., Noguchi, A., Park, C.-H., & Yamada, A. (2011) Gene expression analysis of host innate immune responses in the central nervous system following lethal CVS-11 infection in mice. *Jpn. J. Infect. Dis.*, **64**, 463–472.

Sun, J.-M., Spencer, V. a, Li, L., Yu Chen, H., Yu, J., & Davie, J.R. (2005) Estrogen regulation of trefoil factor 1 expression by estrogen receptor alpha and Sp proteins. *Exp. Cell Res.*, **302**, 96–107.

Tait, E.D. & Hunter, C.A. (2009) Advances in understanding immunity to Toxoplasma gondii. *Mem. Inst. Oswaldo Cruz*, **104**, 201–210.

Taupin, D. & Podolsky, D.K. (2003) Trefoil factors: initiators of mucosal healing. *Nat. Rev. Mol. Cell Biol.*, **4**, 721–732.

Taupin, D., Wu, D.C., Jeon, W.K., Devaney, K., Wang, T.C., & Podolsky, D.K. (1999) The trefoil gene family are coordinately expressed immediate-early genes: EGF receptor- and MAP kinase-dependent interregulation. *J. Clin. Invest.*, **103**, R31–8.

Taupin, D.R., Kinoshita, K., & Podolsky, D.K. (2000) Intestinal trefoil factor confers colonic epithelial resistance to apoptosis. *Proc. Natl. Acad. Sci. U. S. A.*, **97**, 799–804.

Thim, L. (1989) A new family of growth factor-like peptides. "Trefoil" disulphide loop structures as a common feature in breast cancer associated peptide (pS2), pancreatic spasmolytic polypeptide (PSP), and frog skin peptides (spasmolysins). *FEBS Lett.*, **250**, 85–90.

Thim, L. (1997) Trefoil peptides: from structure to function. *Cell. Mol. Life Sci.*, **53**, 888–903.

Thim, L., Madsen, F., & Poulsen, S.S. (2002) Effect of trefoil factors on the viscoelastic properties of mucus gels. *Eur. J. Clin. Invest.*, **32**, 519–527.

Thim, L. & May, F.E.B. (2005) Structure of mammalian trefoil factors and functional insights. *Cell. Mol. Life Sci.*, **62**, 2956–2973.

Thim, L., Wöldike, H.F., Nielsen, P.F., Christensen, M., Lynch-Devaney, K., & Podolsky, D.K. (1995) Characterization of human and rat intestinal trefoil factor produced in yeast. *Biochemistry*, **34**, 4757–4764.

Tobey, N.A. & Orlando, R.C. (1991) Mechanisms of acid injury to rabbit esophageal epithelium. Role of basolateral cell membrane acidification. *Gastroenterology*, **101**, 1220–1228.

Tomasek, J.J., Gabbiani, G., Hinz, B., Chaponnier, C., & Brown, R. a (2002) Myofibroblasts and mechano-regulation of connective tissue remodelling. *Nat. Rev. Mol. Cell Biol.*, **3**, 349–363.

Tomasetto, C. & Rio, M.-C. (2005) Pleiotropic effects of Trefoil Factor 1 deficiency. *Cell. Mol. Life Sci.*, **62**, 2916–2920.

Tomasetto, C., Rio, M.C., Gautier, C., Wolf, C., Hareuveni, M., Chambon, P., & Lathe, R. (1990) hSP, the domain-duplicated homolog of pS2 protein, is co-expressed with pS2 in stomach but not in breast carcinoma. *EMBO J.*, **9**, 407–414.

Tran, C.P., Cook, G. a, Yeomans, N.D., Thim, L., & Giraud, a S. (1999) Trefoil peptide TFF2 (spasmolytic polypeptide) potently accelerates healing and reduces inflammation in a rat model of colitis. *Gut*, **44**, 636–642.

Vaudaux, J.D., Muccioli, C., James, E.R., Silveira, C., Magargal, S.L., Jung, C., Dubey, J.P., Jones, J.L., Doymaz, M.Z., Bruckner, D. a, Belfort, R., Holland, G.N., & Grigg, M.E. (2010) Identification of an atypical strain of toxoplasma gondii as the cause of a waterborne outbreak of toxoplasmosis in Santa Isabel do Ivai, *Brazil. J. Infect. Dis.*, **202**, 1226–1233.

Vries, R.G.J., Huch, M., & Clevers, H. (2010) Stem cells and cancer of the stomach and intestine. *Mol. Oncol.*, **4**, 373–384.

Waligórska-Stachura, J., Jankowska, A., Waśko, R., Liebert, W., Biczysko, M., Czarnywojtek, A., Baszko-Błaszyk, D., Shimek, V., & Ruchała, M. (2012) Survivin--prognostic tumor biomarker in human neoplasms--review. *Ginekol. Pol.*, **83**, 537–540.

Wallace, K., Veerisetty, S., Paul, I., May, W., Miguel-Hidalgo, J.J., & Bennett, W. (2010) Prenatal infection decreases calbindin, decreases Purkinje cell volume and density and produces long-term motor deficits in Sprague-Dawley rats. *Dev. Neurosci.*, **32**, 302–312.

Waree, P. (2008) Toxoplasmosis: Pathogenesis and immune response. *Thammasat Med. J.*, **8**, 487–496.

Watanabe, S., Hirose, M., Yasuda, T., Miyazaki, A., & Sato, N. (1994) Role of actin and calmodulin in migration and proliferation of rabbit gastric mucosal cells in culture. *J. Gastroenterol. Hepatol.*, **9**, 325–333.

Weiss, L.M. & Kim, K. (2000) The development and biology of bradyzoites of Toxoplasma gondii. *Front. Biosci.*, **5**, D391–405.

Weiss, U. (2008) Inflammation. *Nature*, **454**, 427.

Westley, B.R., Griffin, S.M., & May, F.E.B. (2005) Interaction between TFF1, a gastric tumor suppressor trefoil protein, and TFIZ1, a brichos domain-containing protein with homology to SP-C. *Biochemistry*, **44**, 7967–7975.

Wiede, A., Jagla, W., Welte, T., Köhnlein, T., Busk, H., & Hoffmann, W. (1999) Localization of TFF3, a new mucus-associated peptide of the human respiratory tract. *Am. J. Respir. Crit. Care Med.*, **159**, 1330–1335.

Williams, M. a, Westley, B.R., May, F.E., & Feeney, J. (2001) The solution structure of the disulphide-linked homodimer of the human trefoil protein TFF1. *FEBS Lett.*, **493**, 70–74.

Wilson, E.H., Wille-Reece, U., Dzierszinski, F., & Hunter, C. a (2005) A critical role for IL-10 in limiting inflammation during toxoplasmic encephalitis. *J. Neuroimmunol.*, **165**, 63–74.

Wolf, A., Cowen, D., & Paige, B. (1939) Human Toxoplasmosis: Occurrence in infants as an encephalomyelitis verification by transmission of animals. *Science*, **89**, 226–227.

Wong, B. (1984) Parasitic diseases in immunocompromised hosts. *Am. J. Med.*, **76**, 479–486.

Wong, W.M., Poulsom, R., & Wright, N. a (1999) Trefoil peptides. *Gut*, **44**, 890–895.

Wright, N.A., Hoffmann, W., Otto, W.R., Rio, M.C., & Thim, L. (1997) Rolling in the clover: trefoil factor family (TFF)-domain peptides, cell migration and cancer. *FEBS Lett.*, **408**, 121–123.

Wright, N.A., Poulsom, R., Stamp, G., Van Norden, S., Sarraf, C., Elia, G., Ahnen, D., Jeffery, R., Longcroft, J., & Pike, C. (1992) Trefoil peptide gene expression in gastrointestinal epithelial cells in inflammatory bowel disease. *Scand. J. Gastroenterol. Suppl.*, **193**, 76–82.

Yang, J. & Weinberg, R. a (2008) Epithelial-mesenchymal transition: at the crossroads of development and tumor metastasis. *Dev. Cell*, **14**, 818–829.

Yap, G.S. & Sher, A. (1999) Cell-mediated immunity to Toxoplasma gondii: initiation, regulation and effector function. *Immunobiology*, **201**, 240–247.

Zahm, J.M., Kaplan, H., Hérard, a L., Doriot, F., Pierrot, D., Somelette, P., & Puchelle, E. (1997) Cell migration and proliferation during the in vitro wound repair of the respiratory epithelium. *Cell Motil. Cytoskeleton*, **37**, 33–43.

Zhang, B.-H., Yu, H.-G., Sheng, Z.-X., Luo, H.-S., & Yu, J.-P. (2003) The therapeutic effect of recombinant human trefoil factor 3 on hypoxia-induced necrotizing enterocolitis in immature rat. *Regul. Pept.*, **116**, 53–60.

Znalesniak, E.B. (2013) Vergleichende Expressionsanalysen von stationären und migrierenden Epithelzellen nach in vitro-Verwundung (Ph.D. Thesis), Fakultät für Naturwissenschaften der Otto-von-Guericke-Universität Magdeburg.

Znalesniak, E.B., Dürer, U., & Hoffmann, W. (2009) Expression profiling of stationary and migratory intestinal epithelial cells after in vitro wounding: restitution is accompanied by cell differentiation. *Cell. Physiol. Biochem.*, **24**, 125–132.

Znalesniak, E.B. & Hoffmann, W. (2010) Modulation of cell-cell contacts during intestinal restitution in vitro and effects of epidermal growth factor (EGF). *Cell. Physiol. Biochem.*, **25**, 533–542.

Appendix

Appendix I: Body weight of the various mouse strains used in this study

Body weight analysis of all Tff-deficient mice as well as their corresponding wild types was performed. 129/Sv wild type mice (n = 10), Tff1^{KO} mice (n = 26), Tff2^{KO} mice (n = 14) and wild type mice corresponding to Tff3^{KO} mice with mixed background of 129/Sv and C57BL/6 (n = 40, 28 males and 12 females) and Tff3^{KO} mice (n = 31, 21 males and 10 females) were used for the analysis (12 – 16 weeks old). The results show that Tff2^{KO} mice have a significantly reduced body weight (p = 1.56x10^{-3}); whereas Tff3^{KO} mice showed a significantly increased body weight **(A)**. According to a gender analysis, the male Tff3^{KO} mice show a greater increase than the female mice **(B)**.

A: Body weight analysis of all three mouse lines:

B: Body weight analysis sorted by gender (Tff3^{KO} mice)
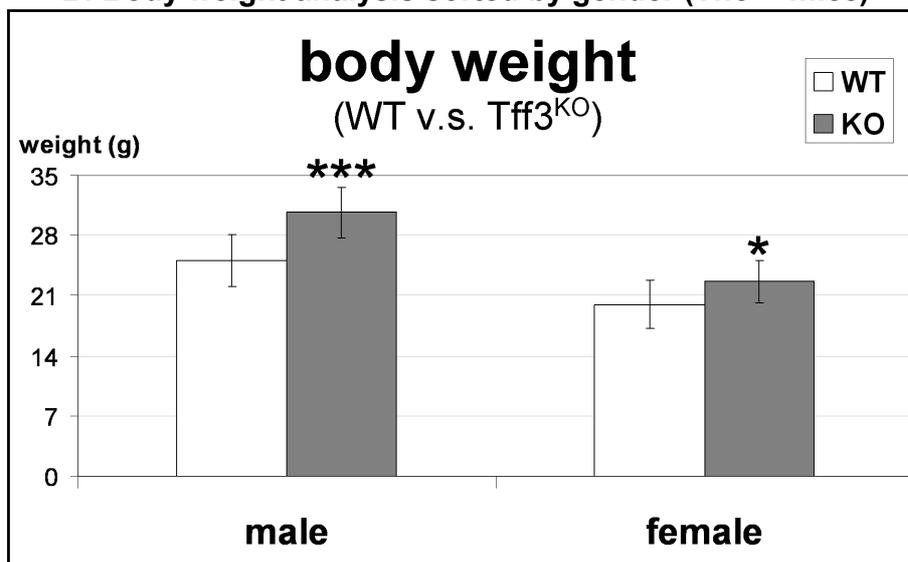
Appendix II: Pedigree of the Tff3^{KO} mouse strain

Tff3^{KO} mice used in this study originated from the Tff3-deficient (Tff3^{KO}) mice with a mixed background of 129/Sv and C57BL/6 (Lubka *et al.*, 2008; Blaschke, 2010). The original strain has been described by Mashimo *et al.* (1996). In order to generate wild type (WT) and Tff3^{KO} mice with nearly identical genetic background, mice heterozygotes (HT) for Tff3 were crossed for more than 10 generations. The numbers refer to the mice used for the breeding. Both mice for each pairing originated from the same parents. The generation number of each pairing is indicated in parentheses on the right side. Pairings of wild type mice are shown in blue, Tff3^{KO} mice are shown in red and the heterozygote mice are shown in black. The yellow background indicates the origin of the mice used in this study.

equivalent to the pedigree from Dr. Blaschke (2010)

	967 x 970	(I)
	1000 x 1002	(II)
	1035 x 1039	(III)
	1099 x 1102	(IV)
	1167 x 1171	(V)
	1222 x 1225	(VI)
	1340 x 1373	(VII)
	1515 x 1497	(VIII)
	1568 x 1569	(IX)
1785 x 1786	1614 x 1617 — 1815 x 1826	(X)
1951 x 1953	1809 x 1814 — 1952 x 1954	(XI)
1994 x 2000	1932 x 1935	(XII)
2047 x 2050	2005 x 2007 — 2033 x 2034	(XIII)
	1998 x 2001	
	2057 x 2060	(XIV)

KO   HT   WT
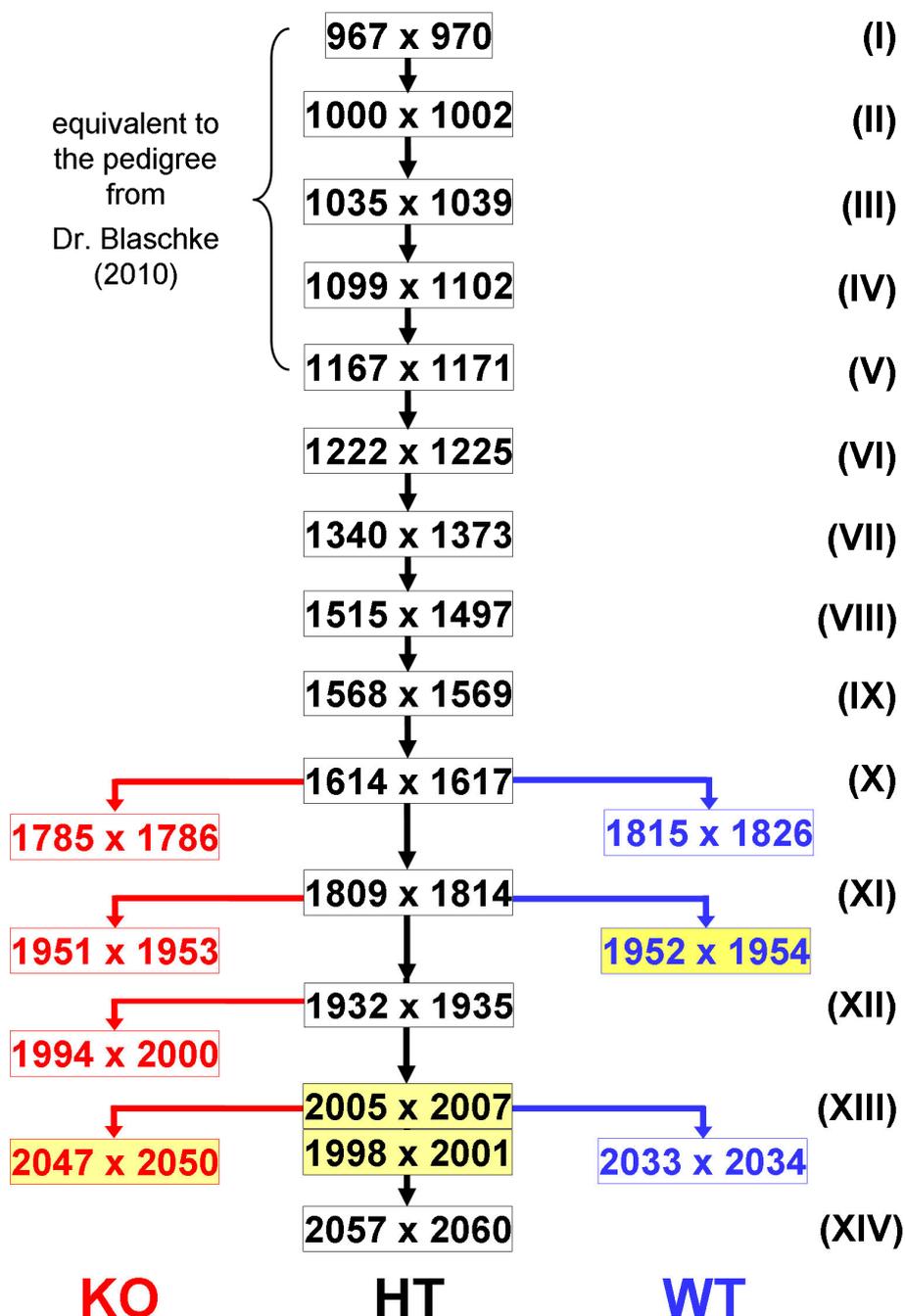
Appendix III: Sequencing of Tff1 and Tff2 (RT-PCR products from mouse brain)

This DNA sequencing was performed via commercial sequencing services of Institut für Biologie (Abt. Genetik), Humboldt Universität Berlin. The accuracy of the sequences was verified by the online software "Pairwise Sequence Alignment" on: http://www.ebi.ac.uk/Tools/psa/emboss_needle/nucleotide.html.

Results are shown as follow:

```
primer forward
primer reverse
stop codon
unpaired base
#=======================================
# Aligned_sequences: 2
# 1: RT-PCR product of Tff1 from mouse brain
# 2: NM_009362.2, Mus musculus trefoil factor 1 (Tff1), mRNA
#=======================================


Tff1 (Brain)     1 GCGAAATCC--------------------GCAAGCT---AT------TTA    21
                     ||||              | ||||| ||       ..|
NM_009362.2      1 -----ATCCATCACTCGTGGTCTTCCCGTG-AAGCTGCCATGGAGCACAA   44

Tff1 (Brain)    22 GGTGA----------CACTATAGAATACTCAAGCATATGCATCCAACGCG   61
                    |||||           |.||.|.| |.|||||.||    ||       ||.
NM_009362.2     45 GGTGATCTGTGTCCTCGCTGTGG--TCCTCATGC---TG--------GCC   81

Tff1 (Brain)    62 TT-GGGAGCTCT--CCCATATGGTCGACCTGCAGGC---GGCCGCGAATT  105
                    || ||.||| || |||| ||.| ||||| ||||
NM_009362.2     82 TTCGGCAGC-CTTGCCCA---GGCC------CAGGCCCAGGCC-------  114

Tff1 (Brain)   106 CA---CTAGTGATTAAACATGTATCATGGCCCCCCGGGAGAGGATAAATT  152
                    ||   |.|| ||..|||||||||||||||||||||||||||||||||||||
NM_009362.2    115 CAGGCCCAG-GAAGAAACATGTATCATGGCCCCCCGGGAGAGGATAAATT  163

Tff1 (Brain)   153 GTGGCTTCCCCGGTGTCACCGCCCAGCAGTGCACGGAGAGAGGTTGCTGT  202
                    ||||||||||||||||||||||||||||||||||||||||||||||||||
NM_009362.2    164 GTGGCTTCCCCGGTGTCACCGCCCAGCAGTGCACGGAGAGAGGTTGCTGT  213

Tff1 (Brain)   203 TTTGATGACAGTGTCCGGGGATTCCCGTGGTGCTTCCACCCCATGGCCAT  252
                    ||||||||||||||||||||||||||||||||||||||||||||||||||
NM_009362.2    214 TTTGATGACAGTGTCCGGGGATTCCCGTGGTGCTTCCACCCCATGGCCAT  263

Tff1 (Brain)   253 CGAGAACACTCAAGAAGAAGAATGTCCCTTCTAAGGTCCATCCTGAGAGA  302
                    ||||||||||||||||||||||||||||||||||||||||||||||||||
NM_009362.2    264 CGAGAACACTCAAGAAGAAGAATGTCCCTTCTAAGGTCCATCCTGAGAGA  313

Tff1 (Brain)   303 ACTGGCTACATCAAGACTTGGCACCCTCCACCTGGGCACTGGAGCCACCT  352
                    ||||||||||||||||||||||||||||||||||||||||||||||||||
NM_009362.2    314 ACTGGCTACATCAAGACTTGGCACCCTCCACCTGGGCACTGGAGCCACCT  363

Tff1 (Brain)   353 GGCCCACCTGCTACATACACACCTACTCTGTGGCTGGATCTGGCTGGTGA  402
                    ||||||||||||||||||||||||||.|||||||||||||||||||||||
NM_009362.2    364 GGCCCACCTGCTACATACACACCTATTCTGTGGCTGGATCTGGCTGGTGA  413

Tff1 (Brain)   403 CACAGTTCAACCCCTCAGACTTTTAGTCCTCGAATTCAATCGAATTCCCG  452
                    |||||||||||||||||||||||||||||||||||
NM_009362.2    414 CACAGTTCAACCCCTCAGACTTTTAGTCCTCGAATT-------------  449
```

```
#========================================
# Aligned_sequences: 2
# 1: RT-PCR product of Tff2 from mouse brain
# 2: NM_009363.3, musculus trefoil factor 2 (Tff2), mRNA
#========================================


Tff2 (Brain)       1 -------------------------------------------------- 0
NM_009363.3        1 ATTCTGCAGGCTGCCCAGGTCCAGTGGAGCAGACATGCGACCTCGAGGTG 50

Tff2 (Brain)       1 -------------------------------------------------- 0
NM_009363.3       51 CCCCCCTGCTGGCAGTGGTCCTGGTTTTGGGACTGCATGCTCTGGTAGAG 100

Tff2 (Brain)       1 ---GCGAA----TCCGCC-------GCTATTTAGG-TGA-----CACTAT 30
                        |.|||    |||.||        || |..||| |||     |||.|.
NM_009363.3      101 GGCGAGAAACCTTCCCCCTGTCGGTGC--TCCAGGCTGACACCCCACAAC 148

Tff2 (Brain)      31 AGAA--TACTCAAGCTAT-----GCATC---------CAACGCGTTG--- 61
                        ||||  .|||...||| |     |||||        ||..||.|||
NM_009363.3      149 AGAAAGAACTGTGGCT-TCCCGGGCATCACCAGTGAGCAGTGCTTTGATC 197

Tff2 (Brain)      62 --GGA-GCT-------CTCCCATATGGTCGACCTGCAGGCGGCCGCGAAT 101
                        ||| |||       ||| ||..|||| |||..|
NM_009363.3      198 TTGGATGCTGCTTTGACTC---TAGCGTCG--CTGGGG------------ 230

Tff2 (Brain)     102 TCACTAGTGAT-TTTCCACCCACTTCCAAACCAAGAATCGGAGCAGTGTG 150
                        ||.|| ||.| |||||||||||||||||||||||||||||||||||||
NM_009363.3      231 TCCCT--TGGTGTTCCACCCACTTCCAAACCAAGAATCGGAGCAGTGTG 278

Tff2 (Brain)     151 TCATGGAAGTGTCAGCTCGCAAGAATTGTGGGTACCCGGGCATCAGTCCC 200
                        ||||||||||||||||||||||||||||||||||||||||||||||||||
NM_009363.3      279 TCATGGAAGTGTCAGCTCGCAAGAATTGTGGGTACCCGGGCATCAGTCCC 328

Tff2 (Brain)     201 GAGGACTGTGCCAGTCGAAACTGCTGCTTTTCCAACCTGATCTTTGAAGT 250
                        ||||||||||||||||||||||||||||||||||||||||||||||||||
NM_009363.3      329 GAGGACTGTGCCAGTCGAAACTGCTGCTTTTCCAACCTGATCTTTGAAGT 378

Tff2 (Brain)     251 GCCCTGGTGTTTCTTCCCACAGTCTGTGGAAGATTGTCACTACTGAGAGT 300
                        ||||||||||||||||||||||||||||||||||||||||||||||||||
NM_009363.3      379 GCCCTGGTGTTTCTTCCCACAGTCTGTGGAAGATTGTCACTACTGAGAGT 428

Tff2 (Brain)     301 TGCTACTGCCGAGCCACCAGTTCCCTGGGAGCTGCAAGCCAGAAGAAAGT 350
                        ||||||||||||||||||.|||||||||||||||||||||||||||||||
NM_009363.3      429 TGCTACTGCCGAGCCACCCGTTCCCTGGGAGCTGCAAGCCAGAAGAAAGT 478

Tff2 (Brain)     351 TCCAACCAGACTTCATCGATCTCTGGGGTTTCTAAAACCATCTTGACCCT 400
                        |.|||||||||||||||.||||||||||||||||||||||||||||||||
NM_009363.3      479 TTCAACCAGACTTCATCAATCTCTGGGGTTTCTAAAACCATCTTGACCCT 528

Tff2 (Brain)     401 TAGCAGTGGCTAGACACAGCATT---------AATCGAA---TTCCCGCG 438
                        |||||||||||||||||||||||         || |||   ||.
NM_009363.3      529 TAGCAGTGGCTAGACACAGCATTTTCCAAGTAAA--GAAAGTTG----- 571
```

Lebenslauf

Persönlichen Daten

Name:	FU, Ting (weiblich)
Geburtsdatum:	25.03.1980
Staatsangehörigkeit:	China
E-Mail:	ftketty@gmail.com
Anschrift:	Fermersleber Weg 45C-0101
	39112 Magdeburg

Bildungen

ab 2008   **Promotionsstudium**
Institut für Molekularbiologie und Medizinische Chemie, Otto-von-Guericke-Universität, Magdeburg
„In vivo and in vitro studies on the expression and function of TFF peptides in the gastrointestinal tract and central nervous system "

2006–2007   **Praktikum**
ECHO Labor, Universitätsklinik und Poliklinik für Allgemein-, Viszeral- und Gefäßchirurgie, Martin-Luther-Universität Halle-Wittenberg (Untersuchungen zur Rolle der sieben-transmembranöse Rezeptoren in humanen Neoplasien)

2003–2006   **Studium für „Master of Biomedical Engineering"**
Martin-Luther-Universität Halle-Wittenberg & Fachhochschule Anhalt
„Assessment of [^{3}H] Digoxin bnding kinetics in rat aorta"

1998–2002   **Studium für „Bachelor of Pharmaceutical Engineering"**
Nanjing Science and Technology University, China
"The improve of synthesize technology of 2,5-dichloroaniline"

Konferenzbeiträge

07-09.12.2006
22. Arbeitstagung Experimental Schilddrüsenforschung, AESF, Berlin.
mündliche Präsentation: *„Prognostic value of Raf kinase inhibitor protein (RKIP) in thyroid carcinoma"*

06-08.12.2007
23. Arbeitstagung Experimental Schilddrüsenforschung, AESF, Lübeck.

Publikationen

Liu, D., Trojanowicz, B., Radestock, Y., **Fu, T.**, Hammje, K., Chen, L., & Hoang-Vu, C. (2010) Role of CD97 isoforms in gastric carcinoma. *Int. J. Oncol.*, **36**, 1401–1408.

Fu, T., Kalbacher, H., & Hoffmann, W. (2013) TFF1 is differentially expressed in stationary and migratory rat gastric epithelial cells (RGM-1) after *in vitro* wounding: influence of TFF1 RNA interference on cell migration. *Cell. Physiol. Biochem.*, **32**, 997–1010

Selbstständigkeitserklärung

Die von mir eingereichte Dissertation „*In vivo* and *in vitro* studies on the expression and function of TFF peptides in the gastrointestinal tract and central nervous system" wurde selbstständig, ohne unzulässige Hilfe Dritter und ohne Verwendung anderer als der angegebenen Hilfsmittel, verfasst. Die aus anderen Quellen übernommenen Daten und Erkenntnisse sind unter Angabe der Quelle gekennzeichnet.
Weiterhin erkläre ich, dass ich weder diese noch eine andere Arbeit zur Erlangung des akademischen Grades doctor rerum naturalium (Dr. rer. nat.) an anderen Einrichtungen eingereicht habe.

Erklärung über Promotionsversuche

Ich erkläre, dass ich keine früheren Promotionsversuche unternommen habe und an keiner anderen Fakultät oder Universität ein Promotionsverfahren anhängig ist.

Magdeburg, den 27.01.2014